HYDRODYNAMICS OF LIQUID HELIUM II

Derek J. Griffiths

A Thesis Submitted for the Degree of PhD
at the
University of St Andrews

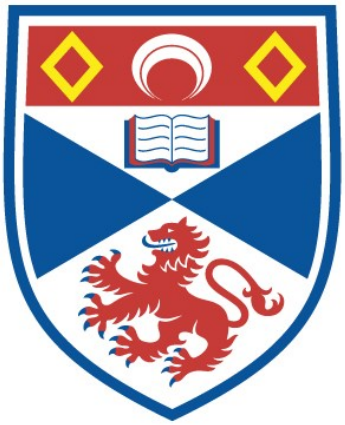

1964

Hydrodynamics of liquid helium II

A thesis presented by

Derek J. Griffiths

to the University of St. Andrews

in application for the degree of

Doctor of Philosophy.

October, 1963

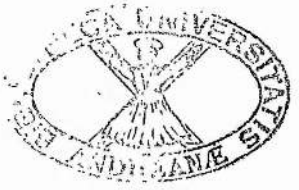

Declaration

I hereby declare that the following thesis is based upon research work carried out by me, that the thesis is my own composition and that it has not previously been presented for a higher degree.

The research has been performed in the Department of Natural Philosophy of the United College of the University of St. Andrews under the supervision of Dr. D. V. Osborne and of Professor J. F. Allen, F.R.S.

Certificate

I certify that Derek J. Griffiths has spent nine terms engaged in research in the Department of Natural Philosophy of the United College of the University of St. Andrews under the direction of Professor J. F. Allen and of myself, that he has fulfilled the conditions of Ordinance No. 16 of the University Court of St. Andrews and that he is qualified to submit the accompanying thesis in application for the degree of Doctor of Philosophy.

Research Supervisor.

Personal Preface

I graduated in 1960 as Bachelor of Arts of the University of Cambridge with first class honours in Part I of the Natural Sciences Tripos and second class honours in Part II of the same Tripos, in which my subject was Physics (with theoretical option). In October of that year I began research in the Department of Natural Philosophy of the United College of the University of St. Andrews under Dr. D. V. Osborne, who has continued to direct me until the present time, with the exception of the academic year 1961/1962 when his place was taken by Professor J. F. Allen. In July, 1961, I attended a course on liquid helium at the Enrico Fermi International School of Physics, Italy, and in September, 1962, the VIIIth International Congress on Low Temperature Physics at Queen Mary College, London.

Acknowledgments

The author offers his sincere thanks to the following people and institutions:

The Department of Scientific and Industrial Research for the award of a Research Studentship and for grants towards the cost of attending the International Summer School course on liquid helium in Italy in 1961 and the VIIIth International Congress on Low Temperature Physics in London in 1962.

Dr. D. V. Osborne for the basic ideas on which the whole work rests; for help with many practical details, especially the design of the electronics; for being always available with help, stimulating ideas and discussion when wanted, and keeping tactfully out of the way otherwise.

Professor J. F. Allen for encouragement and patience throughout the work, especially during the difficult period of the investigation from 1961 to 1962; for discussion of the ideas of the early parts of chapter 3 and of appendix II, and help in the preparation of a paper upon them.

Professor W. F. Vinen for discussion and criticism of the same ideas.

Mr. R. H. Mitchell for designing the final version of the cryostat, and for a steady flow of helium, help and ideas on

experiment and theory, a remarkably high proportion of them bright ones.

Mr. C. F. Mitchell and Mr. T. Marshall for constructing the final version of the cryostat.

Mr. H. Cairns for lending some vital pieces of electrical equipment.

Virtually everyone else in the department for doing and lending things at various times.

Dr. A. Norridge and the Getty Marine Research Laboratory for lending a high-speed pen recorder and other equipment.

Dr. K. Stevens and the Department of Physiology for the temporary loan of a CFO and the permanent loan of a constant-speed camera drive.

Mr. K. Currie and the Department of Natural Philosophy, Glasgow University, for the loan of an 'HT' power supply unit and three photomultiplier tubes.

Mr. J. Cornard for the supply of equipment and for printing the illustrations to this thesis.

Finally, Mrs. M. Cunningham for typing the thesis at high speed for a rather unreliable author.

Summary

Observations have been made of the behaviour of a fine quartz fibre, weighted at its lower end and suspended inside a short, horizontal tunnel in which counterflow of the normal and superfluid components of liquid helium II can be produced by a heater. Section I of this thesis is an introduction to the hydrodynamics of liquid helium II. In section II the interaction with such a fibre of quantized vortex lines in the superfluid is discussed, and the effect of a short heat pulse on the fibre when it is carrying superfluid circulation is calculated approximately. The different responses of the fibre to turbulence in the normal fluid and in the superfluid are contrasted.

In section III, after a description of the apparatus and the experimental method, measurements, deduced from the response to heat pulses, of the circulation about the fibre from 1.3°K to 2.1°K are reported. At all temperatures circulations of the expected order of magnitude are observed to grow and decay with time. At 1.3°K apparent circulations of up to about $\frac{1}{5}$ quantum occur. In undisturbed helium the largest circulations are more stable than other values, persisting for up to five minutes. Measurement of the same circulation both by the heat-pulse method and by the deflection of the fibre in a steady heat current suggests that the large, persistent circulations may in

fact be equal to one quantum. The sense of the observed circulations about the fibre at 1.3°K is strongly biased, this bias being probably associated with the heater geometry. In small heat current no change in the bias or persistence of circulation can be detected, but in currents above $1\frac{1}{2}$-3 mW/cm^2, depending on the heater, the circulation about the fibre is both more variable and of the opposite bias to that in undisturbed helium. This behaviour continues for 100 sec or more after the heat current has been switched off. At higher temperatures there are indications that the behaviour might be similar if it were possible for the helium to regain its undisturbed condition after being stirred up by turbulent heat currents. In fact this seems either to be impossible, or to require many hundreds of seconds, and the situation is therefore rather confused.

In still higher heat currents measurement of superfluid circulation by heat pulses is impossible because the fibre is continuously agitated in a random way. From measurements of the rms deflections of the bob on the end of the fibre a critical heat current for the onset of such turbulence is found at 1.3°K. At higher temperatures the sensitivity is too low for the transition itself, if any, to be detected, but an upper limit to the critical heat current is given. At 1.3°K and 2.1°K the rms deflection increases monotonically with increasing heat currents, but at intermediate temperatures it is variable, because the bob is often hardly agitated for long periods during apparently supercritical heat currents. This is called quiescent behaviour.

When a supercritical heat current is switched on there is a delay before agitation of the fibre begins. The delay time, which is often not very well defined, has been measured as a function of the heat current. When the current is switched off the agitation of the bob decays in a few seconds, but at 1.3°K the circulation about the fibre is small and variable for 100 sec or more, until the persistence and bias characteristic of undisturbed helium are regained.

These results are discussed in section IV. It is believed that at 1.3°K the undisturbed superfluid contains little vorticity, what little there is being perhaps created by the measurement pulses themselves. In very low heat currents the superfluid moves without essential modification, but when the superfluid velocity exceeds $(\frac{1}{2}-1) \times 10^{-2}$ cm/sec extra vorticity appears in the superfluid. It is suggested that this arises from something similar to classical secondary flow, here induced by irregularity and asymmetry in the heater, and that it may be connected with Vinen's (1957d) subcritical turbulence. In heat currents above a critical value given by $Re_v \doteq 1350$ at 1.3°K, both the normal and superfluid components are turbulent. Re_v is a Reynolds' number depending on the mean velocity and the viscosity of the normal fluid, the mean tunnel diameter and the total fluid density (cf. Staas, Taconis and Van Alphen 1961; Chase 1962). At higher temperatures the experimental upper limit to the critical Reynolds' number lies at or just above this value. From comparison with the results of other authors, in particular Vinen (1957a-d) and Chase (1962), the

transition to turbulence is identified with the onset of mutual friction between the normal fluid and the superfluid. No clear explanation of the quiescent behaviour in supercritical heat currents at temperatures intermediate between 1.3°K and the λ-point is found. In general the results at temperatures above 1.3°K are not so clear-cut both because of the lack of sensitivity of the apparatus, and because of the difficulty of attaining undisturbed conditions. It is suggested that the delay time for the onset of turbulence is associated with the propagation of a turbulence front from the heater rather than with the simultaneous growth of turbulence throughout the tunnel.

In the same section some speculations on the nature of superfluid vorticity and turbulence, and the connection of these and normal-fluid turbulence with mutual friction are put forward. Further experiments and possible theoretical investigations are suggested. Appendix I contains some early measurements of the normal viscosity of helium II in an apparatus similar to that of the present experiment. In appendix II Vinen's (1961b) experiment on the detection of single quanta of circulation is discussed in terms of classical vortex-line theory. It is found that his observations can be quite well accounted for without postulating, as he did, an anomalously large vortex-line core.

Apart from the material of section I and where specific references are given in the text or among the acknowledgments, all the work in this thesis is original. The material of chapter 3(a)-(c) and of appendix II has been accepted for publication in the Proceedings of the

Royal Society, and a note on the progress of the experiment was read at the VIIIth International Congress on Low Temperature Physics.

The quotations at the head of each section are taken from Dorothy L. Sayers's translation of Dante's Divine Comedy, published by Penguin Books.

Contents

List of illustrations

I

Introduction

What ill-directed reasonings syllogistical

Weight down thy wings to mundane triviality!

(Paradiso XI, 2-3)

1. Liquid Helium II

Naturally occurring helium, which was first liquefied by Kamerlingh Onnes in 1908, the last of the permanent gases to be so, is found to give a clear, colourless liquid about one-seventh as dense as water. The critical temperature and the boiling point are close to the absolute zero, being 5.20°K and 4.21°K respectively, because the symmetry and simplicity of the He^4 atom lead to very weak interatomic forces. Two extranuclear electrons fill the first atomic shell, and, being close to the nucleus, are firmly bound. Further, the nucleus, which contains two protons and two neutrons, has no resultant angular momentum or magnetic moment. However, liquid helium is not the very simple, classical liquid that might be expected, for the weakness of the classical interactions allows purely quantum-mechanical effects to manifest themselves, the more strongly because of the small mass of the helium atom. It is easily shown, for example, that the zero-point energy of an atom is inversely proportional to its mass. The zero-point energy of helium is so large that it cannot be solidified by cooling alone: a pressure of about 25 atmospheres is necessary for solidification. Liquid helium therefore exists down to the absolute zero.

At the absolute zero classical solids achieve zero entropy, that is perfect order, as is demanded by the third law of thermodynamics, by ordering their atoms or molecules on a lattice in position space. The fact that helium remains liquid implies that ordering takes place not in position space, but in momentum space. One sign of this is that at

2.18°K the properties of the liquid change dramatically, for whereas above 2.18°K it is an ordinary liquid (helium I) of low viscosity (about 2.10^{-5} poise), below this temperature it is able to flow through narrow slits and capillaries with a velocity of many centimetres per second, so that its effective viscosity is less than 10^{-11} poise. It also appears to have a thermal conductivity far greater than that of silver. The low-temperature modification of the liquid having these so-called superfluid properties is known as liquid helium II. It was discovered simultaneously by Allen and Misener and by Kapitza in 1938. No latent heat or volume discontinuity is associated with the transition from helium I to II, but there is a discontinuity, together with a logarithmic singularity, in the specific heat (Fairbank, Buckingham and Kellers 1957). This type of transition, of which that in helium is the earliest and best-known example, is known as a λ-transition. The transition temperature under the saturated vapour pressure is called the λ-point.

The properties of helium II cannot in fact be described in terms of simple viscosity and thermal conductivity coefficients, although the liquid does seem to possess a normal viscosity, similar to that of helium I in magnitude, which controls the damping of the torsional oscillations of a disc immersed in the liquid, for example, but not its flow through narrow channels. A satisfactory description of this behaviour is provided by the two-fluid theory proposed in different forms by Tisza (1940) and Landau (1941). The liquid is considered to be an intimate mixture of two components, a normal one and a superfluid

one, each with its associated density ρ_n or ρ_s, respectively, where the total density $\rho = \rho_n + \rho_s$. The normal component, which has an ordinary viscosity, is responsible for the damping of the oscillations of a disc and similar phenomena, while the superfluid apparently flows almost without friction. It is found that ρ_n/ρ falls monotonically from unity at the λ-point to zero at the absolute zero. With the two components velocity fields $\underset{\sim}{v}_n$ and $\underset{\sim}{v}_s$ are associated, and the thermal effects can then be explained if it is assumed that all the entropy resides in the normal fluid. The apparently high thermal conductivity arises because heat is transported by an internal convection mechanism in which normal fluid moves away from the source of heat while superfluid moves towards it. On this basis the following equations of motion can be tentatively derived (Atkins 1959). By conservation of mass

$$\frac{\partial \rho}{\partial t} + \operatorname{div}\left(\rho_s \underset{\sim}{v}_s + \rho_n \underset{\sim}{v}_n\right) = 0, \qquad (1.1)$$

and by conservation of entropy (S per unit total mass)

$$\frac{\partial(\rho S)}{\partial t} + \operatorname{div}\left(\rho S \underset{\sim}{v}_n\right) = 0. \qquad (1.2)$$

For the superfluid component

$$\rho_s \frac{D\underset{\sim}{v}_s}{Dt} = -\frac{\rho_s}{\rho} \operatorname{grad} p + \rho_s S \operatorname{grad} T, \qquad (1.3)$$

and for the normal component

$$\rho_n \frac{D\underset{\sim}{v}_n}{Dt} = -\frac{\rho_n}{\rho} \text{ grad } p - \rho_s S \text{ grad } T + \eta_n \left(\nabla^2 \underset{\sim}{v}_n + \frac{1}{3} \text{ grad div } \underset{\sim}{v}_n \right), \quad (1.4)$$

where p is the pressure, T is the temperature, η_n is the normal viscosity,

and $$\frac{D}{Dt} \equiv \frac{\partial}{\partial t} + \underset{\sim}{v} \cdot \text{grad}$$

Equations (1.3) and (1.4) are similar to the Navier-Stokes equation for a classical liquid, except for the terms in grad T and the lack of viscous dissipation in the superfluid. They must be supplemented by appropriate boundary conditions, which are usually taken to be

$$\left.\begin{array}{l} \underset{\sim}{v}_n = 0 \text{ at a solid boundary} \\ \text{and } \underset{\sim}{v}_s \text{ is tangential but otherwise unrestricted.} \end{array}\right\} \quad (1.5)$$

This form of the superfluid boundary condition is however not universally accepted (Lin 1961).

From the equations it follows that it should be possible to propagate two forms of wave motion in helium II: a pressure variation, ordinary or first sound, with velocity $u_1 \doteq 240$ m/sec, and a

temperature variation, second sound, with velocity $u_2 \doteq 20$ m/sec in the range from 1°K to 2°K. Both these wave motions have been identified and found to propagate with little dispersion and attenuation.

It is found that frictionless flow of the superfluid seems to occur only at sufficiently small velocities, and so, in order to secure better agreement with experiment, various additional frictional forces acting on and between the two components have been proposed at different times. It is hoped that the present thesis resolves some of the confusion surrounding this topic.

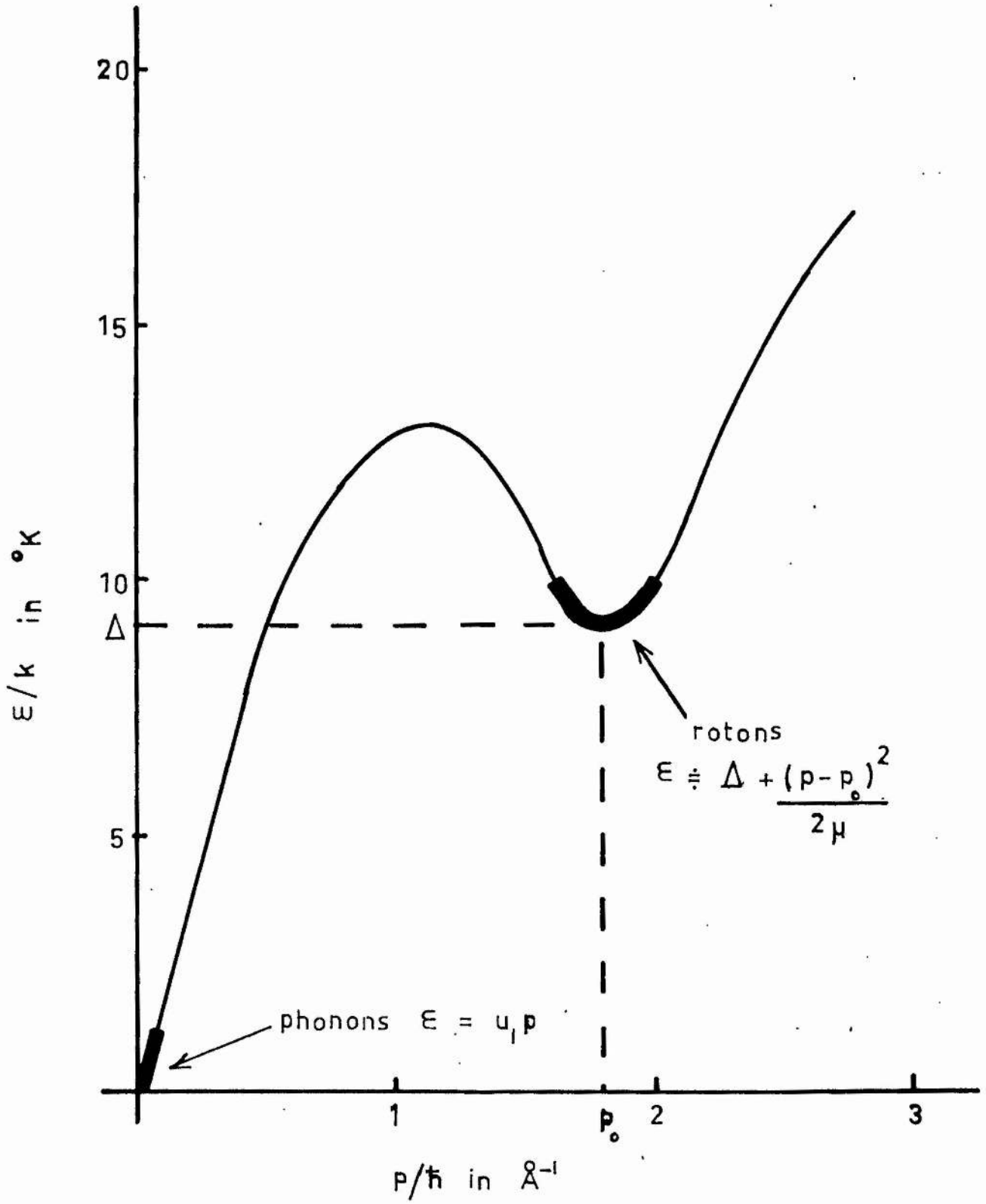

Figure 2.1. Energy and momentum of elementary excitations.

2. Thermohydrodynamics

(a) Critical velocities and mutual friction

The most fruitful approach to the problem of helium II has proved to be that of Landau (1941, 1947), who considered what elementary excitations could exist in a background of undisturbed superfluid, essentially the same as the whole fluid at absolute zero. By identifying these excitations with the normal component he was able to obtain the two-fluid equations of chapter 1. As in a solid there exist quantized sound waves, called phonons, with energy ε and momentum $\underset{\sim}{p}$ related linearly through the velocity of first sound:

$$\varepsilon = u_1 p . \qquad (2.1)$$

Landau showed that the thermodynamic data could be explained if there existed other excitations separated from the phonons by an energy gap and with energy related quadratically to their momentum:

$$\varepsilon = \Delta + \frac{(p-p_0)^2}{2\mu} , \qquad (2.2)$$

where Δ, p_0 and μ are constants, which may however be functions of temperature and pressure. It has been confirmed by neutron diffraction experiments (Palevsky et al. 1957; Yarnell et al. 1959) that the two sorts of excitation fall on two parts of the same dispersion curve, as shown in figure 2.1, where the thickened portions of the curve contain

the excitations normally present in significant numbers, except near the λ-point. The division into phonons and rotons is therefore quite exact. Above about 1.5°K rotons dominate the behaviour of the liquid, phonons being important only at low temperatures.

Landau (1941) pointed out that superfluid flowing past a solid boundary can lose energy and momentum only either by slowing up as a whole, which seems inherently very improbable indeed, or by the creation of an excitation in the fluid. In the latter process energy and momentum can be simultaneously conserved only if $v_s \geq \varepsilon / p$, where ε, p are the energy and momentum of the new excitation, and v_s is the velocity of the superfluid relative to the boundary. If the minimum value of ε/p is greater than zero there will be a critical velocity $v_{s,c} = (\varepsilon/p)_{min}$ below which no interaction between superfluid and solid can occur, and so frictionless flow will take place with velocity up to $v_{s,c}$.

For the phonon-roton spectrum ε/p has a minimum value of Δ/p_0, so that we expect frictionless flow to occur. The value of Δ/p_0 is however about 10^3 cm/sec, which is far in excess of any experimentally observed critical velocity. There must therefore exist other excitations, which may be statistically and thermodynamically insignificant, with lower values of ε/p. Alternatively the observed critical velocities may not be of this ideal type (Vinen 1957d).

Many measurements have been made of critical velocities in various circumstances; that is, of the velocity at which extra frictional forces

not apparently predicted by the simple thermohydrodynamical equations of chapter 1 appear. In such experiments the flow may be induced thermally or by pressure; it may take place with or without net transfer of mass, and in channels, slits or capillaries ranging from 10^{-6} to 1 cm in characteristic dimension; further, the supercritical effects may be detected by measurement of the pressure gradient or the temperature gradient, or by some other method. With so many variations in conditions the results were equally varied and confusing until Gorter and Mellink (1949) suggested that many of them could be explained by adding a new term to the equations of motion for the two fluids, as follows:

$$\rho_s \frac{D\underset{\sim}{v}_s}{Dt} = -\frac{\rho_s}{\rho} \operatorname{grad} p + \rho_s S \operatorname{grad} T - \underset{\sim}{F}_{sn} . \quad (2.3)$$

$$\rho_n \frac{D\underset{\sim}{v}_n}{Dt} = -\frac{\rho_n}{\rho} \operatorname{grad} p - \rho_s S \operatorname{grad} T + \underset{\sim}{F}_{sn} + \eta_n \left(\nabla^2 \underset{\sim}{v}_n + \tfrac{1}{3} \operatorname{grad} \operatorname{div} \underset{\sim}{v}_n \right) . \quad (2.4)$$

$\underset{\sim}{F}_{sn}$, which is a volume force of mutual friction between the two components, and therefore appears with opposite sign in the two equations, has the postulated form

$$\underset{\sim}{F}_{sn} = A \rho_s \rho_n \left| \underset{\sim}{v}_s - \underset{\sim}{v}_n \right|^2 \left(\underset{\sim}{v}_s - \underset{\sim}{v}_n \right) ,$$

where it is hoped that A is independent of channel width and of $\underset{\sim}{v}_s$ or

$\underset{\sim}{v}_n$, and not too dependent on temperature. Study of the results quoted in the original paper suggests that A is in fact a rather poor constant, while in subsequent measurement which have been interpreted in terms of mutual friction (Hung et.al. 1952; Winkel et.al. 1955; Brewer and Edwards 1957; Vinen 1957a,b; Chase 1962) the power of the velocity dependence has varied from 3 up to 4 or 5, and a small velocity v_0 has sometimes been subtracted from $(\underset{\sim}{v}_s - \underset{\sim}{v}_n)$. It appears that agreement with the Gorter-Mellink postulate is better in wider channels and with higher velocities, a conclusion which is confirmed by Brewer and Edwards (1957) for their own results in capillaries of 50, 100 and 366 μ diameter. There is also a critical velocity below which the mutual friction is not detectable.

In the steady state, where $\frac{D}{Dt} \equiv 0$ and div $\underset{\sim}{v}_n = 0$, equations (2.3) and (2.4) are easily solved:

$$\text{grad } p = \eta_n \nabla^2 \underset{\sim}{v}_n \ , \tag{2.5}$$

$$\rho S \text{ grad } T = \eta_n \nabla^2 \underset{\sim}{v}_n + \underset{\sim}{F}_{sn} . \tag{2.6}$$

For sufficiently small velocities $\underset{\sim}{F}_{sn} = 0$, either exactly or approximately, and we obtain the London (1939) relation

$$\text{grad } p = \rho S \text{ grad } T . \tag{2.7}$$

The heat flow per unit cross-sectional area is $\underset{\sim}{W} = \rho S T \underset{\sim}{v}_n$, so that in a parallel-sided channel grad p and $\rho S \operatorname{grad} T$ are equal and proportional to the average heat flow, provided the normal fluid flow remains of the Poiseuille type and F_{sn} is small. When mutual friction is important, $\rho S \operatorname{grad} T$ exceeds grad p, which itself is unaffected unless the normal-fluid flow is altered. If for example the normal fluid became turbulent, grad p would be given by an empirical expression similar to those well-known in classical hydrodynamics, while $\rho S \times$ grad T would continue to exceed it by an amount depending on the mutual friction.

(b) Vortex lines

It was suggested by F. London (1954) and others that frictionless flow of the superfluid might follow from the condition

$$\operatorname{curl} \underset{\sim}{v}_s = 0. \qquad (2.8)$$

That is, that the flow of the superfluid must be potential. It is well known that in this case the superfluid can exert no force on a body submerged in it. London assumed that this implied the absence of viscous dissipation in the superfluid, which is not strictly true (Lin 1961). Nevertheless the condition (2.8) has been generally accepted as containing at least some truth (Feynman 1955; Chester 1961). It follows that in a simply-connected volume the circulation of superfluid velocity around any circuit is zero, and so the superfluid cannot rotate. In a

doubly-connected volume (a torus) however the circulation around all circuits enclosing the central portion of the torus may have a constant, non-zero value. Since the superfluid is found to rotate experimentally (Osborne 1950; Walmsley and Lane 1958), Onsager (1949) and Feynman (1955) suggested that it might become multiply connected by the formation of line singularities parallel to the axis of rotation, with curl $\underset{\sim}{v}_s = 0$ everywhere except on the singularities. Arguing from the single-valuedness of the wave function, Feynman inferred that at absolute zero the superfluid circulation about such a singularity should be quantized in units of h/m, where h is Planck's constant and m is the mass of a helium atom. This result is assumed to hold at finite temperatures also. The tangential superfluid velocity at distance r from an isolated, straight line singularity is $nh/2\pi mr$, where n is the quantum number of the circulation. Because of the atomic structure of the fluid, the singularity cannot be mathematically ideal, but must be smeared out over a core of diameter at least as great as the interatomic spacing. It turns out to be energetically favourable for all singularities to have a single quantum of associated circulation (Hall 1960). Such singularities, with finite core size and unit circulation, are called vortex lines.

The superfluid is able to simulate solid-body rotation of angular velocity ω if it contains vortex lines parallel to the rotation axis so arranged that the average circulation per unit area is equal to the curl of the velocity in true solid-body rotation. That is $Nh/m = 2\omega$,

where N is the number of vortex lines per unit area normal to the axis of rotation. The distance between neighbouring lines is of the order of $N^{-\frac{1}{2}}$, which is about 1 mm when $\omega = 0.1$ rad/sec.

A vortex line has a kinetic energy per unit length of $\pi \rho_s \kappa^2 \ln \frac{b}{a_0}$, where $2\pi\kappa = h/m$ is the circulation about the vortex line and b is a length of the order of the size of the containing vessel or the separation between lines (whichever is the smaller), and a_0 is of the order of the vortex-core radius. The line therefore appears to be in tension, and it is possible to propagate circularly polarized waves on it. Hall (1958) has done calculations and experiments on wave propagation on an array of parallel vortex lines, of the sort expected in rotating helium, and the agreement obtained provides general support for the existence of vortex lines, although the behaviour is probably not critically dependent on such quantitative details of the theory as exact quantization. A vortex-core radius of $6.8\ 10^{-8}$ cm is deduced from the experimental results.

Hall and Vinen (1956) measured the extra attenuation of second sound in steadily rotating helium, finding that it was small when the second sound was propagated along the axis of rotation, but readily detectable and proportional to the angular velocity of rotation for propagation normal to the axis. Now in a second-sound wave the periodic temperature variation is produced by alternate concentration and rarefaction of the normal-fluid excitations. The normal fluid and the superfluid therefore oscillate in antiphase, and any mutual friction

between them would attenuate the second sound. Hall and Vinen found that their results could be interpreted in terms of a mutual friction

$$\underset{\sim}{F}_{sn} = B \frac{\rho_s \rho_n}{\rho} \omega \left(\underset{\sim}{v}_s - \underset{\sim}{v}_n \right) , \qquad (2.9)$$

where B is a temperature-dependent parameter of order unity. The dependence of the attenuation on direction of propagation and on angular velocity suggested that the mutual friction might be due to collisions of normal-fluid excitations with vortex lines in the superfluid. On this assumption Hall and Vinen calculated the expected size and temperature dependence of the parameter B. They obtained good agreement with experiment when the circulation about each of the vortex lines was taken as exactly one quantum, and the radius of the vortex core as about 10^{-8} cm. Although this experiment provides further support for the theory of vortex lines, it again depends on the properties of an array of many lines, and is therefore not too sensitive to the details of the theory.

The only direct support for the quantization of circulation comes from Vinen's (1961b) work on the detection of single quanta. He measured the superfluid circulation about a wire stretched along the axis of a slowly rotating, cylindrical vessel of helium, with results which proved rather difficult to interpret, although he was able to show that an apparent circulation of exactly one quantum was a particularly stable value. The theory and interpretation of this experiment

are further discussed in appendix II.

The connection between superfluid vorticity and mutual friction was further explored by Vinen (1957a-d) in a series of experiments on heat currents in wide channels. Below 1.8°K the temperature gradient and the heat flow W were related by

$$\text{grad}\, T \propto (W - W_0)^3 \quad , \tag{2.10}$$

leading to a mutual friction of the form

$$F_{sn} = A \rho_s \rho_n (|\underset{\sim}{v}_s - \underset{\sim}{v}_n| - v_0)^3 \quad . \tag{2.11}$$

W_0 and v_0 are empirical constants. The value of A, determined as a function of temperature, agreed with the scattered values calculated by Gorter and Mellink from previous measurements. A was independent of channel width over the range investigated (about 2 to 4 mm).

The mutual friction was also determined from the attenuation of second sound propagated across the channel, which was used as a resonator. Provided the heat flow W was fairly large, the attenuation coefficient α varied as

$$\alpha = \alpha_0 + C(W - W_0)^2 \quad , \tag{2.12}$$

where α_0 is the attenuation coefficient of second sound in undisturbed

helium. Neglecting W_o, this implies a mutual friction

$$\underset{\sim}{F}_{sn} = A' \rho_s \rho_n \left| \overline{\underset{\sim}{v}_s - \underset{\sim}{v}_n} \right|^2 \left(\underset{\sim}{v}_s - \underset{\sim}{v}_n \right) , \qquad (2.13)$$

where $\overline{\underset{\sim}{v}_s - \underset{\sim}{v}_n}$ is the time average of $\underset{\sim}{v}_s - \underset{\sim}{v}_n$ over one period of the second sound. That is, it is the relative velocity produced by the heat current alone. The values of A' agreed with those of A. Below a critical heat flow W_{crit} the mutual friction fell sharply to a value indistinguishable from zero.

The mutual friction normally took some seconds to reach its equilibrium value after the switching on of a supercritical heat current. This time τ_o was dependent on the history of the helium, but attained a reproducible maximum value when the helium had been left undisturbed for a time of the order of 10^2 sec. Detectable mutual friction decayed within a few seconds of the switching off of the heat circuit, but the variability of τ_o implied that the helium remained in some way modified for 100 sec or more. By measuring the reduction in τ_o for a supercritical heat flow after a subcritical one had been allowed to flow, Vinen was able to show that except at the lowest temperatures ($\sim 1.3°K$) the helium was modified in some way even in subcritical heat currents. This modification, which he called subcritical turbulence, was greater in wider channels and at higher temperatures; so much so that, above about 1.4°K to 1.5°K, the transition was completely blurred and no critical heat input could be defined.

Vinen interpreted his results in terms of laminar flow of the normal fluid together with turbulence in the superfluid, which he imagined as a tangle of vortex lines with equilibrium density proportional to $\left| \overline{\underset{\sim}{v}_s - \underset{\sim}{v}_n} \right|^2$ in the supercritical case. He developed theories of the growth and decay of such turbulence (1957c,d) which, although they agree qualitatively with experiment in their predictions of growth and decay times, critical heat input and subcritical turbulence, are nevertheless speculative.

Townsend (1963) has pointed out some serious difficulties in this interpretation of mutual friction. While the Gorter-Mellink force is a volume force, the Hall-Vinen force acts only at or near the cores of the vortex lines, and it is difficult to see how it can balance the driving force ($-\text{grad}\, p + \rho S \,\text{grad}\, T$), which is uniform over the channel cross-section. Under the Hall-Vinen force the vortex lines themselves move across the channel perpendicular to the heat flow and are destroyed at the walls. There is thus a continuous loss of vorticity by the superfluid, and the mutual friction force cannot be maintained unless there is some other mechanism which generates vorticity. Townsend shows that with the assumed structure of the heat flow there is no such mechanism, and suggests that the difficulty can be overcome by assuming that the mutual friction acts not just on the vortex cores but on the whole superfluid. This is liable to lead to distributed vorticity in the superfluid, and he suggests that there should be provision in the classical expression of the quantum-mechanical

properties of the superfluid for the destruction of such unquantized vorticity. It is not sufficient to show that distributed vorticity does not arise in critically irrotational flow. This problem is explored further in chapter 9.

Staas, Taconis and van Alphen (1961) investigated the temperature and pressure gradients in flow through wide capillaries (80-250 μ) under a great variety of circumstances (not restricting themselves to the case of zero net mass transfer). They found that the pressure gradient was always related to the normal-fluid flow in a way very similar to that for ordinary fluids, independent of the superfluid velocity through the capillary, provided that a Reynolds' number defined as

$$Re_v = \frac{\overline{v_n} d \rho}{\eta_n} \qquad (2.14)$$

was used to describe the flow, where $\overline{v_n}$ is the mean normal-fluid velocity, d is the capillary diameter and ρ is the total density of the helium. At a Reynolds' number of about 1200 there was a transition to a regime which appeared identical to the turbulence of a classical fluid, although hysteresis was observed in which laminar flow persisted up to hipher Reynolds' numbers. In a classical fluid the lowest Reynolds' number at which turbulence can occur is 2300.

Chase (1962) measured the temperature gradient in heat currents in wide capillaries (0.08 to 0.4 cm) and found that the onset of mutual friction was well described by a critical Reynolds' number of the same

type, having a value almost constant and approximately equal to the classical value below 1.6°K, and falling sharply to zero at the λ-point. The critical heat input was not very well defined in the range 1.7°K to 1.9°K, particularly in the larger channels. He suggested that below 1.6°K mutual friction was associated with turbulence in the normal fluid or the whole fluid, rather than just the superfluid, and that near the λ-point possibly another mechanism, such as a critical superfluid velocity, caused the critical Reynolds' number to drop from the classical value towards zero. If this Reynolds' number is calculated for Vinen's critical heat inputs for the onset of mutual friction, which are in the range from 1.3°K to 1.5°K, it is found to lie between 1500 and 2300 in all cases, in approximate agreement with Chase's results.

Apart from doubt in the interpretation of critical heat inputs in wide channels, the whole vortex-line hypothesis has recently been questioned (Lin 1961; Pellam 1962, 1963). Further experiments in this field are therefore useful. The origin of the present work was as follows. The author was measuring the viscous drag exerted on a fine fibre by a heat current, in an effort to observe and interpret effects due to the phonon mean free path, which was comparable with the fibre diameter at low temperatures. Since the first exploratory results, which are given in appendix I, showed that the experiment was not likely to prove fruitful it was discontinued. It had however been noticed that the fibre suffered random deflections in conditions where

a classical fluid with the density, viscosity and velocity of the normal fluid would not have been turbulent. It was thought that the deflections might be due to vortex lines in the turbulent superfluid striking the fibre, and that the phenomenon should be investigated in more detail.

II

Theory: Superfluid circulation about a fibre

... and each and all
More slowly turned as they were more removed
Numerically from the integral.

(Paradiso XXVIII, 34-36)

3. Interaction of a vortex line with a straight fibre

(a) Introduction

Just as the superfluid circulation about a vortex line is quantized, so is the circulation about a fibre or any solid body which makes the superfluid doubly connected. Such circulation can arise either when the superfluid is created or by subsequent capture of vortex lines from the superfluid. Since vortex lines may be attached to the fibre at various points along its length, with corresponding quantum changes in the circulation about it, the mean circulation over a given length of fibre may be fractional. Further, the circulation about a body which projects into the helium without making it truly doubly connected will behave in a similar way, for a vortex line can continue the circulation from the free end of the projection to the wall of the containing vessel, as shown in figure 3.1.

We shall first consider the interaction between two straight, parallel vortex lines in otherwise undisturbed helium. (Alternatively the analysis applies approximately to the interaction between any two lines of the equilibrium array in rotating helium, the velocity fields of the remainder being smoothed to give solid-body rotation. If many lines are present the omission of two in this process will have negligible effect on the mean angular velocity of the superfluid, which will continue to rotate with the normal fluid). Let the separation of the two vortex lines be $2r$. Then the velocity induced on the axis of one line by the other is $q_t = \kappa/2r$ in a direction normal to the plane

containing both lines. In the absence of normal fluid the lines would circle each other with this velocity. If on the other hand they were both bound at rest in the helium, for example by being centred on fine fibres, a Magnus force would act on each given by

$$\underset{\sim}{f} = 2\pi\rho_s \underset{\sim}{q_{vt}} \times \underset{\sim}{\kappa} \quad \text{per unit length,} \tag{3.1}$$

where $2\pi\underset{\sim}{\kappa}$ is the vector circulation about either vortex line. This force is repulsive when the circulations are in the same sense.

In practice a vortex line is neither completely bound nor completely free, for the normal fluid exerts upon a moving line a viscous drag $\underset{\sim}{p}$ per unit length, which gives rise to an extra drift velocity $\underset{\sim}{\delta q_v}$, given by

$$\underset{\sim}{p} = 2\pi\rho_s \underset{\sim}{\delta q_v} \times \underset{\sim}{\kappa}. \tag{3.2}$$

Set up a cylindrical coordinate system at rest in the helium and with its axis parallel to the vortex lines and lying midway between them (figure 3.2). Then each line is at distance r from the axis and q_{vt} is tangential. Equation (3.2) shows that the radial component of the drag $\underset{\sim}{p}$ leads to a tangential component δq_{v_t} of $\underset{\sim}{\delta q_v}$, that is a change in the apparent magnitude of q_{vt}, while the tangential component of $\underset{\sim}{p}$ leads to a radial component δq_{v_r}. Now

$$\underset{\sim}{p} = -\left(C + [C'/\kappa]\,\underset{\sim}{\kappa}\times\right)\left(\underset{\sim}{q_{vt}} + \underset{\sim}{\delta q_v}\right), \tag{3.3}$$

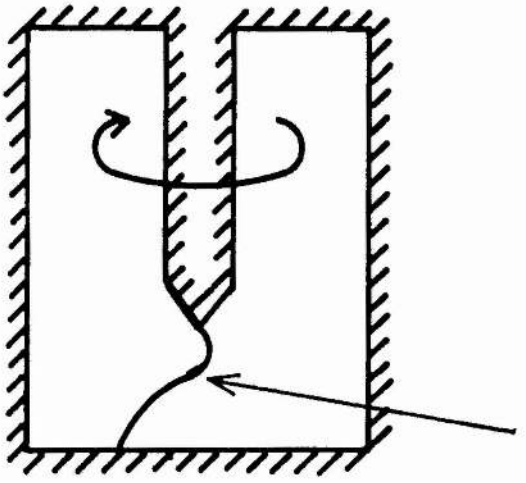

Figure 3.1.
Superfluid circulation about a projection

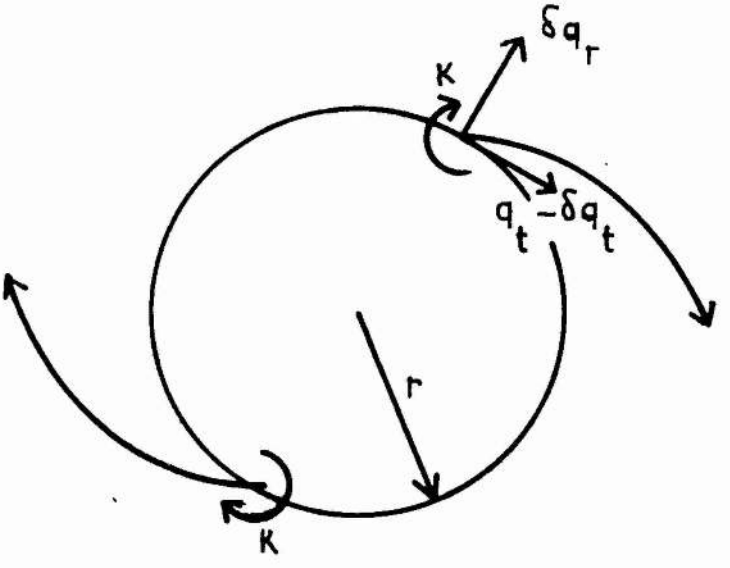

Figure 3.2. Paths of parallel vortex lines under the influence of roton drag

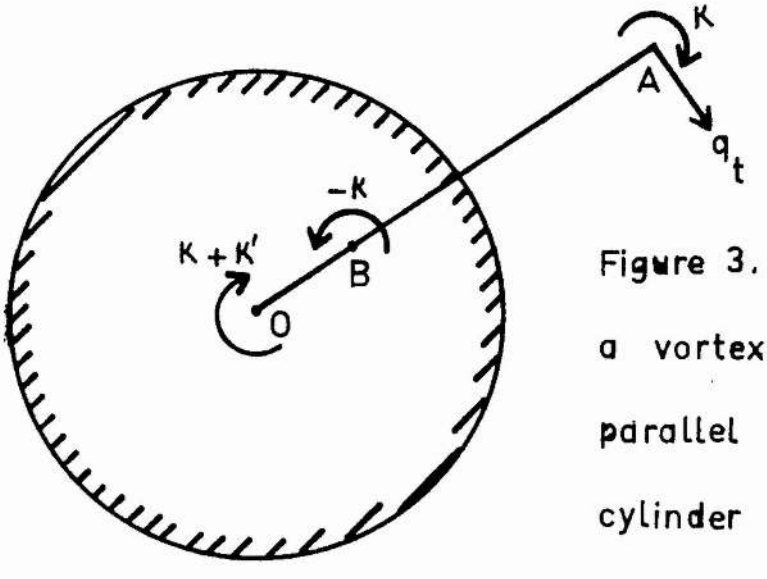

Figure 3.3. Images of a vortex line in a parallel circular cylinder

where C and C' are positive coefficients specifying the drag components in the directions parallel to and normal to the relative velocity of the line and the normal fluid. Therefore

$$2\pi\rho_s \, \delta\underset{\sim}{q} \times \underset{\sim}{\kappa} = -\left(C + [C'/\kappa]\,\underset{\sim}{\kappa}\times\right)\left(\underset{\sim}{q}_t + \delta\underset{\sim}{q}\right). \qquad (3.4)$$

Whence, after some manipulation,

$$\delta q_r / q_t = \frac{2\pi\rho_s \kappa C}{(2\pi\rho_s\kappa - C')^2 + C^2}, \qquad (3.5)$$

where δq_r is taken as positive in the direction of $\underset{\sim}{q}_t \times \underset{\sim}{\kappa}$. This ratio depends on temperature through C, C' and ρ_s, but, if $C' \ll C$, it cannot exceed $\frac{1}{2}$. The value of C, which increases steeply with temperature, is of the order of $2\pi\rho_s\kappa$ at about 1.3°K, while C' is probably no larger than C (Hall 1960), and quite possibly zero (Townsend 1963).

Hence the effect of roton drag is to superimpose an outward radial velocity on the tangential velocity of each vortex line. If the lines had been completely free they would have circled each other with constant separation; if bound, a repulsive Magnus force would have acted between them. The situation in liquid helium is intermediate: under the combined influence of their own velocity fields and of roton drag the lines trace out spiral paths away from each other, as shown in figure 3.2.

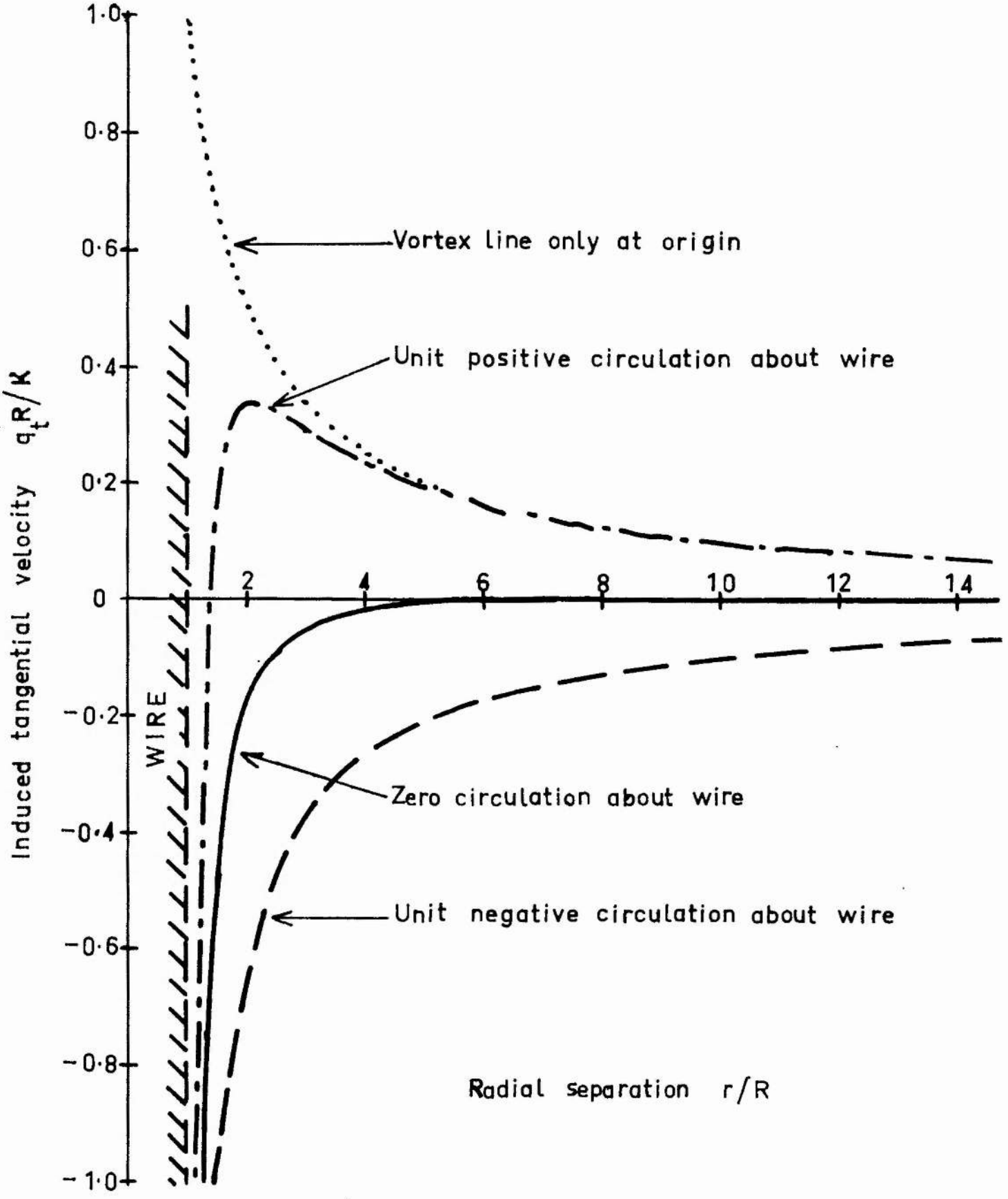

Figure 3.4. Induced tangential velocity of a vortex line parallel to a circular wire of radius R

(b) The interaction between a fibre and a parallel vortex line

If a long, straight fibre of circular cross-section is immersed in the helium, the interaction which occurs between it and a parallel vortex line can be determined by an image method. The axis of the fibre is taken as the axis of a cylindrical coordinate system.

Let the superfluid circulation about the fibre be $2\pi\kappa'$, the radius of the fibre be R, and the radial distance OA of the vortex line from the axis be r. Then the image system is as shown in figure 3.3, where $OB = d = R^2/r$ (Milne-Thomson 1960, p.362). Hence the induced radial velocity of the vortex line in the absence of normal fluid is

$$q_t = \frac{\kappa + \kappa'}{r} - \frac{\kappa}{r - d}$$

$$= \frac{\kappa + \kappa'}{r} - \frac{\kappa r}{r^2 - R^2} . \qquad (3.6)$$

If there is no circulation about the fibre, $\kappa' = 0$, and so

$$q_t = \frac{-\kappa R^2}{r\left(r^2 - R^2\right)} , \qquad (3.7)$$

the negative sign showing that it is in the opposite direction to that which would be induced by a circulation about the origin in the same sense as the vortex line. The variation of q_t with r is shown in figure 3.4. From equation (3.4) δq_r is directed inwards, and so the path of the line is a spiral towards the fibre with the same ratio

$\delta q_r / q_t$ as that in (a). After a certain time it is annihilated at the surface of the fibre, about which unit circulation simultaneously appears.

In the case that there is unit circulation about the fibre in the opposite sense to that about the vortex line $\kappa' = -\kappa$, and

$$q_t = \frac{-\kappa r}{r^2 - R^2} . \qquad (3.8)$$

This function is shown in figure 3.4. Its negative sign indicates that the vortex line follows a spiral path towards the fibre, where it is captured with the annihilation of the circulation.

Finally, let the fibre have unit positive circulation about it $\left(\kappa' = \kappa \right)$. Then

$$q_t = \frac{2\kappa}{r} - \frac{\kappa r}{r^2 - R^2}$$

$$= \frac{\kappa \left(r^2 - 2R^2 \right)}{r \left(r^2 - R^2 \right)} \quad \text{(figure 3.4)} \qquad (3.9)$$

Therefore $q_t < 0$ for $R < r < \sqrt{2}R$

and $q_t > 0$ for $r > \sqrt{2}R$ (3.10)

So a line within $\sqrt{2}R$ of the axis of the fibre would be captured, making a total of two quanta of circulation, while beyond this critical

distance it would be repelled. Asymptotically for large r, $q_t \sim \kappa / r$, which is identical with the velocity field of a vortex line lying on the axis. For small r, when the fibre itself is more important than the circulation about it, the induced velocity is reversed.

(c) The stability of a completely attached quantum of circulation

The induced tangential velocity q_t of an ideal vortex line becomes infinite (negative in our sign convention) as it approaches the surface of the fibre. A real vortex line has a finite core, inside which the velocity is not defined, or there is perhaps distributed vorticity. $|q_t|$ therefore reaches an upper limit, which may be written as $\kappa / 2\delta$, the induced velocity of an ideal line at distance δ from the surface, if $\delta \ll R$. We expect $\delta \sim a_0$, an estimate consistent with the energy calculations of appendix II. The quantum-mechanical details of the capture or loss process will not be considered. If we assume that, in the loss process, a vortex line is first formed in the fluid at the surface of the fibre, it will immediately be recaptured unless its motion through the normal fluid is reversed. Since the normal fluid is bound to the fibre by viscosity near the surface, the line can escape only if the superfluid is streaming past the fibre with a local velocity greater than $\kappa / 2\delta$. Hence the criterion for loss is, in order of magnitude,

$$q_s > \kappa / 2a_0 , \qquad (3.11)$$

where q_{v_s} is the component normal to the fibre of the relative velocity of fibre and superfluid. An estimate of a_0 can therefore be obtained in principle by measurement of the minimum value of q_{v_s} needed to cause loss of a completely attached quantum of circulation.

Since (3.11) is independent of R, it applies to the creation of a vortex line at any solid boundary with radius of curvature large compared with a_0. If a_0 is of the order of the interatomic spacing, the criterion is satisfied for almost any surface (unless roughness on an atomic scale is important). Hence the critical superfluid velocity for the creation of vortex lines at a solid boundary is

$$q_{v_s} \sim \kappa / 2a_0$$

$$\doteq 10^3 \text{ cm/sec with } a_0 = 10^{-7} \text{ cm.} \qquad (3.12)$$

(d) The capture of vortex lines from moving superfluid

In stationary superfluid the induced velocity q_{v_t} of a vortex line lying parallel to a straight fibre is given by equation (3.6). If the superfluid is given a stream velocity $\underset{\sim}{v}_s$ relative to the fibre the vortex-line velocity will be, neglecting normal-fluid drag,

$$\underset{\sim}{q}_{v_l} = \underset{\sim}{q}_{v_t} + \underset{\sim}{v}_s^{*}. \qquad (3.13)$$

$\underset{\sim}{v}_s^{*}$, the local superfluid velocity, is equal to $\underset{\sim}{v}_s$ far from the

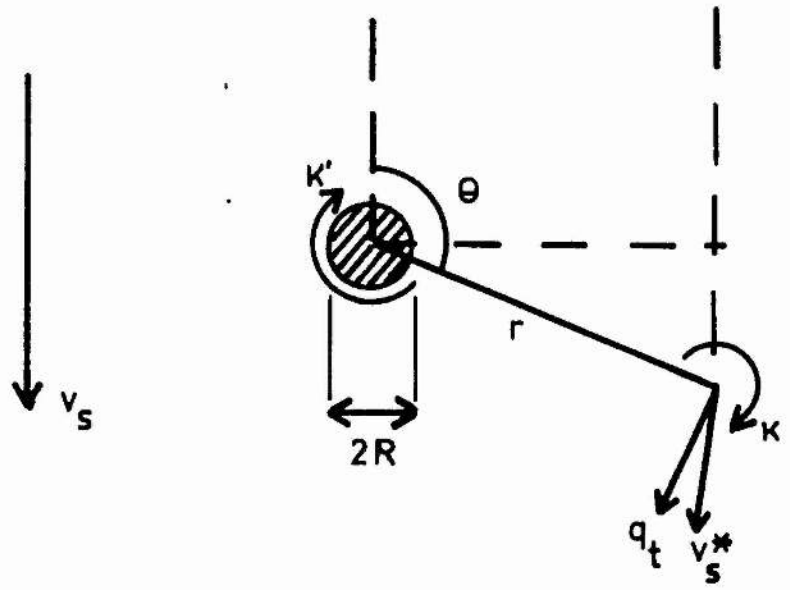

Figure 3.5. Coordinate system for path of vortex line past fibre in superfluid stream

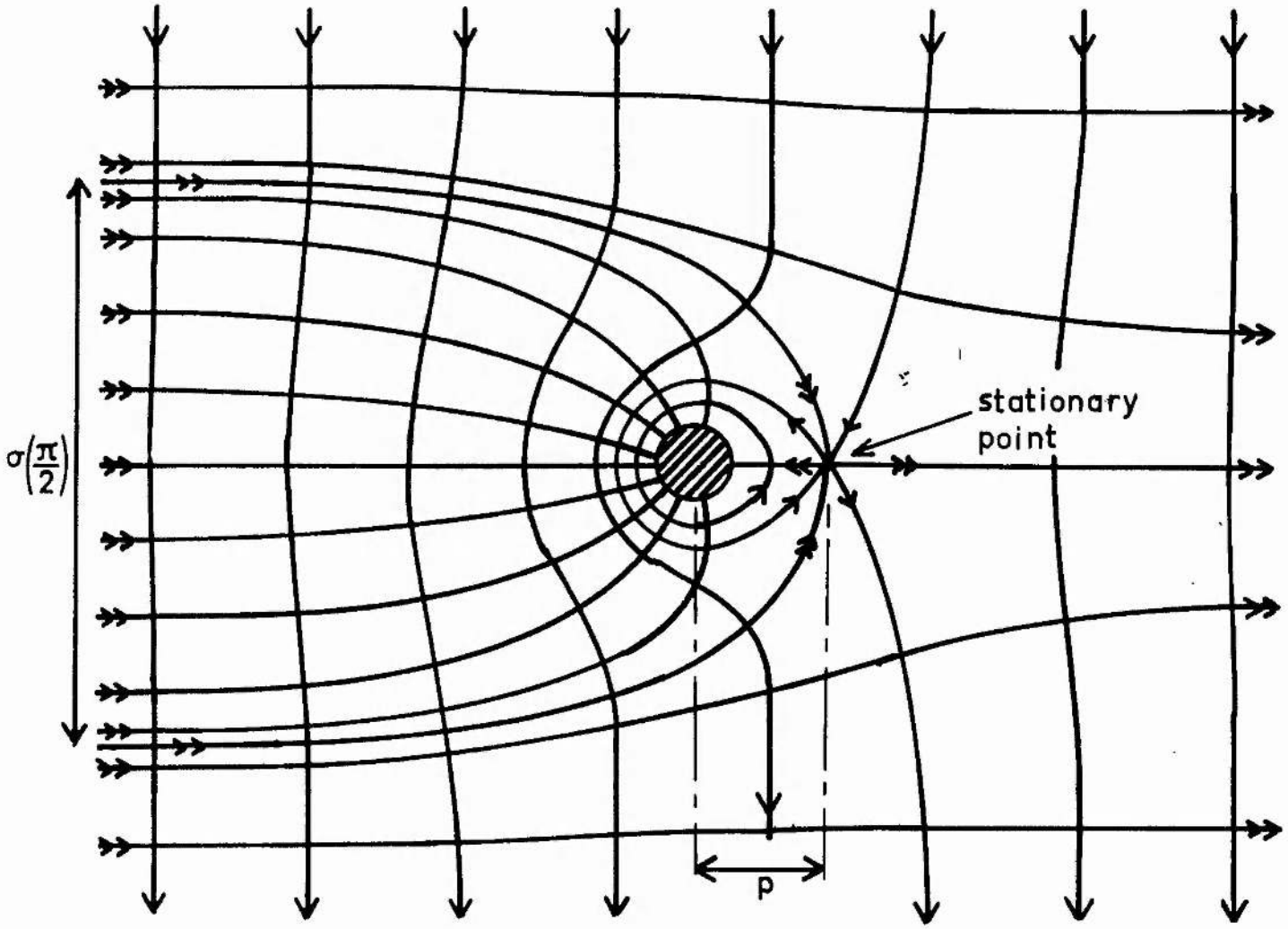

Figure 3.6. Paths of a vortex line past fibre with $\kappa' = 0$; ⟶ χ - lines ($\varepsilon = 0$), ⟶⟶ path lines for $\varepsilon = \pi/2$

perturbing effect of the fibre. The path of the vortex line in the absence of normal fluid (Milne-Thomson 1960, p.365) is given by

$$\chi = -v_s\left(r - R^2/r\right)\sin\theta + \kappa' \ln r - \tfrac{1}{2}\kappa \ln\left(1 - R^2/r^2\right)$$

$$= \text{constant}, \qquad (3.14)$$

where the variables are as shown in figure 3.5. Suppose for simplicity that there is no circulation about the fibre $(\kappa' = 0)$. Then on one side of the fibre $\underset{\sim}{q_{l_t}}$ and $\underset{\sim}{v_s}^*$ are in the same direction, while on the other side they are opposed. At the point where they are equal and opposite the vortex line would be stationary. Without solving (3.14) the form of the lines of constant χ is seen to be as in figure 3.6.

Since no χ-line touches the surface of the fibre, except the one which wholly coincides with it, no vortex line can be captured in the absence of normal fluid. We know from § (a) that the presence of stationary normal fluid will add a drift velocity $\underset{\sim}{\delta q}$ to $\underset{\sim}{q_l}$, and that $\delta q \perp q_l$, the angle between the two velocities being fixed. Hence the path of the vortex line will cut the χ-lines at a constant angle ε given by

$$\varepsilon = \tan^{-1}\frac{\delta q_p}{q_l - \delta q_l}, \qquad (3.15)$$

where $\delta q_{\parallel}$ and δq_{ρ} are the components of δq parallel and perpendicular respectively to $q_{\parallel}$. If $\varepsilon = 0$ the χ-lines and path lines coincide and no vortex line is captured by the fibre.

In the limit $\varepsilon = \frac{\pi}{2}$ the capture diameter $\sigma\left(\frac{\pi}{2}\right)$ can be estimated from figure 3.6, where some typical path lines are drawn for this value of ε (with the correct sign). Clearly $\sigma\left(\frac{\pi}{2}\right)$ is related to ρ, the distance of the stationary point from the axis of the fibre. We guess that

$$\sigma\left(\frac{\pi}{2}\right) \sim 2\rho \quad . \tag{3.16}$$

As ε varies from 0 to $\pi/2$, $\sigma(\varepsilon)$ varies smoothly from 0 to $\sigma\left(\frac{\pi}{2}\right)$, and it is therefore natural to interpolate from the formula

$$\sigma(\varepsilon) \sim 2\rho \sin\varepsilon \qquad \left(0 \leqslant \varepsilon \leqslant \frac{\pi}{2}\right). \tag{3.17}$$

ρ is given by

$$q_t(\rho) = v_s^*$$

$$\doteq v_s \text{ for } \rho \gg R. \tag{3.18}$$

With $K' = 0$, $q_t = \dfrac{\kappa R^2}{r(r^2 - R^2)}$ by eq. (3.7),

$$\doteq \frac{\kappa R^2}{r^3} \quad \text{for} \quad r \gg R \ . \tag{3.19}$$

Therefore

$$\rho \doteq \left(\frac{\kappa R^2}{v_s}\right)^{\frac{1}{3}}, \tag{3.20}$$

provided

$$\rho \gg R \ ,$$

that is

$$v_s \ll \kappa / R \ .$$

Therefore the diameter for capture of a single quantum is

$$\sigma_1(\varepsilon) \sim 2\left(\frac{\kappa R^2}{v_s}\right)^{\frac{1}{3}} \sin\varepsilon \ , \tag{3.21}$$

for

$$v_s \ll \kappa / R \ .$$

If the circulations about fibre and vortex line are equal and opposite $(K' = -\kappa)$, the χ-lines are topologically unaltered, but ρ is now given by

$$v_s^* = \frac{\kappa\rho}{\rho^2 - R^2} \quad \text{(see equation (3.8))} \tag{3.22}$$

that is

$$v_s \doteq \kappa/\rho \quad \text{for} \quad \rho \gg R \ ,$$

or $$p \doteq \kappa / v_s \quad \text{for} \quad v_s \ll \kappa / R . \tag{3.23}$$

Therefore the capture diameter for annihilation of an established quantum of circulation is

$$\sigma_0(\varepsilon) \sim \frac{2\kappa}{v_s} \sin \varepsilon , \tag{3.24}$$

for $$v_s \ll \kappa / R .$$

As $v_s \to \infty$, $p \to R$ in both cases. Hence in the opposite limit $(v_s \gg \kappa / R)$

$$\sigma_1(\varepsilon) \sim \sigma_2(\varepsilon) \sim 2R \sin \varepsilon . \tag{3.25}$$

If there are equal circulations in the same sense about fibre and vortex line, the behaviour is quite different. We know that

$$q_t = \frac{\kappa (r^2 - 2R^2)}{r (r^2 - R^2)} \quad \text{by eq. (3.9).}$$

This function is shown in figure 3.4. For $v_s \ll \kappa / R$ there are three roots to the equation

$$v_s^* = | q_t (p) | \tag{3.26}$$

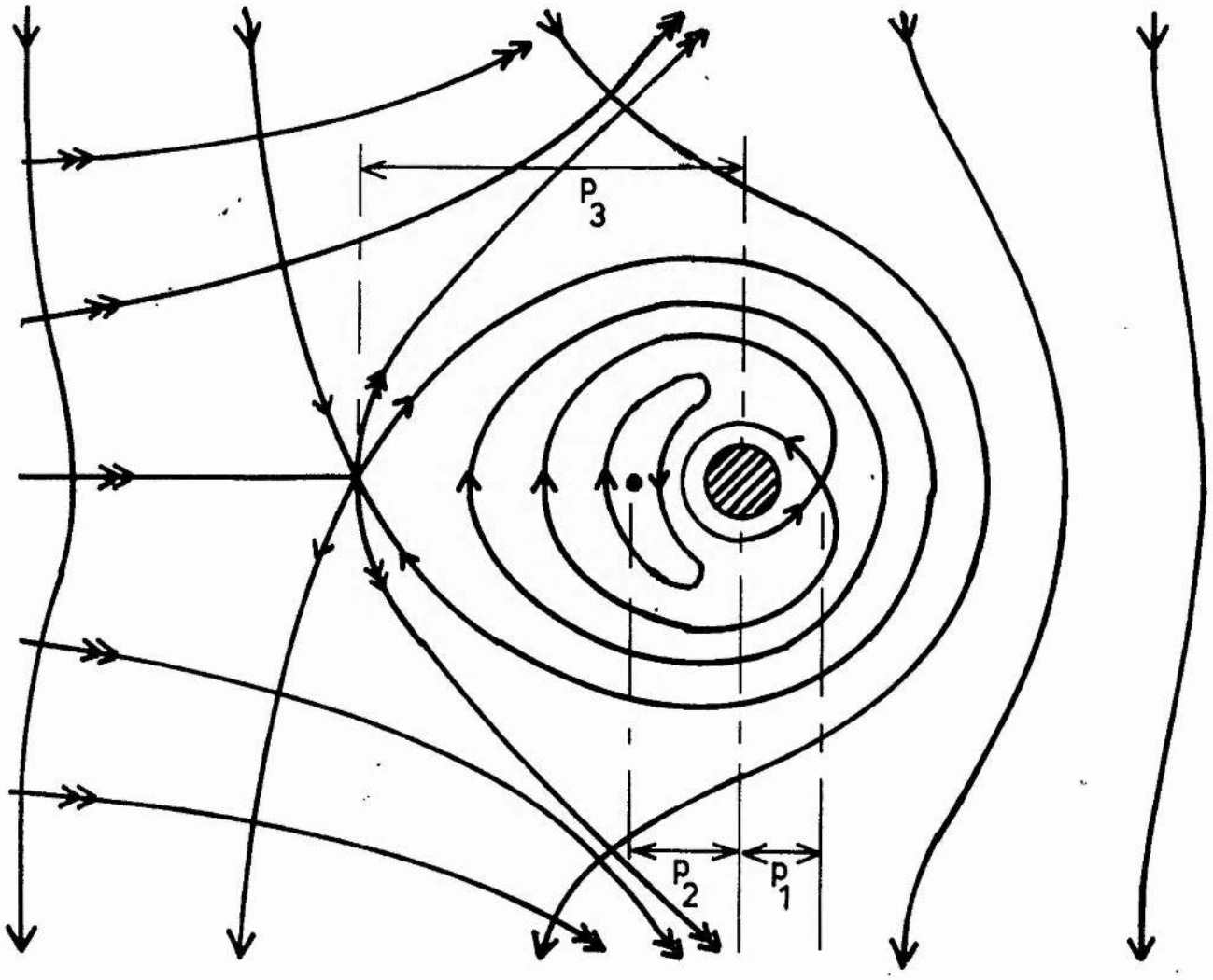

Figure 3.7. Paths of a vortex line past fibre with $\kappa' = +\kappa$;

——→—— X-lines, ——»—— path lines for $E = \pi/2$

and correspondingly three stationary points, of which the nearest to the fibre is on the opposite side of it to the other two. The χ-lines have the form shown in figure 3.7, where the path lines for the case $\varepsilon = \frac{\pi}{2}$ are also drawn. Hence

$$\sigma_2\left(\frac{\pi}{2}\right) = 0 \quad \text{for} \quad V_s \ll K/R . \tag{3.27}$$

This result is true for all ε in the first quadrant.

As V_s increases P_1 and P_2 move together and eventually coincide at $r \doteq 2R$, when

$$V_s^{*}\left(P_{1,2}\right) = \left(q_t\right)_{max}$$

$$\doteq K/3R . \tag{3.28}$$

If V_s is further increased there remains a single root $\left(P_1\right)$ to equation (3.26), the topology of the χ-lines changes to that of the cases $K' = 0$ and $K' = -K$, and $\sigma_2\left(\frac{\pi}{2}\right)$ begins to rise from zero. Replacement of V_s^{*} by V_s gives as an estimate of the critical superfluid velocity for the capture of a second vortex line

$$V_c \sim K/3R . \tag{3.29}$$

As $V_s \to \infty$, $\sigma_2(\varepsilon) \to 2R \sin\varepsilon$, but remains smaller than $\sigma_1(\varepsilon)$

and $\sigma_0(\varepsilon)$. Its behaviour as a function of v_s in the three cases studied is sketched in figure 3.8.

The value of ε can in principle be found as a function of temperature from equation (3.4). Although the coefficients C and C' are not known exactly, ε is probably of the order of 30° or 45° at temperatures between 1°K and the λ-point, so that $\sin\varepsilon$ may reasonably be taken as unity.

In a counterflow experiment the normal fluid is not stationary but moving with such a velocity that there is no net mean mass transfer. At low temperatures its velocity is many times greater than that of the superfluid and the resulting roton drag on the vortex line leads to a large extra contribution to the drift velocity of the line through the superfluid, δq . Far from the fibre the local velocities v_n^* and v_s^* are oppositely directed (in non-turbulent flow) and so the path of the vortex cuts the χ-lines at a larger angle ε than when the normal fluid is stationary. ε may even exceed $\frac{\pi}{2}$ radians. Very close to the fibre the normal fluid is held at rest by viscosity, and so the final stages of capture are independent of its stream velocity. At distances of order ρ from the fibre, where the capture or loss of the vortex line is decided, ε is a complicated function of position.

If the contribution δq_n to the drift velocity from the motion of the normal fluid is small compared with q_l when $r \sim \rho$, then the above analysis will remain correct. Clearly a sufficient condition for this is that $v_n \ll v_s$, where v_n is the stream velocity of the

normal fluid. This condition is satisfied in a counterflow experiment only very close to the λ-point. Alternatively ρ must be close enough to R to lie in the region where the normal fluid is held at rest by viscosity.

At temperatures low enough for v_n to be very much greater than v_s we have

$$\delta q_n \gg v_s^* \qquad (3.30)$$

everywhere except very close to the fibre. In this case the motion of the vortex line will be dominated, through δq_n, by v_n rather than by v_s. From the qualitative picture obtained by replacing v_s in the above analysis by δq_n we see that the main effect of the normal-fluid motion is to increase the effective value of v_s and to make the vortex lines drift in a direction quite different from that of the superfluid stream. This leads to problems in the maintenance of superfluid vorticity (Townsend 1963; see also chapter 2(b)).

(e) <u>The probability distribution of the mean circulation about a fibre</u>

In the experiment the circulation was measured about a fibre of diameter 0.7 μ, for which $K/R \doteq 5$ cm/sec. By (3.29) $v_c \sim 2$ cm/sec, which is greater than both normal-fluid and superfluid velocities in the experimental conditions where circulation was measurable. Hence $\sigma_2 = 0$, and no circulation greater than one quantum should have been observed if the vortex-line hypothesis is correct.

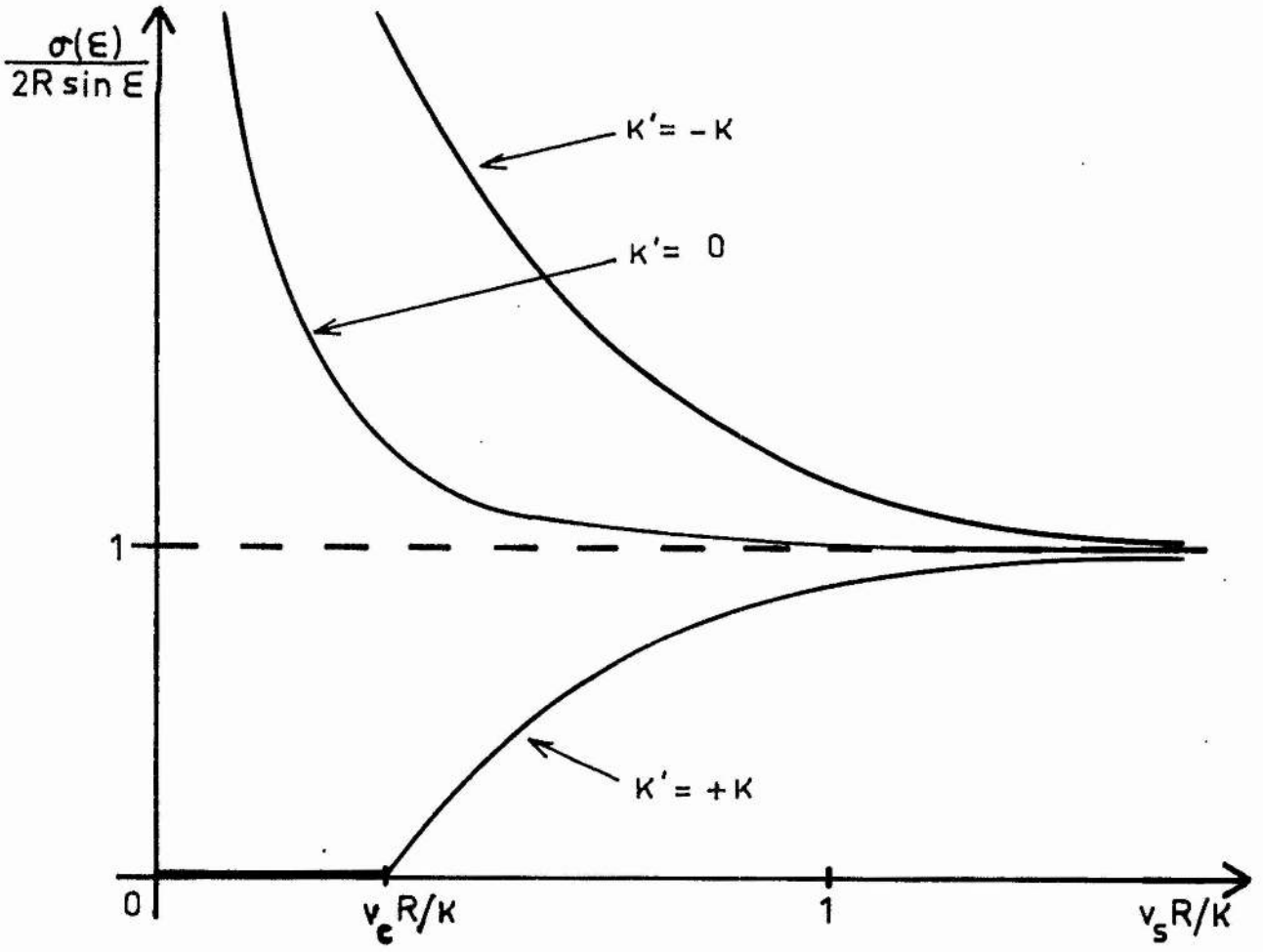

Figure 3.8. Sketch of the variation of capture diameter with superfluid stream velocity for various circulations about fibre

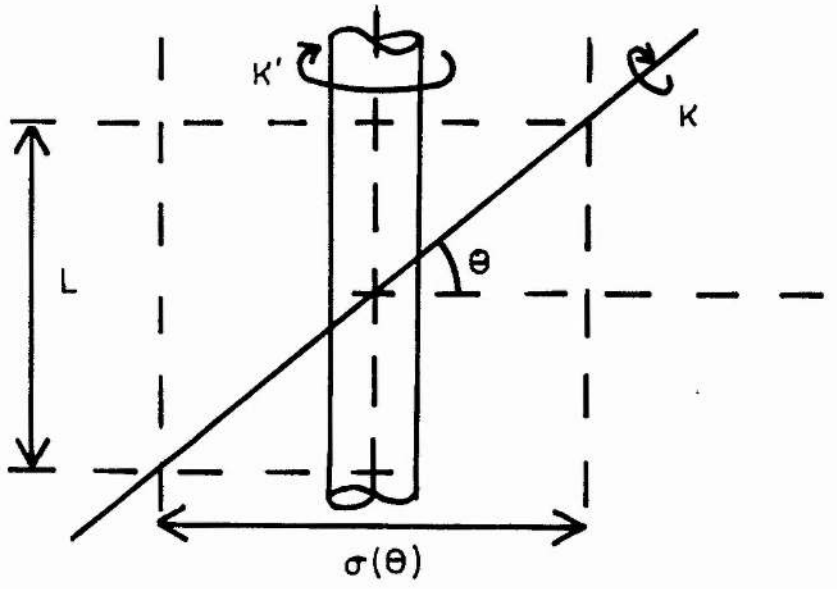

Figure 3.9. Capture of a vortex line inclined to the fibre

At such low velocities κ_0 is considerably larger than κ_1 (see figure 3.8). The a priori probability of the annihilation of established circulation is therefore considerably greater than that of the capture of fresh circulation. It is immediately clear that in a stream of randomly orientated vortex lines large mean circulations (approaching one quantum) are likely to exist for significant times only if vortex lines are sufficiently rare for annihilation to be an infrequent process. In order to proceed further the interaction between the fibre and an inclined vortex line must be considered.

Suppose that an inclined vortex line is carried towards the fibre as shown in an idealised form in figure 3.9. It eventually cuts the fibre at some point, and a length L of it is captured, the two remaining portions of free vortex line being attached to the fibre at points distance L apart. These points of attachment may then move along the fibre. It is shown in appendix II that in certain conditions vortex lines partly attached to the fibre in this way are metastable, but that these conditions can hardly be fulfilled in the experimental geometry when the helium is stationary, and hence even less so when it is moving. Nevertheless it does seem that the peeling of a partly attached vortex line on or off the fibre may be a slow process, so that we can sensibly refer to the capture of a given length L of vortex line.

From figure 3.9, L can be written as $\sigma^*/|\tan\theta|$, where σ^* is an appropriate capture diameter. Because the interaction between an

inclined vortex line and a fibre is less strong than when they are parallel, we guess that

$$\sigma^* \sim \sigma_{0,1,2} \left| \sin\theta \right| , \qquad (3.31)$$

where $\sigma_{0,1,2}$ is the appropriate capture diameter from (d). Hence

$$L \sim \sigma_{0,1,2} \left| \sin\theta \tan\theta \right| . \qquad (3.32)$$

This function is so sharply peaked at $|\theta| = \frac{\pi}{2}$ that, to a first approximation, only vortex lines which are very nearly parallel to the fibre can significantly alter the circulation about it. The captured length of such vortex lines is limited in the first place by the length of the fibre itself, and in the second place by the curvature of the vortex lines, which are likely to be straight only over distances of the order of λ, the mean separation of the lines, or of the tunnel width if that is smaller. Therefore, if there are so few vortex lines in the flow that λ is large compared with the tunnel width and the length of the fibre, we may expect occasionally to capture a length L of vortex line which is a fair fraction of the length of the wire. Mean circulations of up to one quantum are possible (larger circulations being forbidden because $\sigma_1 = 0$ in the experimental conditions) and will grow or decay as the vortex line peels on or off the fibre. They may eventually be annihilated by the capture of a vortex line of opposite sense.

If λ is much smaller than the length l of the fibre we may suppose that circulation is captured in short lengths of exactly λ. We take as the idealized structure of the circulation about the fibre a number $N = l/\lambda$ of statistically independent lengths λ, about each of which the circulation may be clockwise ($+2\pi\kappa$), anti-clockwise ($-2\pi\kappa$) or zero, with probabilities $\frac{\sigma_1}{2\sigma_1+\sigma_0}$, $\frac{\sigma_1}{2\sigma_1+\sigma_0}$ and $\frac{\sigma_0}{2\sigma_1+\sigma_0}$ respectively, proportional to the relevant capture diameters. This distribution is trinomial, with mean zero and standard deviation approximately $\frac{2\sigma_1}{2\sigma_1+\sigma_0}$. By the central limit theorem the average circulation over the whole wire has a near-normal distribution with mean zero and standard deviation $\left(\frac{2\sigma_1}{2\sigma_1+\sigma_0}\sqrt{\frac{\lambda}{l}}\right)2\pi\kappa$ for $\lambda \ll l$. Since $2\sigma_1 \ll \sigma_0$ at low velocities, the probability of observing mean circulation approaching one quantum drops rapidly as λ decreases through values comparable with l. The mere observation of such circulations, quite apart from their persistence, is therefore in itself a sign of the presence of few vortex lines.

(f) Summary

A fibre with no circulation about it has a weak attraction for vortex lines, but once circulation is established there is a strong tendency to annihilate it by the capture of lines of opposite sense, together with a tendency to repel lines of the same sense as the circulation about the fibre. Except at relatively high fluid velocities, of the order of 2 cm/sec in the experimental apparatus, circulations greater than one quantum cannot be established. /s well as by

annihilation, circulation can change by the peeling of a partly attached vortex line on or off the fibre. A wholly attached quantum of circulation cannot be removed bodily from a fibre except by superfluid flow of very high velocity, of the order of 10^3 cm/sec.

When the separation of the vortex lines is much larger than the length of the fibre, slowly-changing mean circulations of up to one quantum should be observable, while when it is smaller than the length of the fibre the mean circulation should be smaller and more rapidly varying.

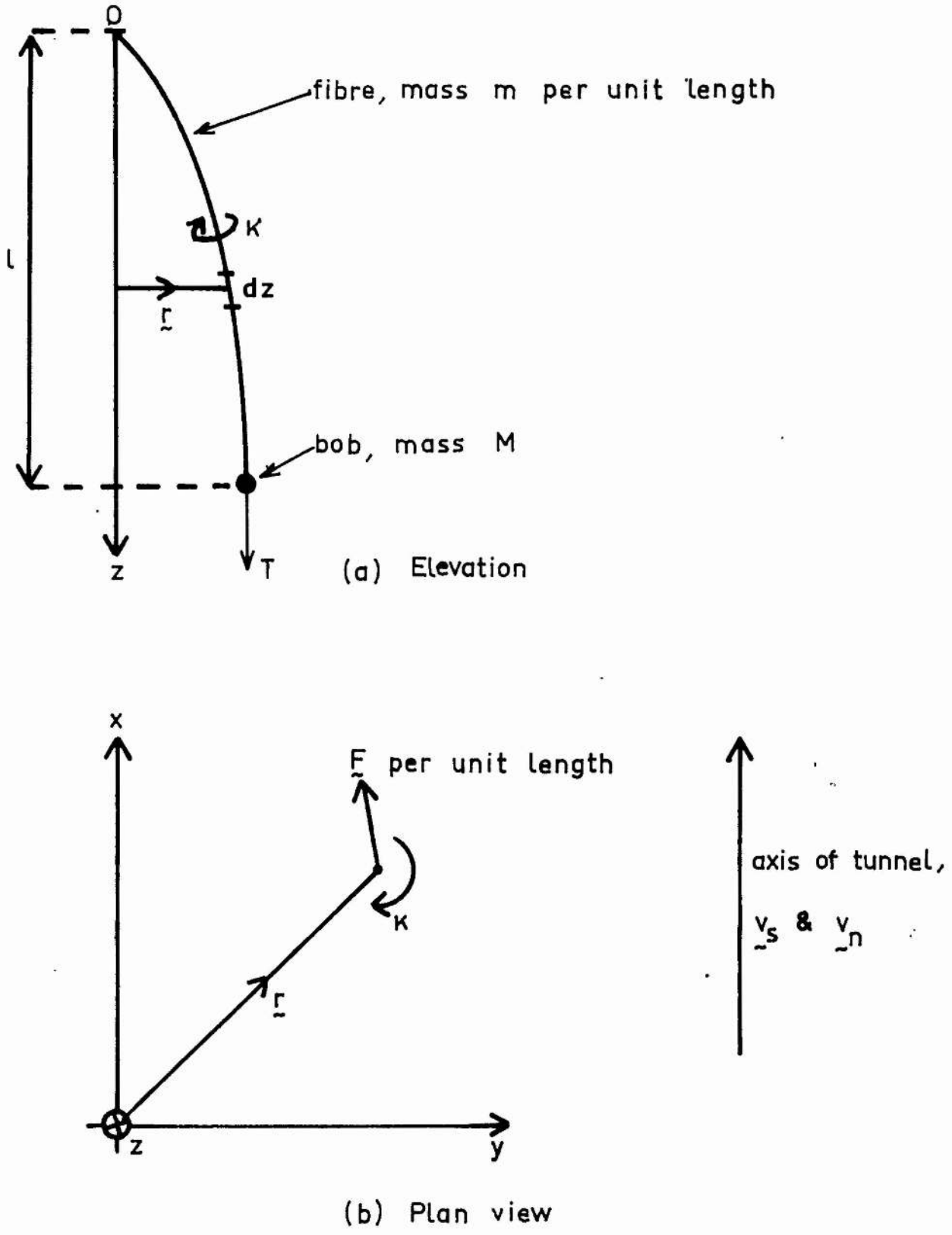

Figure 4.1. Coordinate system for calculation of transient fibre response

4. Response of a fibre carrying superfluid circulation to a heat pulse

(a) The solution of the equation of motion of the fibre

When superfluid is made to stream with velocity $\underset{\sim}{v_s}$ past a fibre carrying circulation $2\pi\underset{\sim}{\kappa}$, a Magnus force acts upon the fibre given by

$$\underset{\sim}{F} = 2\pi\rho_s \underset{\sim}{v_s} \times \underset{\sim}{\kappa} \quad \text{per unit length,} \tag{4.1}$$

If the fibre is suspended vertically with a weighted bob at its lower end as shown in figure 4.1, the force can be detected by the deflection of the bob, which will also respond to the viscous drag of the normal fluid. Neglecting the stiffness and weight of the fibre, a uniform, steady force F per unit length produces a steady bob deflection given by

$$y = \frac{Fl^2}{2T}, \tag{4.2}$$

where l is the length of the fibre and T is the tension provided by the bob. The configuration of the fibre is a quadratic curve, and the bob deflection is normal to the superfluid velocity in the case of a Magnus force, but in the direction of the normal-fluid velocity for a viscous force.

The response of the fibre to a varying force is more difficult to calculate, because its flexibility precludes treatment as a simple pendulum. With the coordinate system of figure 4.1 the equation of motion

of a length element dz of the fibre is

$$\underset{\sim}{F}\,dz + T\frac{\partial^2 \underset{\sim}{r}}{\partial z^2}\,dz = \ddot{\underset{\sim}{r}}\,m\,dz \quad , \tag{4.3}$$

where m is the effective mass per unit length of the fibre, and the force $\underset{\sim}{F}$ per unit length acting on it is given by

$$\underset{\sim}{F} = B\left(\underset{\sim}{v}_n - \dot{\underset{\sim}{r}}\right) + \frac{D}{\kappa}\left(\underset{\sim}{v}_s - \dot{\underset{\sim}{r}}\right) \times \underset{\sim}{\kappa} . \tag{4.4}$$

B and D are coefficients characterising the viscous and Magnus forces respectively, and $\underset{\sim}{v}_n$ and $\underset{\sim}{v}_s$ are the externally imposed, time-dependent velocities of the normal and superfluid components. Hence

$$m\ddot{\underset{\sim}{r}} + B\dot{\underset{\sim}{r}} + \frac{D}{\kappa}\left(\dot{\underset{\sim}{r}} \times \underset{\sim}{\kappa}\right) - T\frac{\partial^2 \underset{\sim}{r}}{\partial z^2} = B\underset{\sim}{v}_n + \frac{D}{\kappa}\left(\underset{\sim}{v}_s \times \underset{\sim}{\kappa}\right). \tag{4.5}$$

In a counterflow wind tunnel $\underset{\sim}{v}_n$ and $\underset{\sim}{v}_s$ are anti-parallel. For simplicity we take them both to be conventionally in the positive x-direction. We shall require the response of the fibre to a short square velocity pulse of height v_n, v_s and length τ. This may be written approximately:

$$v_n(t) = v_n \tau\, \delta(t) \tag{4.6}$$

and similarly for v_s. Remembering that $\underset{\sim}{\kappa}$ is in the positive

z-direction, (4.5) may now be resolved into two simultaneous, scalar differential equations as follows:

$$\left.\begin{aligned} m\ddot{x} + B\dot{x} + D\dot{y} - T\frac{\partial^2 x}{\partial z^2} &= Bv_n\tau\,\delta(t) \\ m\ddot{y} + B\dot{y} - D\dot{x} - T\frac{\partial^2 y}{\partial z^2} &= -Dv_s\tau\,\delta(t) \end{aligned}\right\} \qquad (4.7)$$

Taking Laplace transforms with the boundary condition $x = y = 0$ at $t = 0$ for all z, and solving for the transformed transverse displacement $Y(p)$, we obtain

$$Y\left[\left(mp^2 + Bp - T\frac{\partial^2}{\partial z^2}\right)^2 + D^2p^2\right] = -Dv_s\tau\left(mp^2 + Bp\right) + Bv_n\tau Dp, \qquad (4.8)$$

where we have assumed that D, i.e. the circulation, is independent of z. Apart from the term D^2p^2Y on the left hand side Y is proportional to D, and so the transverse displacement is a measure of the Magnus force, and hence of the circulation.

The first term on the right hand side is the direct contribution from the superfluid pulse; the second arises because the fibre is dragged with the normal fluid, and so the relative velocity between fibre and superfluid is increased, v_n and v_s being anti-parallel. The terms $\left(mp^2 + Bp - T\frac{\partial^2}{\partial z^2}\right)Y$ lead to damped oscillations of the

fibre, while the term D^2p^2Y arises because the plane of the oscillations precesses under the influence of the Magnus force. If the circulation is small enough $D^2 \ll B^2$, i.e. the period of precession is much longer than the decay time of the oscillations, and the precession may be neglected. Although this approximation is not a good one if the circulation is near one quantum, particularly at low temperatures, it will be used because the labour of numerical calculation is then very much reduced, the form of $y(t)$ (but not its amplitude) being then independent of the size of the circulation at a given temperature.

In the easier case of a rigid simple pendulum it has been verified that the main effect of the term D^2p^2Y is to lengthen the apparent period of the oscillations and to reduce the apparent damping. The size of the initial transient deflection is reduced by 10% or 20%. It is probable that the precession would have a similar effect in the full calculation.

The simplified equation, valid in the limit of small circulation, is

$$T\frac{\partial^4 Y}{\partial z^4} - 2m\rho T\left(p + \frac{B}{m}\right)\frac{\partial^2 Y}{\partial z^2} + m^2p^2\left(p + \frac{B}{m}\right)^2 Y = -Dv_s\tau m\rho\left(p + \frac{B}{m}\left[1 - e^*\right]\right), \quad (4.9)$$

where $e^* = v_n / v_s$, with regard to sign.

This has the solution

$$Y = P + Qe^{\mu z} + Re^{-\mu z} , \qquad (4.10)$$

where $$P = \frac{-Dv_s\tau\left(p + \frac{B}{m}\left[1 - e^{*}\right]\right)}{mp\left(p + \frac{B}{m}\right)^2} ,$$

$$\mu = \sqrt{\frac{mp}{T}\left(p + \frac{B}{m}\right)} ,$$

and Q and R are to be determined from the boundary conditions:

$$\left.\begin{aligned} &\text{on } z = 0, && y = 0, \text{ i.e. } Y = 0 \\ &\text{on } z = l, && M\ddot{y} = -T\frac{\partial y}{\partial z}, \text{ i.e. } Mp^2Y = -T\frac{\partial Y}{\partial z} \end{aligned}\right\} \qquad (4.11)$$

The boundary condition on $z = l$ is the equation of motion of the bob, neglecting the viscous drag on it.

The solution on $z = l$ is found to be

$$Y(l,p) = \frac{\mu P\left(\operatorname{ch}\mu l - 1\right)}{\mu \operatorname{ch}\mu l + \frac{p^2M}{T}\operatorname{sh}\mu l} . \qquad (4.12)$$

By the inversion theorem (Jaeger 1951) the untransformed, transverse deflection of the bob is given by

$$y(l,t) = \sum_{\alpha_n}\left[\frac{\mu P\left(\operatorname{ch}\mu l - 1\right)}{\frac{d}{dp}\left(\mu \operatorname{ch}\mu l + \frac{p^2M}{T}\operatorname{sh}\mu l\right)}\right]_{p=\alpha_n} \cdot e^{\alpha_n t} \qquad (4.13)$$

where $p = \alpha_n$ gives the singularities of $Y(l,p)$ in the complex p-plane.

Remembering that μ and P are functions of p, we find that $Y(l,p)$ remains finite as $p \to 0$, but that at $p = -B/m$ there is a singularity which leads to the contribution to $y(l,t)$

$$y^*(l,t) = Dv_s \tau \frac{B}{m} e^{*\frac{l^2}{2T}} \frac{e^{-Bt/m}}{1 + \frac{B^2 M l}{m^2 T}} . \qquad (4.14)$$

For a light fibre B/m is a frequency or decay constant much higher than any we are interested in, and so we take the limit as $B/m \to \infty$:

$$\lim_{B/m \to \infty} y^*(l,t) = 0 \quad \text{for all} \quad t \geqslant 0. \qquad (4.15)$$

This contribution is therefore neglected.

The remaining singularities are given by the roots of

$$\text{th}\, \mu l = -\mu T / p^2 M . \qquad (4.16)$$

Let $\mu = \mu_n$ when $p = \alpha_n$, so that

$$\left.\begin{aligned} \mu_n &\doteq \left(\frac{B}{T}\alpha_n\right)^{\frac{1}{2}} \quad \text{for} \quad |\alpha_n| \ll B/m \\ &\doteq \left(\frac{m}{T}\right)^{\frac{1}{2}} \alpha_n \quad \text{for} \quad |\alpha_n| \gg B/m \end{aligned}\right\} \qquad (4.17)$$

Let $$\left(\frac{B}{T}\alpha_n\right)^{\frac{1}{2}} l = \mu_n l = \varepsilon + i\delta \qquad (4.18)$$

for $|\alpha_n| \ll B/m$.

Then (4.16) becomes

$$th(\varepsilon + i\delta) = -\frac{B^2 l^3}{MT}\,\frac{1}{(\varepsilon + i\delta)^3} \qquad (4.19)$$

in the limit that $B/m \to \infty$, i.e. for a light fibre.

This equation has solutions with $\varepsilon = 0$ given by

$$\tan\delta = -\frac{B^2 l^3}{MT}\,\frac{1}{\delta^3} \,. \qquad (4.20)$$

In the experimental conditions $\frac{B^2 l^3}{MT} \sim 1$, so that the solutions are

$$\left.\begin{aligned} \delta &\doteq \pi(-)\,,\ 2\pi(-)\,,\ 3\pi(-)\,,\ \ldots) \\ \varepsilon &= 0 \end{aligned}\right\} \qquad (4.21)$$

Since in our present approximation $\alpha_n \propto \mu_n^2$, these singularities of $Y(l,p)$ give non-oscillatory, exponentially decaying contributions to $y(l,t)$ with decay constants

$$\alpha_n = \frac{\pi^2 T}{B l^2}\,,\ \frac{4\pi^2 T}{B l^2}\,,\ \frac{9\pi^2 T}{B l^2}\,,\ \ldots \qquad (4.22)$$

For very large values of δ the approximation $|\alpha_n| \ll B/m$ is no longer valid and so the contributions to $y(l,t)$ are not purely exponential. In the extreme opposite limit, where $B/m \ll \alpha_n \ll \mu_n$, equation (4.16) becomes

$$th\left(\frac{ml^2}{T}\right)^{\frac{1}{2}}\alpha_n = -\left(\frac{mT}{M^2}\right)^{\frac{1}{2}}\frac{1}{\alpha_n}, \qquad (4.23)$$

which has solutions

$$\left(\frac{ml^2}{T}\right)^{\frac{1}{2}}\alpha_n \doteq \pm n\pi i \qquad (4.24)$$

with n a large integer. These almost undamped, oscillatory contributions to $y(l,t)$ are nevertheless not physically important, because their actual amplitude is very small.

In order to find singularities of $Y(l,p)$ with non-zero values of ε, equation (4.19) is separated into real and imaginary parts, giving the simultaneous equations

$$\frac{\frac{1}{\varepsilon}th\varepsilon\left(1+\tan^2\delta\right)}{1+th^2\varepsilon\tan^2\delta} = -\frac{B^2l^3}{MT}\,\frac{\varepsilon^2-3\delta^2}{(\varepsilon^2+\delta^2)^3} \qquad (4.25)$$

$$\frac{\frac{1}{\delta}\tan\delta\left(1-th^2\varepsilon\right)}{1+th^2\varepsilon\tan^2\delta} = \frac{B^2l^3}{MT}\,\frac{3\varepsilon^2-\delta^2}{(\varepsilon^2+\delta^2)^3} \qquad (4.26)$$

These equations are unchanged by the simultaneous reversal of the signs of ε and δ, as we expect since it is only $(\varepsilon+i\delta)^2$ that has

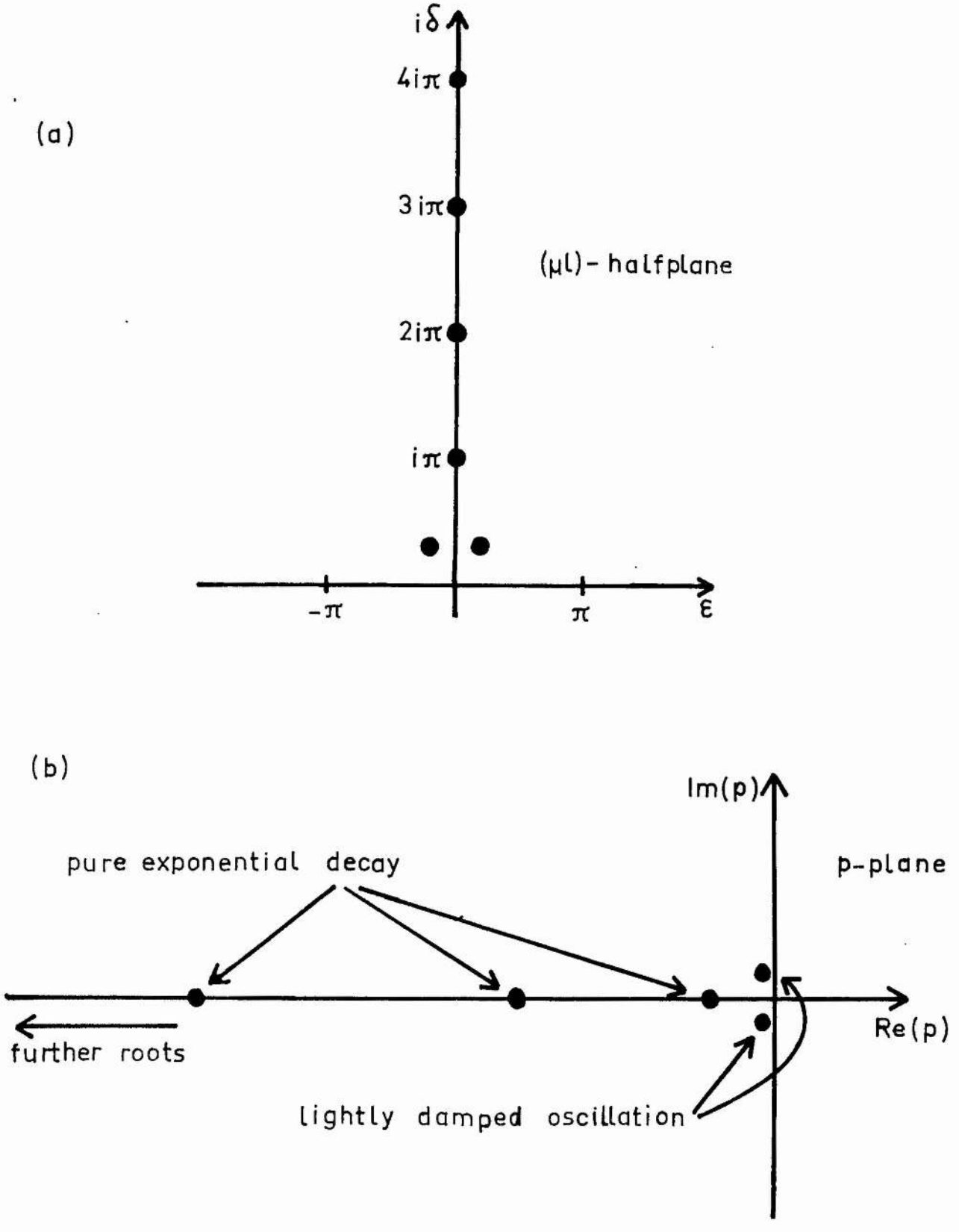

Figure 4.2. Singularities of $Y(l,p)$ in (a) the $\frac{1}{2}$-plane of (μl) (b) the p-plane

physical significance. They are also unchanged if the sign of only one of ε or δ is reversed. Hence if $[\varepsilon, \delta]$ is a solution, so is $[\varepsilon, -\delta]$, and we need look only for positive values. With $\frac{B^2 l^3}{MT} \sim 1$ there is a root with $\varepsilon \neq 0$ and δ near the middle of the interval $(0, \frac{\pi}{2})$. Good analytical approximation is cumbersome, but it can be verified that the first approximation $\varepsilon^2 = \delta^2$ leads to an oscillatory solution with period $\sqrt{2}$ times that of a rigid simple pendulum of the same length. A better approximation can be obtained numerically by an iteration procedure.

There appears to be no further root with ε of similar magnitude but different δ, and no root with smaller but non-zero ε. If ε is large, $\text{th}\,\varepsilon \doteqdot 1$, and so by equation (4.26)

$$3\varepsilon^2 \doteqdot \delta^2 \quad .$$

However, further approximation on this basis leads to the same root as that obtained from $\varepsilon^2 = \delta^2$. The singularities of $Y(l, p)$ which have been found for a light fibre are mapped in the complex half-plane of (μl) in figure 4.2(a). In figure 4.2(b) they are mapped in the complex p-plane, where imaginary parts lead to oscillatory contributions to $y(l, t)$ and real parts to exponential contributions. For a fibre of small but finite mass the series of singularities along the negative real axis of p begins to diverge from that axis near the particular singularity at $p = -B/m$ (see (4.14)) and to wheel back

symmetrically towards the positive and negative imaginary axis as $|p|$ increases.

The only important oscillatory contributions come from the two roots near the origin, which have equal, negative real parts, and equal and opposite imaginary parts. Together they therefore give to $y(l,t)$ a contribution which is a damped sine wave, probably phase-shifted with respect to the zero of time.

(b) The numerical evaluation of the solution

This physically interesting, oscillatory contribution is evaluated as follows. Equations (4.25) and (4.26) are added and subtracted to give the equations

$$\frac{\frac{1}{\varepsilon}\,\mathrm{th}\,\varepsilon\left(1+\tan^2\delta\right)+\frac{1}{\delta}\tan\delta\left(1-\mathrm{th}^2\varepsilon\right)}{1+\mathrm{th}^2\varepsilon\tan^2\delta}=\frac{2B^2l^3}{MT}\,\frac{1}{\left(\varepsilon^2+\delta^2\right)^2} \qquad (4.27)$$

$$\frac{\frac{1}{\varepsilon}\,\mathrm{th}\,\varepsilon\left(1+\tan^2\delta\right)-\frac{1}{\delta}\tan\delta\left(1-\mathrm{th}^2\varepsilon\right)}{1+\mathrm{th}^2\varepsilon\tan^2\delta}=\frac{4B^2l^3}{MT}\,\frac{\delta^2-\varepsilon^2}{\left(\varepsilon^2+\delta^2\right)^3} \qquad (4.28)$$

When B^2l^3/MT has been calculated as a function of temperature for the given experimental conditions, first estimates ε_1 and δ_1 are substituted in the left hand sides of (4.27) and (4.28) to give $\left(\varepsilon_2^2+\delta_2^2\right)^2$ and $\frac{\delta_2^2-\varepsilon_2^2}{\left(\varepsilon_2^2+\delta_2^2\right)^3}$ respectively. ε_2 and δ_2 can then be found and the whole process repeated. This is continued until ε_n and δ_n attain sufficiently stable values. The resulting contribution to $y(l,t)$ is given by

$$y_0(l,t) \propto \exp\left[-\frac{T}{Bl^2}\left(\delta^2-\varepsilon^2\right)t\right]\exp\left[\pm\frac{2T}{Bl^2}\varepsilon\delta\,it\right] \qquad (4.29)$$

with coefficients $\left[\dfrac{\mu P\left(ch\,\mu l - 1\right)}{\dfrac{d}{dp}\left(ch\,\mu l + \dfrac{p^2 M}{T} sh\,\mu l\right)}\right]$ evaluated at

the two singularities.

Now

$$\left[\frac{d}{dp}\left(ch\,\mu l + \frac{p^2 M}{T} sh\,\mu l\right)\right]_{p=\alpha_n}$$

$$= \frac{m}{2\mu_n T}\left(2\alpha_n + B/m\right)\left[1 + \frac{\alpha_n^2 M l}{T}\right] ch\,\mu_n l$$

$$+ \left[\frac{Bl}{2T} + \frac{\alpha_n}{T}\left(ml + 2M\right)\right] sh\,\mu_n l$$

$$\sim \frac{B}{2\mu_n T}\left(1 + \frac{Ml}{T}\alpha_n^2\right) ch\,\mu_n l + \left(\frac{Bl}{2T} + \frac{2M}{T}\alpha_n\right) sh\,\mu_n l \quad (4.30)$$

in the limit as $B/m \to \infty$. From equation (4.10)

$$\lim_{B/m\to\infty} P = -\frac{Dv_s\tau\left(1 - e^*\right)}{Bp}. \quad (4.31)$$

Therefore

$$\left[\mu P\left(ch\,\mu l - 1\right)\right]_{p=\alpha_n} = -\frac{Dv_s\tau\left(1-e^*\right)}{B}\,\frac{\mu_n}{\alpha_n}\left(ch\,\mu_n l - 1\right) \quad (4.32)$$

in this limit.

Substituting for α_n and μ_n from equation (4.18) we find that the coefficients of the exponentials in relation (4.29) are

$$\frac{\left[-2Dv_s\tau\left(1-e^{*}\right)/B\right]\left[ch\left(\varepsilon+i\delta\right)-1\right]}{\left[1+\frac{MT}{B^2l^3}\left(\varepsilon+i\delta\right)^4\right]ch\left(\varepsilon+i\delta\right)+\left[1+\frac{4MT}{B^2l^3}\left(\varepsilon+i\delta\right)^2\right]\left(\varepsilon+i\delta\right)sh\left(\varepsilon+i\delta\right)} \quad (4.33)$$

with $(\varepsilon\delta)$ taking the appropriate sign. This function is even in $(\varepsilon+i\delta)$. Hence it is of the form $F(\varepsilon^2,\delta^2)+i(\varepsilon\delta)G(\varepsilon^2,\delta^2)$; i.e. the sign of the imaginary part but not that of the real part depends on the sign of $(\varepsilon\delta)$. Therefore

$$y_o(l,t)=\exp\left[-\frac{T}{Bl^2}\left(\delta^2-\varepsilon^2\right)t\right]\left\{\begin{array}{l}F(\varepsilon^2,\delta^2)\left[e^{+i\frac{2T}{Bl^2}\varepsilon\delta t}+e^{-\frac{2T}{Bl^2}\varepsilon\delta t}\right]\\ +i(\varepsilon\delta)G(\varepsilon^2,\delta^2)\left[e^{+i\frac{2T}{Bl^2}\varepsilon\delta t}-e^{-i\frac{2T}{Bl^2}\varepsilon\delta t}\right]\end{array}\right\}$$

$$=\exp\left[-\frac{T}{Bl^2}\left(\delta^2-\varepsilon^2\right)t\right]\left[2F\cos\left(\frac{2T}{Bl^2}\varepsilon\delta t\right)-2\varepsilon\delta G\sin\left(\frac{2T}{Bl^2}\varepsilon\delta t\right)\right], \quad (4.34)$$

where F and G are calculated only for positive ε and δ. This is the expected damped, phase-shifted sine wave.

Expressions (4.30) to (4.33) are in fact perfectly general and can be used to evaluate the fast-decaying exponential contributions to $y(l,t)$. These have $\varepsilon=0$ and $\delta\doteq\pi,2\pi,3\pi\ldots$ (see equation (4.21)). For the experimental fibre this approximation becomes better for higher values of δ and even for the lowest value is in error by only a few degrees. From (4.33) we find that the coefficient of $\exp\left[-\frac{T}{Bl^2}\delta^2t\right]$ in $y(l,t)$ is zero if $\delta=2n\pi$ with $n=1,2,3\ldots$, while ~~the~~ when $\delta=(2n-1)\pi$ the corresponding exponential contribution is

$$y_{2n-1}(l,t) = \frac{-4Dv_s\tau(1-\rho^*)}{B\,\frac{MT}{B^2l^3}\left[(2n-1)\pi\right]^4} \exp\left[-\frac{T\left[(2n-1)\pi\right]^2 t}{BL^2}\right] \quad (4.35)$$

Hence for a light fibre the contribution to $y(l,0)$ from the sum of exponentials is approximately

$$\sum_{n=1}^{\infty} y_{2n-1}(l,0) = -\frac{1}{24}\frac{B^2l^3}{MT}\frac{Dv_s\tau(1-\rho^*)}{B}, \quad (4.36)$$

since $\sum_{n=1}^{\infty} \frac{1}{(2n-1)^4} = \frac{\pi^4}{96}$.

From the boundary condition $y = 0$ at $t = 0$ we expect that

$$\sum_{n=1}^{\infty} y_{2n-1}(l,0) = -y_0(l,0) \quad (4.37)$$

within our approximation. This relation is a useful check on the numerical work since $y_0(l,0)$ depends sensitively on the values of ε and δ obtained by iteration, while $\sum_{n=1}^{\infty} y_{2n-1}(l,0)$ is calculated directly from the experimental constants.

Because over 98% of $\sum_{n=1}^{\infty} y_{2n-1}(l,0)$ is contributed by the singularity at $\delta \doteq \pi$, the form of $y(l,t)$ can be found with sufficient accuracy by adding the single exponential contribution $y_1(l,t)$ to the oscillatory term $y_0(l,t)$.

The length of the fibre with which most of the measurements of circulation were made (fibre I) was, from the point of suspension to the

centre of the bob,

$$l = 0.91 \text{ cm.} \tag{4.38}$$

The bob had a true mass of 0.9 μgm. Its effective hydrodynamic mass was therefore (Birkhoff 1950)

$$M = 0.9.10^{-6} \frac{\rho' + \frac{1}{2}\rho}{\rho'} \text{ gm,} \tag{4.39}$$

where ρ is the total density of liquid helium and ρ' is that of nylon, the material of the bob. Taking ρ' as 1.15 gm cm^{-3},

$$M \doteq 1.0.10^{-6} \text{ gm.} \tag{4.40}$$

The tension in the fibre is equal to the weight of the bob less the Archimedean upthrust.

i.e.
$$T = M_{bulb} \frac{\rho' - \rho}{\rho'} g$$

$$\doteq 0.77.10^{-3} \text{ dyne.} \tag{4.41}$$

The steady viscous drag of a moving fluid on a long circular cylinder is not exactly proportional to the relative velocity of fluid and cylinder, but depends on the velocity in a complicated way (see

appendix I). It might be thought that in flow of varying velocity there was no uniquely defined viscous drag coefficient, but Sewell (1910; see Vinen 1957c) showed that in a sound wave of frequency $\frac{\omega}{2\pi}$ the drag on a circular cylinder of diameter d was given by

$$|F| \doteq \frac{-4\pi\eta v}{\ln\left(\frac{d}{4}\sqrt{\frac{\rho\omega}{\eta}}\right)} \quad \text{per unit length} \qquad (4.42)$$

at low frequencies, where v is the instantaneous velocity of the fluid in the sound wave, ρ is its density, and η its viscosity. Hence the drag coefficient B is in this case given by

$$B = -4\pi\eta / \ln\left(\frac{d}{4}\sqrt{\frac{\rho\omega}{\eta}}\right). \qquad (4.43)$$

Since the dependence on frequency is slight we estimate B by taking $\omega = 30$ rad/sec, which is approximately the fundamental angular frequency of the fibre. The required density and viscosity are those of the normal fluid.

The diameter of the fibre was

$$d = 0.7 \cdot 10^{-4} \text{ cm.} \qquad (4.44)$$

Its true mass per unit length was therefore

$$m = \frac{\pi d^2}{4} \rho_{\text{quartz}}$$

$$\doteq 10^{-8} \text{ gm/cm}, \qquad (4.45)$$

which may be neglected in comparison with the weight of the bob, as assumed in equation (4.2). With a restoring force due only to the stiffness of the fibre the deflection of the lower end would be given by

$$y = \frac{F l^4}{8 E I}, \qquad (4.46)$$

where $E \doteq 3.5.10^{11}$ dyne cm^{-2} is Young's modulus for quartz and $I = \pi d^4/64$ is the geometrical moment of cross-section of the fibre. For a given F, (4.46) predicts a deflection about 400 times as great as that given by equation (4.2). Hence treatment of the fibre as completely flexible is justified.

Although the general form of the variation of normal viscosity with temperature is well known, the measured values have quite a large scatter (e.g. Atkins 1959; Lane 1962; Dash and Taylor 1957). The transient response of the fibre has been computed at three temperatures using the following values of η_n :

$$\left.\begin{aligned} \eta_n &= 22.10^{-6} \text{ poise at } 1.30^\circ\text{K} \\ &= 10.10^{-6} \text{ poise at } 1.64^\circ\text{K} \\ &= 16.10^{-6} \text{ poise at } 2.10^\circ\text{K} \end{aligned}\right\} \qquad (4.47)$$

Although these values lie within the range of the measurements they are rather extreme, that at 1.30°K being high, and that at 1.64°K, low. It is however of interest to see how variation of η_n affects the computed transient behaviour. Values of ρ_n have been taken from NIT tables (1960).

At 1.3°K the value of the drag coefficient from (4.43) is

$$\mathcal{B} = 4.4.10^{-5} \text{ dyne-sec/cm}^2.$$

Hence $$\mathcal{B}l^2/T = 4.7.10^{-2} \text{ sec}$$

and $$\frac{MT}{\mathcal{B}^2 l^3} = 0.53.$$

By the iteration procedure we find

$$\varepsilon = 0.73, \quad \delta = 0.93.$$

The oscillatory part of the transverse motion of the bob is

$$y_0(l,t) = \frac{Dv_s\tau(1-e^*)}{\mathcal{B}} e^{-\lambda t} \frac{4}{13.1} (0.32 \cos \omega t - 2.5 \sin \omega t)$$

$$= -0.76 \frac{Dv_s\tau(1-e^*)}{\mathcal{B}} e^{-\lambda t} \sin(\omega t - \alpha), \qquad (4.48)$$

where $$\omega = 2\varepsilon\delta T/\mathcal{B}l^2 = 28.(9) \text{ rad/sec},$$

$$\lambda = \left(\delta^2 - \varepsilon^2\right) T / Bl^2 = 7.0(2) \text{ sec}^{-1}$$

and $\tan \alpha = 0.13$; i.e. $\alpha = 0.13$ rad $\doteq 7\frac{1}{2}^{\circ}$.

Therefore $$y_0(l,0) \doteq 0.09 \frac{D v_s \tau (1 - \rho^*)}{B},$$

while the sum of all the remaining exponential roots at $t = 0$ is approximately, by (4.36),

$$\sum_{n=1}^{\infty} y_{2n-1}(l,0) = -0.08 \frac{D v_s \tau (1 - \rho^*)}{B}.$$

Therefore $$y_0(l,0) \doteq -\sum_{n=1}^{\infty} y_{2n-1}(l,0).$$

Since this boundary condition is obeyed to within our approximations we may have confidence both in the algebraic solution of the original differential equation and in the numerical results based upon it.

The decay mode $y_1(l,t)$ has decay constant $\lambda_1 = \pi^2 T / Bl^2 = 210 \text{ sec}^{-1}$ and initial amplitude very nearly equal to $\sum_{n=1}^{\infty} y_{2n-1}(l,0)$. Hence

$$y_1(l,t) \doteq -0.08 \frac{D v_s \tau (1 - \rho^*)}{B} e^{-210t}, \qquad (4.49)$$

and to a good approximation

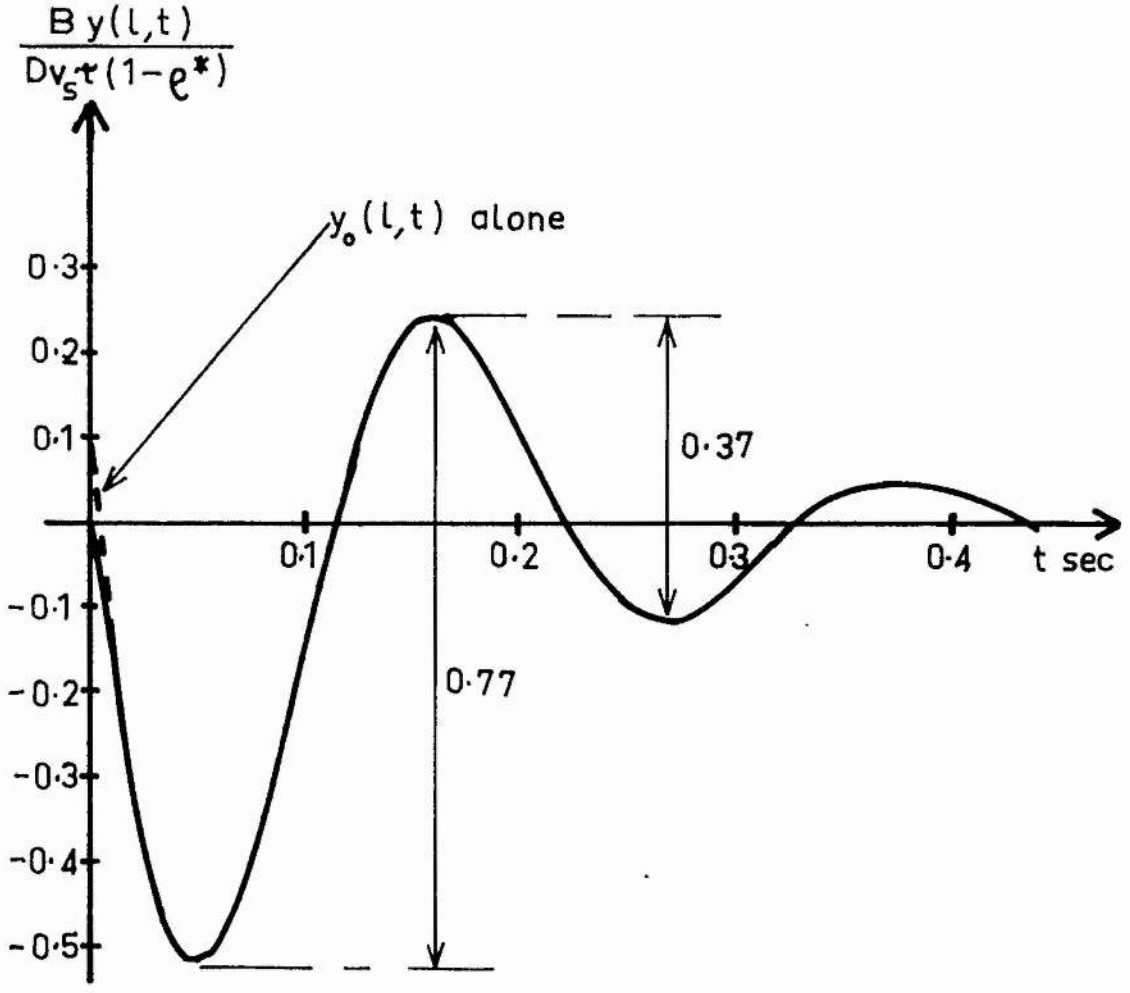

Figure 4.3. Transient transverse response of bob calculated at 1·3°K.

$$y(l,t) = y_0(l,t) + y_1(l,t) . \qquad (4.50)$$

This function is shown in figure 4.3. The peak-to-peak magnitude of the transient is

$$\frac{0.77\, D v_s \tau \left(1 - e^*\right)}{B} \qquad (4.51)$$

while the difference between the second and third extrema is

$$\frac{0.37\, D v_s \tau \left(1 - e^*\right)}{B} . \qquad (4.52)$$

At 1.64°K $B = 2.4.10^{-5}$ dyne-sec/cm^2, whence $Bl^2/T = 2.6.10^{-2}$ sec and $\frac{MT}{B^2 l^3} = 1.78$. By iteration $\varepsilon = 0.57$ and $\delta = 0.65$, and we find that

$$y_0(l,t) = - 0.42 \frac{D v_s \tau \left(1 - e^*\right)}{B} e^{-\lambda t} \sin\left(\omega t - \alpha\right) , \qquad (4.53)$$

where $\omega = 28.(5)$ rad/sec, $\lambda = 3.7(5)$ sec^{-1} and $\tan \alpha = 0.07$; i.e. $\alpha = 0.07$ rad $\doteq 4°$.

$$y_0(l,0) = 0.02(7) \frac{D v_s \tau \left(1 - e^*\right)}{B}$$

while $$\sum_{n=1}^{\infty} y_{2n-1}(l,0) = - 0.02(4) \frac{D v_s \tau \left(1 - e^*\right)}{B}$$

The boundary condition at $t = 0$ is therefore satisfied to within our approximation. At this temperature

$$y_1(l,t) \doteq -0.02 \frac{Dv_s\tau\,(1-e^*)}{B}\, e^{-380t} \qquad (4.54)$$

The general form of $y(l,t) \doteq y_0(l,t) + y_1(l,t)$ is similar to that at 1.3°K. The peak-to-peak transient deflection at 1.64°K is

$$0.61 \frac{Dv_s\tau\,(1-e^*)}{B} \qquad (4.55)$$

At 2.10°K $B = 4.2.10^{-5}$ dyne-sec/cm^2, whence $Bl^2/T = 4.5.10^{-2}$ sec, $\frac{MT}{B^2l^3} = 0.58$. We find that $\Sigma = 0.73$, $\delta = 0.90$ and

$$y_0(l,t) = -0.66 \frac{Dv_s\tau\,(1-e^*)}{B}\, e^{-\lambda t} \sin(\omega t - \alpha), \qquad (4.56)$$

where $\omega = 29.(2)$ rad/sec, $\lambda = 6.1(5)$ sec^{-1} and $\tan\alpha = 0.10$; i.e. $\alpha = 0.10$ rad $\doteq 6°$.

$$y_0(l,0) \doteq 0.07 \frac{Dv_s\tau\,(1-e^*)}{B},$$

while $$\sum_{k=1}^{\infty} y_{2k-1}(l,0) = -0.07 \frac{Dv_s\tau\,(1-e^*)}{B}.$$

The boundary condition at $t = 0$ is therefore satisfied. At this temperature

$$y_1(l,t) \doteq -0.07 \frac{\mathcal{D} v_s \tau (1 - e^*)}{B} e^{-220t}, \qquad (4.57)$$

and the calculated peak-to-peak transient deflection is

$$\frac{0.80\, \mathcal{D} v_s \tau (1 - e^*)}{B} \qquad (4.58)$$

Bearing in mind that B enters not only through the calculated, numerical coefficients but also through the factor $\mathcal{D} v_s \tau (1 - e^*)/B$, we see that the initial amplitude and the frequency of $y_0(l,t)$ are almost independent of B, which affects strongly only the damping of the oscillations.

We have computed the transient form for a light fibre. To check that this is a valid approximation, the values of $|\alpha_n|$ for $y_0(l,t)$ and $y_1(l,t)$ must be compared with the value of B/m in the experiment, where m, the effective mass per unit length of the fibre, is for an ideal fluid equal to its true mass plus the mass of displaced fluid (Lamb 1945, p.85 and Birkhoff 1950, p.151). m is of the order of 10^{-8} gm/cm, so that $B/m \sim 2\text{-}4.10^3$ sec^{-1}, while by equation (4.18)

$$|\alpha_n| = \frac{T}{Bl^2} |\varepsilon + i\delta|^2$$

$$\sim (20\text{-}40)\, |\varepsilon + i\delta|^2 . \qquad (4.59)$$

Therefore $|\alpha_n| \ll \beta/m$ provided that

$$|\epsilon + i\delta|^2 \ll 100. \qquad (4.60)$$

This condition is easily satisfied for $y_0(l,t)$ and reasonably well so for $y_1(l,t)$, where $|\epsilon + i\delta|^2 \sim 10$. Hence the approximation seems to be justified.

There are however some difficulties. It is not certain that the concept of effective hydrodynamic mass is applicable to the motion of a circular cylinder through a viscous fluid. If it is, it may be frequency-dependent, so that at the beginning of the transient when very high-frequency fourier components are present the effective mass of the fibre may be very much greater than we have supposed. Certainly it is true that for these high-frequency components the formula (4.43) for β is incorrect and the drag is probably higher. We shall consider this possibility further in relation to the experimental results.

Some of the results were obtained with another fibre (fibre II). This had the same diameter as fibre I ($0.7.10^{-4}$ cm). Its length from support to the centre of the nylon bob was

$$l = 0.90 \text{ cm}.$$

The weight of the bob was $0.87.10^{-6}$ gm, and so its effective hydrodynamic mass was

$$M = 0.99.10^{-6} \text{ gm},$$

while the tension in the fibre was

$$T = 0.75.10^{-3} \text{ dyne}.$$

The diameter and principal period of this fibre are very similar to those of fibre I. Therefore the drag coefficient B will be the same for both. $\frac{MT}{B^2L^3}$ and $\frac{BL^2}{T}$ differ by only a few percent for the two fibres, so that to our approximation the transient responses of the fibres should be indistinguishable.

5. Differing fibre responses to turbulence in the two fluids

The superfluid interacts with a fibre only through the Magnus force. From chapter 3 we know that, if turbulence in the superfluid takes the form of a tangle of closely spaced vortex lines, as is often supposed (e.g. Vinen 1957c), the mean circulation about the fibre must be small. The mean Magnus force on it will therefore also be small, and so little agitation of the fibre is to be expected. Superfluid turbulence can probably be detected only by measurement of the mean circulation about the fibre, which will be much smaller and more variable than when the superfluid is not turbulent.

The normal fluid interacts with the fibre through viscous forces. Assuming that it is similar to a classical, viscous fluid, its random motion in turbulent flow can be spatially analysed into a series of superimposed eddies of wave-number (size) ranging downwards from the order of the width D of the channel in which flow is occurring (Batchelor 1953). Alternatively the motion can be analysed temporally into a spectrum ranging from very high frequencies to frequencies of order $\overline{v_n}/D$, where $\overline{v_n}$ is the mean flow velocity of the normal fluid along the channel. The fibre, whose length in the experimental conditions is also of order D, responds mainly to the largest eddies, since the average effect of a large number of small, random eddies is close to zero. The mean force on the fibre therefore has a Fourier spectrum with a peak at a frequency of order $\overline{v_n}/D$.

Lin (1943) has shown that the Fourier spectrum of the displacement

of a simple pendulum subject to a random force is related to the spectrum of the force by a simple resonance relation, which has a peak at the natural frequency of the pendulum, and a quality factor Q governed by the viscous damping. Although the fibre used in the experiment is not a simple pendulum, it does oscillate naturally with a frequency and damping that are calculated in chapter 4 (equations (4.48), (4.53) and (4.56)). The natural angular frequency $\omega \doteq 29$ rad/sec at the three given temperatures, and the decay constant for this mode of oscillation is given by

$$\left.\begin{aligned} \lambda &= 7.0 \text{ sec}^{-1} \text{ at } 1.30^\circ\text{K} \\ &= 3.8 \text{ sec}^{-1} \text{ at } 1.64^\circ\text{K} \\ &= 6.2 \text{ sec}^{-1} \text{ at } 2.10^\circ\text{K} \end{aligned}\right\} \qquad (5.1)$$

Although the damping varies slowly with frequency (see equation (4.43)), we can calculate an approximate quality factor

$$\left.\begin{aligned} Q &= \tfrac{1}{2}\,\omega/\lambda \\ &\sim 2 \text{ at } 1.3^\circ\text{K and } 2.1^\circ\text{K} \\ &\sim 4 \text{ at } 1.64^\circ\text{K} \end{aligned}\right\} \qquad (5.2)$$

Since Q is low the fibre is not sharply tuned and will respond adequately to a wide range of frequencies.

The maximum normal-fluid velocity in the large eddies is classically of the order of $\overline{v_n}$, the mean flow velocity. A steady velocity of this size would exert a force

$$F = \frac{4\pi\eta_n \overline{v_n}}{2 - \ln Re'} \qquad (5.3)$$

on unit length of the fibre (see appendix I), where Re' is the Reynolds' number for the flow, based on the fibre diameter and (probably) the normal-fluid density. The slowly-varying denominator of (5.3) is approximately equal to 5 in the experimental conditions.

If the eddy velocity varied at an angular frequency of 30 rad/sec, the instantaneous force acting on the fibre when it was equal to $\overline{v_n}$ would be, by equation (4.42),

$$\overline{F} = \frac{4\pi\eta_n \overline{v_n}}{-\ln \frac{d}{4}\sqrt{\frac{\rho_n 30}{\eta_n}}} . \qquad (5.4)$$

Again the slowly-varying denominator is approximately 5 in the experimental conditions.

Hence we may take

$$\overline{F} \doteq \frac{4}{5}\pi\eta_n \overline{v_n} , \qquad (5.5)$$

independent of frequency. A steady force of this size would deflect the bob on the end of the fibre by an amount

$$y = \frac{Fl^2}{2T} \quad \text{(equation (4.2))}$$

$$\sim 10^3 \eta_n \overline{v_n} \quad \text{cm} \qquad (5.6)$$

with the experimental constants. Remembering the low Q of the fibre

we take (5.6) to be true independently of frequency, in order of magnitude. Hence we expect that in fully-developed normal-fluid turbulence the bob will be randomly agitated with a spectrum having a maximum near frequencies of order $\overline{v_n}/D$, and with maximum deflection of order $10^3 \eta_n \overline{v_n}$ cm. The root-mean-square deflection of the bob, which is found experimentally to be about one-fifth of the largest deflection, will be

$$y_{rms} \sim 200\, \eta_n \overline{v_n} \quad \text{cm.} \tag{5.7}$$

That is, the rms deflection is proportional to the mean flow velocity of the normal fluid, with a constant of proportionality of the order of 4.10^{-3} cm/cm sec^{-1} at 1.3°K and 2.1°K, falling to about 2.10^{-3} cm/cm sec^{-1} between about 1.6°K and 1.85°K.

A classical viscous fluid does not become turbulent unless it is flowing fast enough for the Reynolds' number to exceed a critical value which is normally about 2300. The Reynolds' number is defined as

$$Re = \frac{\overline{v}\, D \rho}{\eta}, \tag{5.8}$$

η and ρ being respectively the viscosity and density of the fluid, $\overline{v}$ the mean flow velocity, and D the diameter of the channel in which flow is occurring. For non-circular channels D is defined as $4A/P$, where A is the area and P the perimeter of the cross-section. It is

possible that a similar criterion may determine the occurrence of normal-fluid turbulence in helium II. Further discussion of the phenomena associated with classical turbulence is given by Batchelor (1953), Landau and Lifshitz (1959), and Prandtl (1952).

III

Experiment

... like tempestuous ocean birling
In the batter of a two-way wind's buffet and fight.

(Inferno V, 29-30)

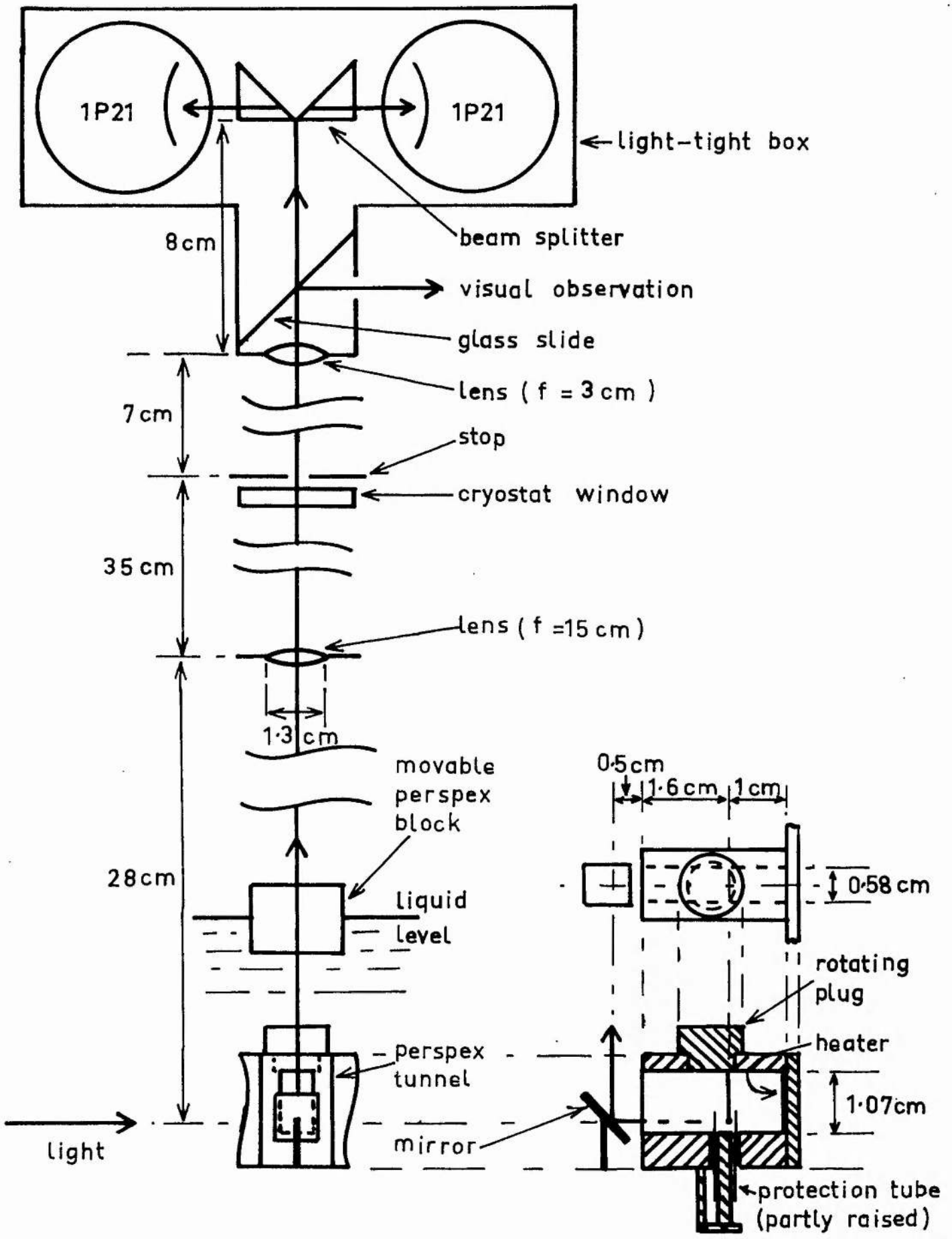

Figure 6.1. Wind tunnel II and optical system

6. Apparatus and experimental details

(a) Description of the apparatus

The heart of the apparatus, which is shown in figure 6.1, is a horizontal, perspex tube of rectangular section, closed at one end by a mica or glass plate on which is painted a carbon-film (aquadag) heater. Hanging inside this tube is a quartz fibre about one centimetre long and less than a micron in diameter, carrying at its lower end a bob of weight just under a microgram. For small displacements from the vertical the fibre behaves like a light, flexible string, and the steady deflection of the bob is simply related to the mean force acting normally on unit length of the fibre. When the apparatus is immersed in helium II and the heater switched on, the superfluid component flows towards the heater and the normal component away from it, in such a way that there is no net mass flow along the tube. The apparatus is therefore called a counterflow wind tunnel.

For the measurements of viscosity reported in appendix I the deflection of the bob in the direction of normal-fluid flow was observed through the wall of the tunnel, the surface of the helium and a window in the cryostat cap, by means of a mirror just outside the tunnel. Illumination was provided by a light beam shining through a clear strip in the dewar assembly and through the open end of the tunnel. In the superfluid circulation and turbulence measurements which form the subject of this thesis the fibre is illuminated through the tunnel wall, while deflections normal to the heat flow are observed by placing the

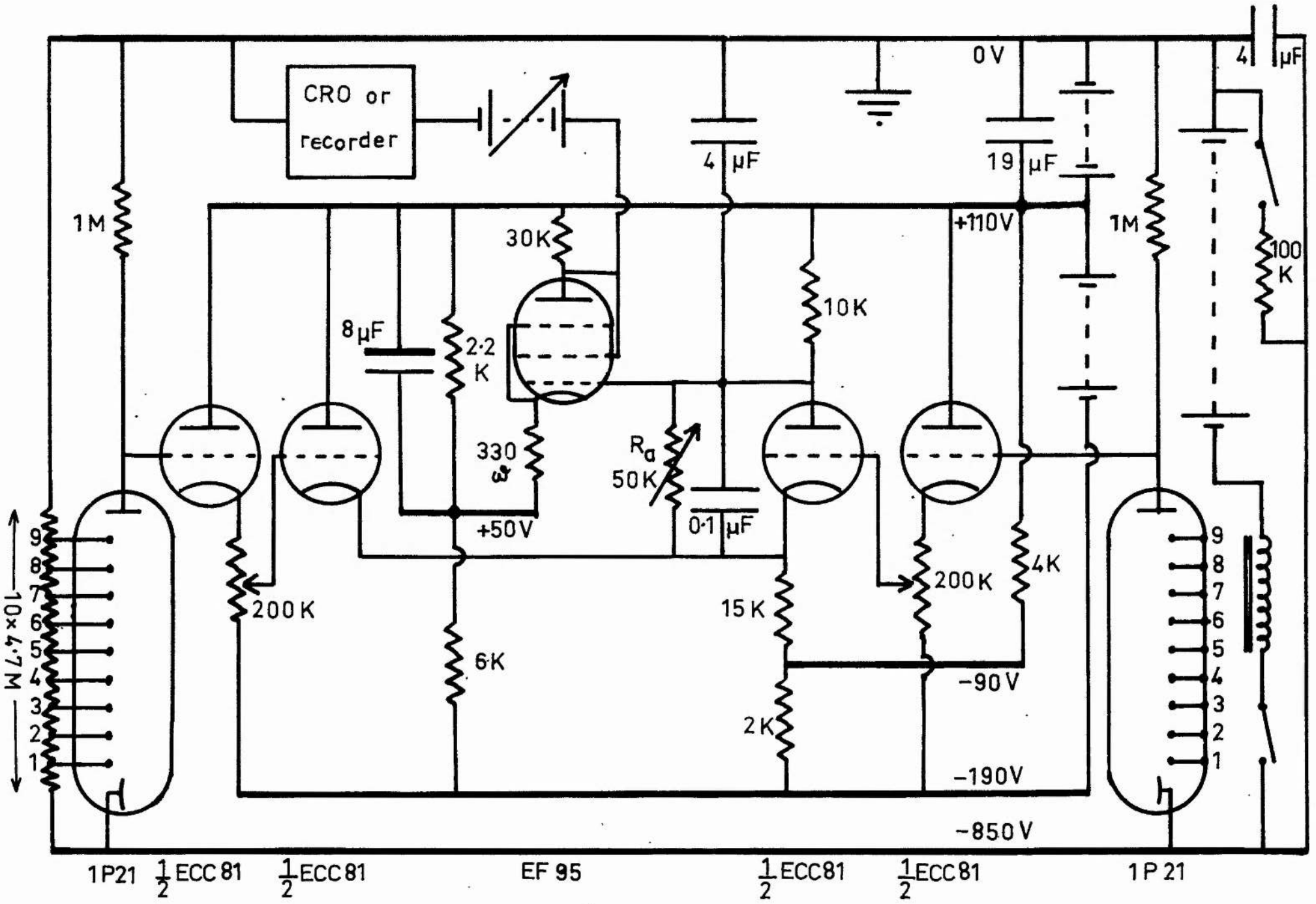

Figure 6.2. Recording system (electronics)

mirror just outside the open end of the tunnel, as shown in figure 6.1.

To avoid disturbance by ripples on the helium surface, the image passes through a thick perspex plate which can be adjusted to remain in the falling surface of the liquid during a run. By a lens above the liquid the image is focused at a window in the top of the cryostat, where it can be isolated from unwanted reflections and stray illumination by a stop. For recording the motion of the bob on the end of the fibre a further assembly, also shown in figure 6.1, is mounted on the cryostat cap. This consists of another lens, a prismatic beam-splitter and two photomultipliers in a light-tight box. The position of the lens is horizontally adjustable to allow the defocused image to be centred on the beam-splitter. The light beam is intercepted between the lens and the beam-splitter by an unsilvered microscope cover slide at 45° to the optic axis, so that the image can be observed during recording.

The electrical part of the recording system is shown in figure 6.2. Two RCA 1P21 photomultipliers are run from an 850-volt battery with choke-condenser smoothing to reduce crackle. Their outputs are fed via cathode followers into a DC-coupled difference amplifier, which gives an overall one-sided voltage gain of about 50:1 and a common-mode rejection ratio of better than 100:1 when resistor R_a is adjusted to its optimum value. Since the photomultipliers were manufactured in the same batch and share a common voltage-divider chain, they have similar sensitivities. It has not been found necessary to provide separate gain controls on the two channels.

A condenser connected across the anode load of one of the amplifier stages removes high-frequency noise, the RC time-constant being 4.10^{-2} sec. Thermal drift is reduced to an acceptable level by shielding the amplifier and its HT supply from draughts. The remaining noise has been measured and found to correspond to the expected photomultiplier noise (which is almost entirely shot noise from the first photocathode). Dark-current noise is not detectable. The output signal, which is taken across the anode load of the final stage of the amplifier and is backed off to zero DC level by a battery, can be displayed on a CRO with its time-base switched off, where it is photographed on continuously moving recording paper. Alternatively the signal can be fed into a high-speed pen recorder (DC-70 c/s flat response) which has high input impedance and contains its own power amplifier. Although the first method probably gives a more accurate record of events, the second method allows better use to be made of running time, since it is possible to see what is happening in the cryostat as it occurs, and to act accordingly.

The bob on the end of the fibre is illuminated by a 36-watt bulb focused on it through the side of the dewar. By passing the light through a Chance glass infra-red filter and an inch thickness of dilute, aqueous, copper sulphate solution, and by allowing the direct light beam to pass straight through and out of the helium dewar through the clear strip, the measured equivalent heat input from the illumination is limited to about 5 mW. Screens are placed outside the tunnel to

prevent light from falling on the aquadag heater as far as possible, where it would be absorbed and cause a heat current to flow in the tunnel.

The electro-optical recording system has a non-linear response to motion of the bob, due mainly to the fact that the patch of light which falls on the beam-splitter is circular and non-uniform in intensity. The extreme measurable deflection is reached when the patch falls entirely on one or other of the prisms. With the given dimensions and component values, movement of the bob between the two extreme positions, which are about 0.2 mm on either side of the zero position, gives a peak-to-peak signal of 20 to 30 volts. In most of the measurements the excursions of the bob did not exceed 0.05 mm from the zero position, so that departures from linearity were relatively unimportant.

Experiments on turbulence in steady heat currents have been carried out in two wind tunnels. The first of these (tunnel I in figure 6.1) has a cross-section 2.3 x 1.0 cm, is 3.5 cm long, and has an aquadag heater on a mica backing held against one end by a spring clip. The quartz fibre is suspended from a metal pin projecting from a plug in the roof of the tunnel. In the floor of the tunnel below the fibre is a hole through which a vertical metal plate can be raised and swung into contact with the whole length of the fibre. The fibre is held against the plate by electrostatic and Van-der-Waals forces during the filling of the cryostat with liquid helium. Once the helium is below the λ-point the wind tunnel is X-rayed to remove electrostatic charge and the

metal plate is then lowered out of the tunnel by remote control from the cryostat cap. In this tunnel the only reliable observations of the motion of the fibre and bob are purely visual.

Tunnel II (see figure 6.1) has a cross-section (1.07 ± 0.03) x $(0.57(5) \pm 0.01)$ cm, and the heater is held in position by a screw clamp. At first an aquadag heater on a mica backing (heater I) was used, but after it had been damaged heater II on a glass backing was substituted, and has proved very satisfactory. The fibre is suspended one centimetre in front of the heater from a plug in the tunnel roof which can be rotated from outside the cryostat. By this means the fibre can be moved through known distances across the tunnel in order to calibrate the recording system. When the apparatus was designed it was expected that movements of up to a millimetre each side of the central position might be necessary, but in fact the deflections in the most interesting experimental conditions are less than this by an order of magnitude. The calibration system is therefore rather too coarse, and its results not very accurate because of backlash.

The method used for calibration is as follows. At the beginning of a run, after going through the λ-point, the illumination of the fibre is optimised, the optical system lined up and the electrical system zeroed. The whole recording system is then calibrated as fully as possible by moving the fibre to known positions in the tunnel, and at the same time the peak-to-peak signal as the light patch from the bob is moved from one prism of the beam splitter on to the other is measured.

The calibration can then be checked during the rest of the run, and any variation allowed for, by measuring the peak-to-peak signal, a simple and quick operation.

In tunnel II it was found that a metal plate was insufficient protection for the fibre during filling. It was therefore replaced by a metal tube, sliding through an annular hole in the floor of the tunnel and completely enclosing the fibre when raised (see figure 6.1). Used in conjunction with the X-raying procedure, this has proved entirely satisfactory. It is hoped that the annular hole, which has a cross-sectional area less than 10% of that of the tunnel, is not large enough to produce significant changes in behaviour.

Temperature is measured by a differential oil manometer, the correction for backing-pump pressure on the low-pressure side being read on a Vacustat (McLeod type) gauge. A temperature-sensitive resistor which is immersed in the helium is included in a Wheatstone's bridge network, and the temperature kept constant by altering pumping speed or heat input to keep the bridge balanced. With care the temperature variation can be kept to within about 0.01°K. Originally the temperature-sensitive resistor was a carbon film on a mica backing, but recently an Allen Bradley resistor (nominally 49 ohm) has been used. It has a resistance of over 1000 ohm in liquid helium, and gives fairly reproducible results from run to run, but has the disadvantage of poor thermal contact with the helium bath, so that, when the two-volt driving accumulator is switched on, a relatively large current flows

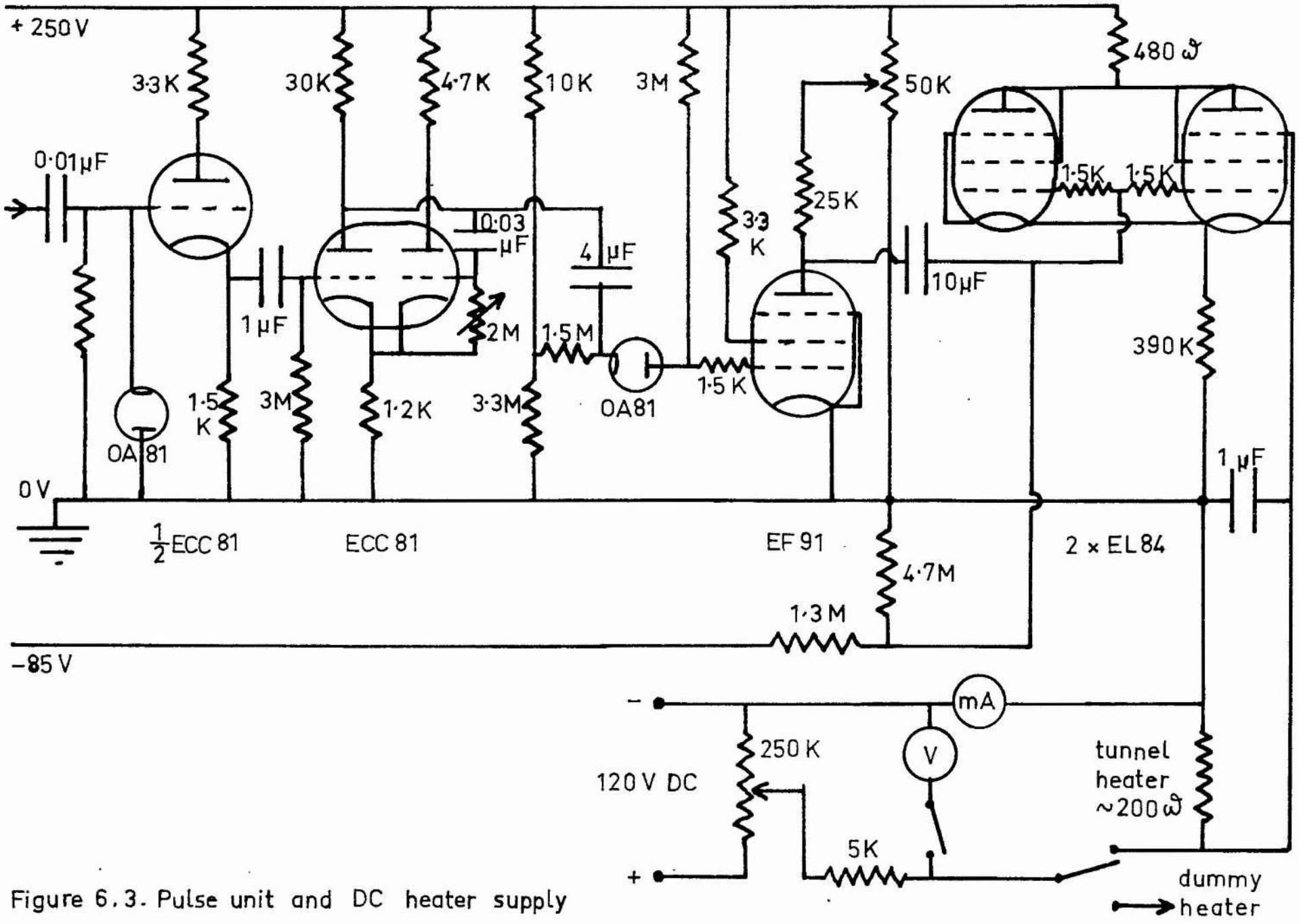

Figure 6.3. Pulse unit and DC heater supply

through the galvanometer until thermal equilibrium is established in about 0.1 sec. A dummy resistor of similar characteristics to the tunnel heater is usually included in the cryostat so that the heat flow in the tunnel can be turned on and off without substantially altering the total heat input to the helium, and hence its temperature.

Provision is made for a pulsed input to the tunnel heater, using the fairly standard circuit shown in figure 6.3. The pulse unit is triggered by a counter and scaler unit, which in turn is driven by a variable frequency oscillator. The pulses are displayed and measured on the second channel of the CRO. They can also be fed to the second channel of the pen recorder, and it is possible to superimpose them upon a steady heat input to the tunnel.

Heat pulses are propagated through helium II as pulses of second sound (e.g. Osborne 1951). The second-sound signal has been detected with a small carbon-resistance thermometer placed at the open end of the tunnel. For short pulses a train of gradually diminishing reflected pulses was observed to follow the main pulse, but for pulses longer than the time taken for second sound to travel the length of the tunnel the main pulse only was detectable. This time is less than about 2 msec for all temperatures at which pulse measurements have been made, while pulses of from 5 msec duration upwards have been employed.

(b) Special techniques

Heaters on a mica backing have been made by evaporating two silver contacts on to the mica plate and then painting a layer of aquadag

between the contacts. The whole heater is then baked at a few hundred degrees centigrade for about half an hour. Contact is made to the silver by nuts and bolts screwed tightly through holes in the mica.

The heater on a glass backing was made by first painting an aquadag layer on a microscope slide. A piece of thin copper wire was then wound tightly round the slide beside the aquadag layer, and its ends twisted together to hold it firmly in place. Another wire was fixed on the other side of the aquadag. Contact between each of the wires and the aquadag was made with a painted layer of Dag dispersion 915 (silver in MIBK), which also served to cement the wires to the glass. The heater was gently baked before use.

Quartz fibres are made by melting the tips of two $\frac{1}{8}$-inch quartz rods together in a fierce oxygas flame, and then immediately separating them by about 30 cm on removal from the flame. The thick fibre so formed is broken in the middle and shortened so that each quartz rod has about 10 cm of stiff fibre projecting from its tip. The oxygas flame is adjusted to be about 30 cm long, steady, with a long central blue cone, and inclined at an angle of 20° to 30° above the horizontal. The stiff fibre is then fed into the flame, using the quartz rod as a handle, where it is melted and blown out into a fine fibre which hangs in the air above the flame. With a black background and side lighting it can be seen and captured with sticky paper tabs. This technique produces fibres with long central sections of diameter $\frac{1}{2}$ to 2 μ, uniform to within a few percent.

The fibre diameter is measured by attaching a bar of known (calculated) moment of inertia to a few centimetres of fibre with shellac, and measuring the period of torsional oscillation. Because viscous damping by the air is very high this can be done only in a diffusion-pump vacuum, where the mean free path of the air molecules is large compared with the thickness of the inertia bar. Torsional oscillations are induced by an electric discharge between the inertia bar and the container supporting the vacuum. From the relation

$$T = 2\pi\sqrt{\frac{Il}{c}}, \qquad (6.1)$$

where T is the period of oscillation, I is the moment of inertia of the bar, l is the length of the fibre and $c = \frac{\pi}{32} d^4 Z$, the fibre diameter d can be deduced provided Z, Young's modulus for quartz, is known. In the older literature (e.g. Strong 1938) it is stated that Young's modulus increases with decreasing fibre size, but it is now thought probable (see Tighe 1956) that this is a spurious effect arising from inaccurate measurement of the true fibre diameter. It has therefore been assumed that Z remains equal to the bulk value for all fibre sizes. In any case the effect on the measured diameter, which is not a very critical constant of the experiment, is small.

Fibres are prepared and mounted in the tunnel as follows (see figure 6.4). A length of fibre is suspended vertically and a small shellac blob is melted on to it a few centimetres below the upper paper

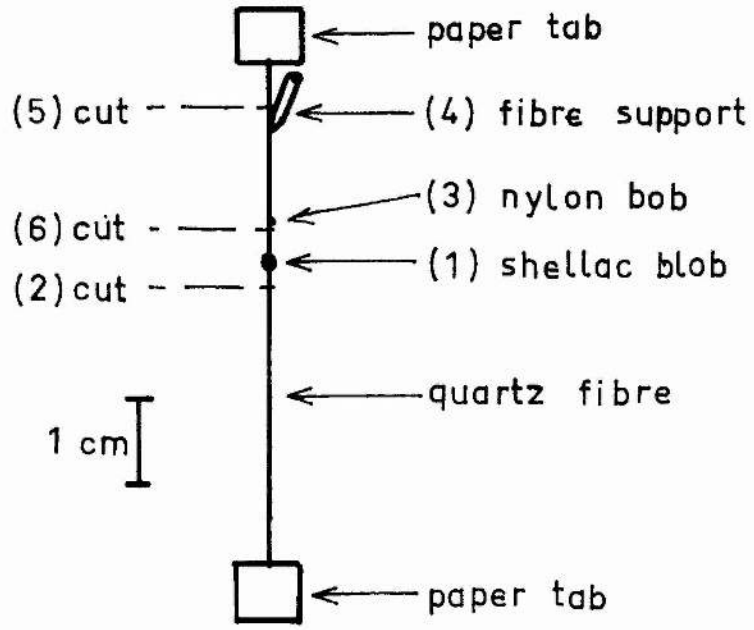

Figure 6.4. Operation sequence for preparation of fibre

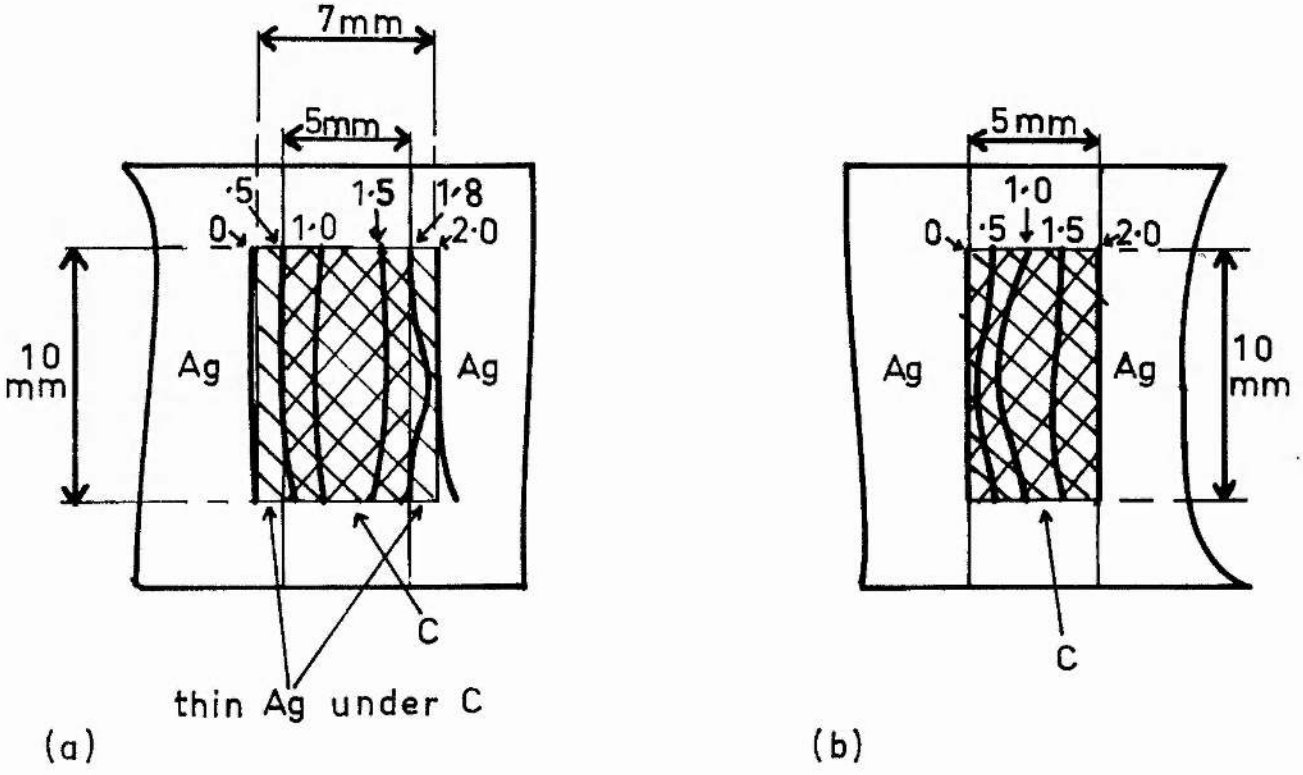

Figure 7.1, Potential distribution across (a) heater I

(b) heater II

tab. The portion below the blob is then cut off and stored. A short length (about $\frac{1}{2}$ mm) of nylon thread is then cut from a long length of known weight per unit length (1.8 μgm/mm) and, after being measured under a microscope, is transferred with a stiff quartz bristle to a position on the quartz fibre about 1 cm above the shellac blob, where it sticks by electrostatic forces. It is then melted into position with an electrically heated tungsten wire, and forms a white sphere about $\frac{1}{10}$ mm in diameter attached to the fibre on one side, being unfortunately prevented by surface tension from wetting the fibre completely. The plug or pin from which the fibre is to be suspended is then painted with nail varnish and brought against the fibre about 1 cm above the nylon sphere. More nail varnish is applied to ensure that the fibre is completely immersed, and, when it is dry, the fibre remaining above the nail varnish is cut away. The whole assembly is then lowered into place in the wind tunnel, the shellac blob hanging through the hole in the floor, and the fibre is cut just below the nylon sphere, as near to it as is possible without damage, by scissors inserted through the open end of the tunnel. The metal plate or tube is then raised to protect the fibre from convection currents.

A disadvantage of this technique is that the weight of the nylon bob is not known as certainly as we should like. Shellac was at first used instead of nylon, but uniform shellac fibres could not be drawn, and weight was certainly lost on melting. Commercial nylon fibre is very uniform, and it is believed that the weight per unit length of the

sample used is known accurately to 2% or 3%. However, the cut ends of the fibre are inevitably ragged, so that the length of a $\frac{1}{2}$ mm piece cannot be measured to better than about 10% accuracy. It is believed that the nylon does not lose much weight on melting (it does not boil or change colour), but a satisfactory test of this has not been devised.

7. Experimental results

(a) General survey

In wind tunnel I visual observations of turbulence have been made over the temperature range from 1.2°K to the λ-point, using a fibre of similar characteristics to fibres I and II (see chapter 4(b)). Since the rms deflection of the bob could not be measured, the rather rough criterion of the largest sudden change in its position, estimated by viewing the image against a graticule, was used to measure the intensity of the turbulence. There exist also some rather sketchy data on turbulence from the original experiment designed to measure the viscosity of the normal fluid (see appendix I).

With tunnel II, in which measurements of both turbulence and superfluid circulation were made, heater I (on a mica backing) was used for the exploratory runs and for the first successful measurement run (at 1.3°K). In this run the heater was found to have increased in resistance through mechanical damage, so that the true heat currents are slightly uncertain. Nevertheless the behaviour of the heater before it was damaged is known, and since no damage to the carbon film itself can be detected it is assumed in calculating the heat flow that the extra resistance is entirely in the contacts, and that the carbon film behaves exactly as it did before the damage occurred. The original resistance of the heater was about 400 ohm, and the extra contact resistance after damage is about 300 ohm. The resistance of all carbon-film resistors is not constant in a helium bath of fixed temperature, but falls with

increasing power dissipation, because the Kapitza resistance to heat exchange between the heater and the bath produces a temperature difference between them (Atkins 1959, pp. 144, 201). The temperature difference takes a certain time to be established: it is assumed that this time is long compared with 5 msec, so that the electrical resistance appropriate to the short pulses used to measure circulation is that for zero power dissipation. In the calculation of heat inputs allowance is made for the lead resistance of 15 ohm, measured with helium in the cryostat.

The potential distribution over the surface of heater I when 2 volts DC is applied between its terminals is sketched in figure 7.1(a). It is very asymmetric, the mean resistance of the left half of the heater being almost twice that of the right half (viewed from the open end of the wind tunnel).

Heater II, on a glass backing, was used for the remaining runs. It has a resistance of about 200 ohm, and its asymmetry is similar to that of heater I, although perhaps slightly less pronounced (see figure 7.1(b)).

Fibre I, for which detailed calculations are given in chapter 4(b), was used in the first three successful measurement runs, at 1.30°K, 2.10°K and 1.64°K respectively. It was lost when an attempt to check that no apparent superfluid circulation could be detected above the λ-point caused the helium to boil. (This particular experiment was not repeated). Fibre II, which is very similar to I (see chapter 4(b)), has

been especially subject to electrostatic charging, and has a permanent kink, obtained during separation from the wall of the tunnel with a fine wire. It therefore does not hang exactly vertically. Although in itself not serious, this prevents the fibre from reflecting much light into the detection system. The nylon bob reflects properly, but the sensitivity and signal/noise ratio are smaller with fibre II than with fibre I.

The temperatures at which measurements have been made with the various modifications of tunnel II are summarised in the following table.

	heater I	heater II
fibre I	1.30°K	1.64°, 2.10°K
fibre II		1.30°, 1.64°, 1.84°, 2.10°K

(b) Measurements of superfluid circulation in undisturbed helium

(i) Factors controlling rate, length and height of pulses.

Reliable circulation measurements have been made in tunnel II only. They are obtained by observing the fibre's transient response to heat pulses, produced at a rate of one every three or four seconds. This rate is chosen so that, while the mean heat current in the tunnel

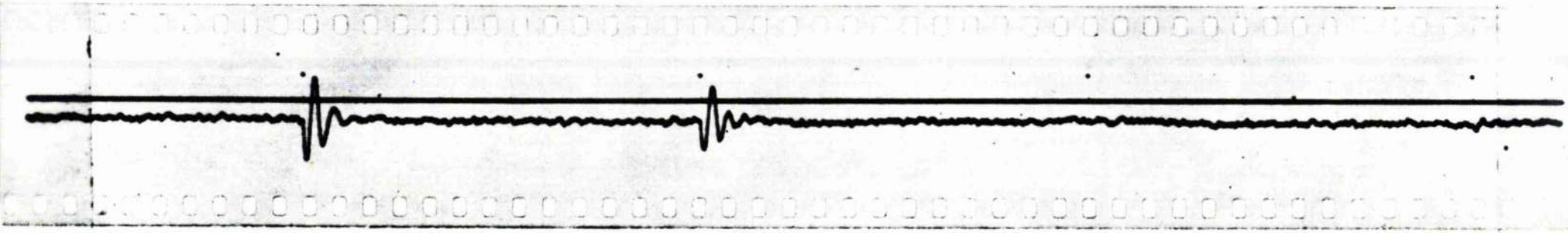

Figure 7.2(a). Subcritical pulse response. T = 1·64°K, pulse length = 15 msec, pulse power = 360 mW/cm^2

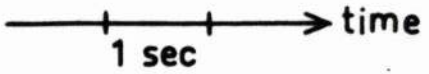

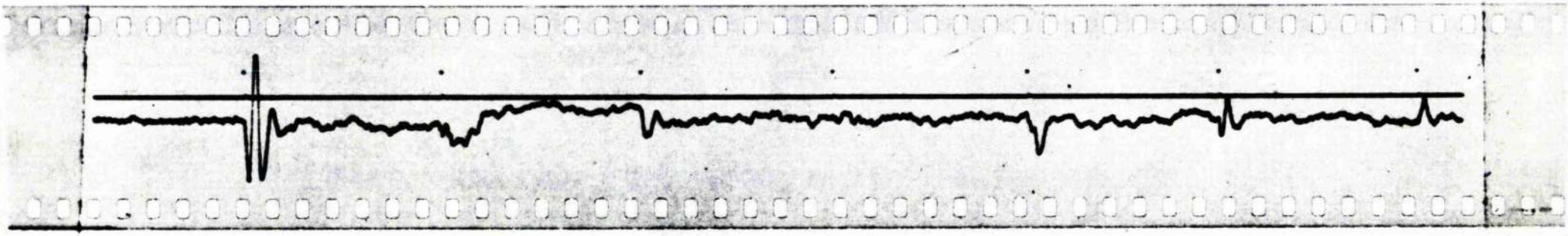

Figure 7.2(b). Supercritical pulse response. T = 1·30°K, same pulse as (a).

(Pulses on the upper trace, response on the lower, in each case)

due to the pulses is small, the variation of slowly changing circulations can be easily followed. Occasionally the persistence of an apparently well-established circulation has been checked by allowing a much longer time to elapse between pulses.

Although in some early exploratory runs pulses of up to 200 msec duration were used, it eventually seemed best to simplify the interpretation of the results by making the pulses as short, i.e. as near to δ-functions, as possible. On the other hand the pulse has to be longer than the time taken for second sound to travel the length of the tunnel in order to avoid reflected pulses (see chapter 6(a)). Five msec was taken as a suitable compromise. It is much shorter than the principal period of the fibre (about 0.2 sec), so that treatment of the pulse as a δ-function is justified.

The heat flow during the pulse is fairly closely controlled by opposing factors. On the one hand it must be as large as possible so that the transient signal is well above the noise level. On the other hand too large a pulse may alter the circulation it is designed to measure. Although this may sometimes have occurred, the stability and persistence of certain circulations suggest that it is not a serious weakness of the method. There is however a more severe upper limit to the pulse height. It is found that up to a certain critical height the bob remains steady between transients, and that the size and direction of the transients varies in a slow and regular way. Above the critical pulse height the bob is agitated between the transients, which are

Figure 7.3. Typical transients at 1·30°K

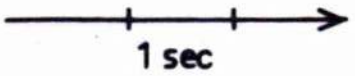

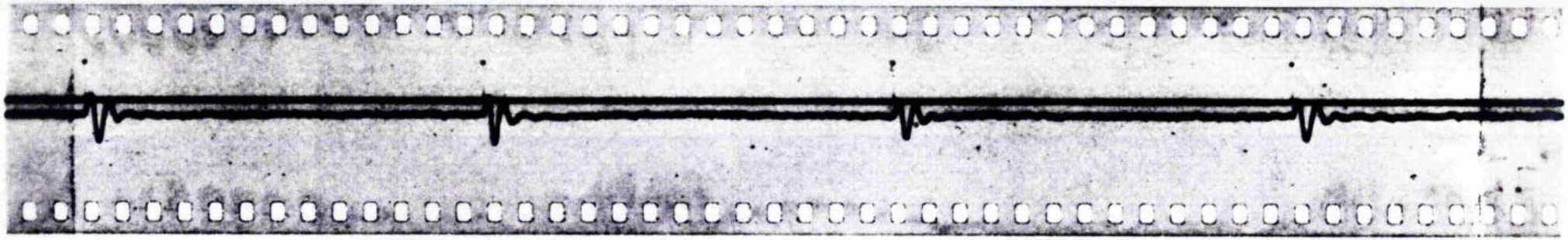

(a) persistent circulation

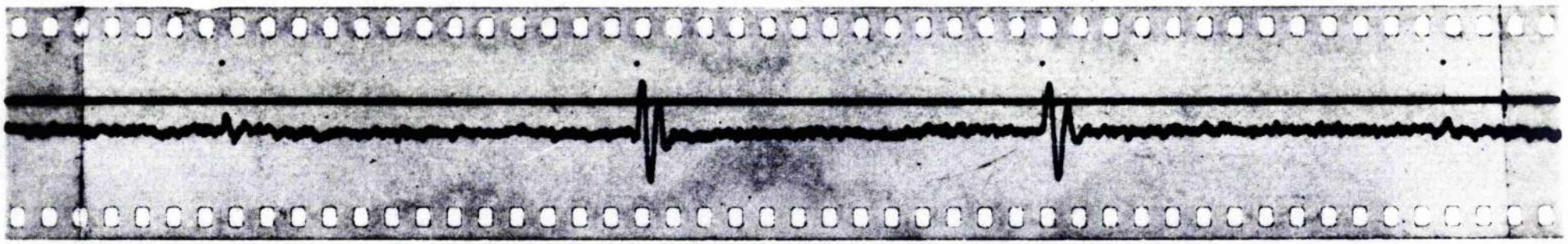

(b) variable circulation

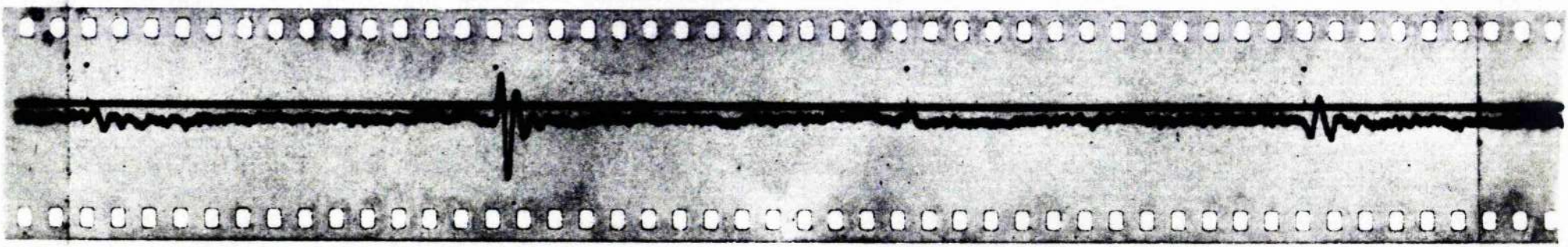

(c) variable circulation

themselves very variable in form and in magnitude, although biased in direction. Examples of subcritical and supercritical behaviour are shown in figures 7.2(a) and (b). This behaviour seems not to depend greatly on the pulse rate, but to be a property of the individual pulses, although it is clear that once one supercritical pulse has disturbed the helium a second one can further amplify the disturbance. For results which are in any sense characteristic of undisturbed helium rather than of the pulses, the heat flow during the pulses must be kept below the critical value W_c, which for 5 msec pulses is as follows.

$$\left.\begin{aligned} W_c &= 210 \pm 40 \text{ mW/cm}^2 \text{ at } 1.30^\circ\text{K} \\ &= 380 \pm 50 \text{ mW/cm}^2 \text{ at } 1.64^\circ\text{K} \\ &= 540 \pm 60 \text{ mW/cm}^2 \text{ at } 2.10^\circ\text{K} \end{aligned}\right\} \qquad (7.1)$$

The variation of W_c with the pulse length τ has not been investigated in detail, but it seems that W_c decreases rather slowly as τ increases, so that the product $W_c\tau$ is an increasing function of τ.

(ii) Results at 1.30°K.

Transient deflections of the bob corresponding to circulations of the expected order of magnitude have been observed at this temperature, but the form of the transients (see figure 7.3) is neither constant nor in complete agreement with the theory developed in chapter 4. Typically the first and third extreme deflections are of similar magnitude, while the second is larger than (and opposite in direction to) them both. The

principal period and damping of the transients are as expected, but it seems that the first maximum is partially suppressed and that the phase of the oscillation with respect to the zero of time has not been correctly predicted. Caution is therefore necessary in the deduction of the size of circulation from an observed transient. The method adopted is to measure the maximum peak-to-peak deflection of each transient, ignoring the details of its form, and to calculate the apparent circulation γ quanta from the theory of chapter 4, according to which the peak-to-peak deflection at 1.30°K would be, by equation (4.51),

$$\frac{0.77\, D v_s \tau\, (1 - \rho^*)}{B}, \qquad (7.2)$$

where $D = \gamma . 2\pi\kappa . \rho_s$ is the coefficient characterising the Magnus force on a circulation of γ quanta. Because of the partial suppression of the first maximum of the transient, circulations calculated in this way are likely to be underestimated by a factor of at least 2. That is, the transient due to a completely attached vortex line would be ascribed to an apparent circulation of half a quantum or less: for partly attached vortex lines the definition of the size of the apparent circulation is in any case a matter of convenience. More quantitative results can be obtained if the transient deflection due to the action of a heat pulse on a given circulation can be compared with the steady transverse deflection in a uniform heat current. The latter does not depend on the viscous drag, but only on the known fibre con-

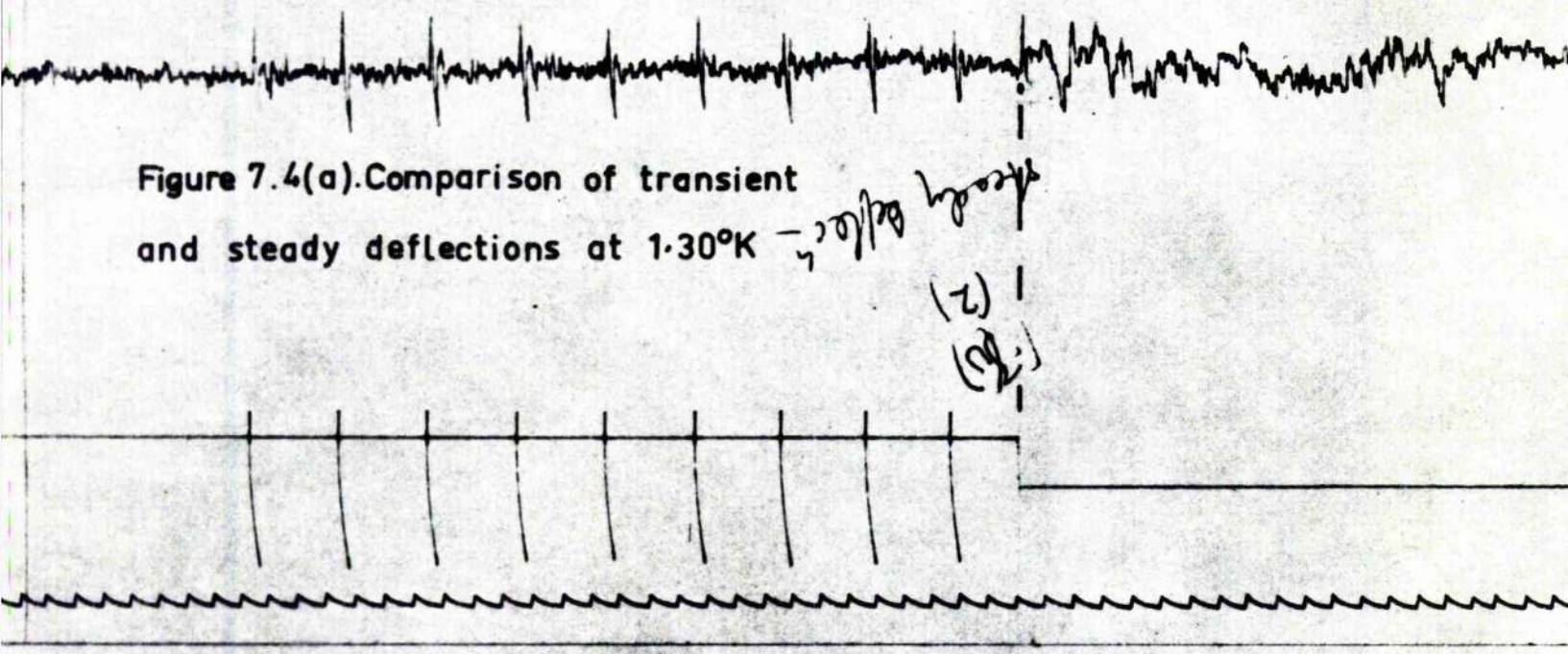

Figure 7.4(a). Comparison of transient and steady deflections at 1·30°K

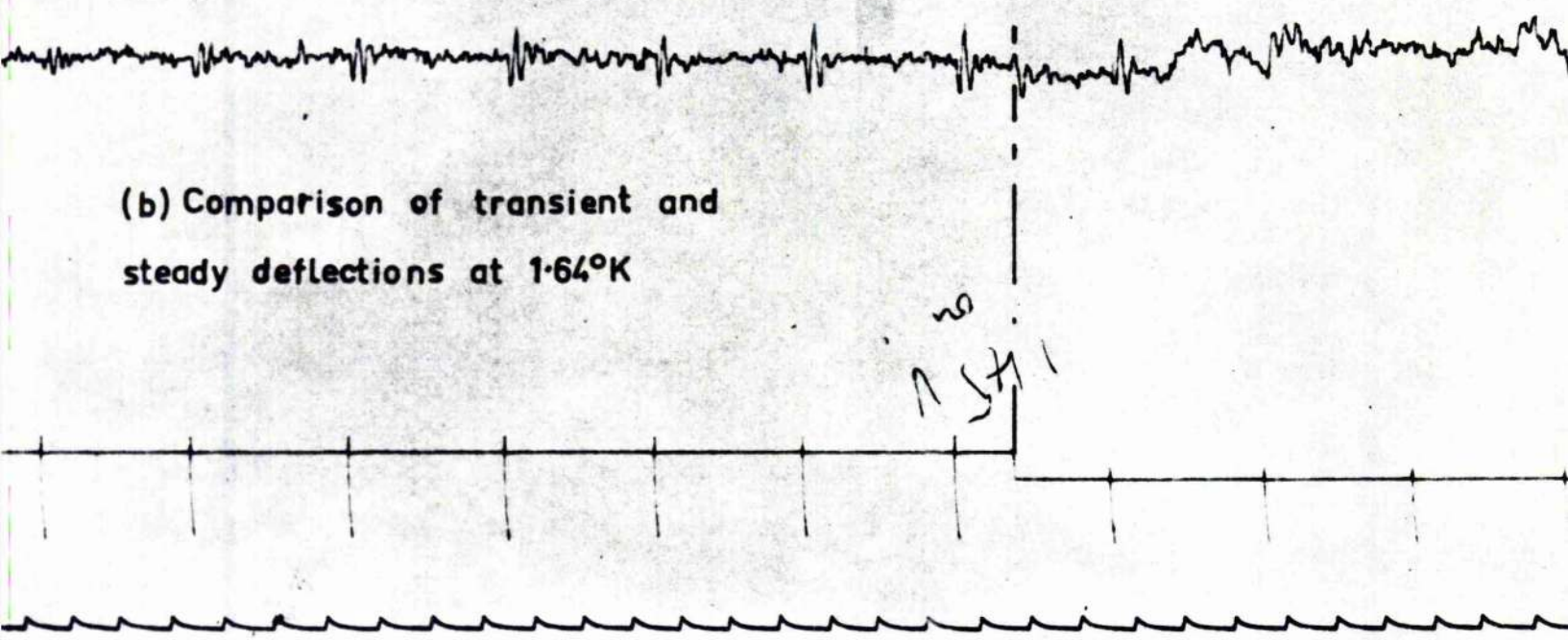

(b) Comparison of transient and steady deflections at 1·64°K

stants, the circulation and the superfluid density and velocity. Ideally we require to observe a series of identical heat-pulse transients, to switch on a heat current and observe the steady deflection, and then to superimpose at least one more heat pulse and verify that the circulation is unchanged. At 1.3°K this ideal is particularly difficult to attain because any heat current large enough to give a measurable steady deflection is inevitably highly supercritical (see below), and the steady deflection is quickly lost in general turbulence. Superposition of a heat pulse only precipitates the development of turbulence, so that the transient deflection due to the circulation cannot be checked after the heat current has been switched on. Only one successful comparison of transient and steady deflections has been made at 1.3°K. It is reproduced in figure 7.4(a), where the top trace is the signal from the bob, the middle trace shows the pulses and the steady heater voltage, and the sawtooth trace indicates seconds. Heater II and fibre II were used for this comparison, which is not very satisfactory, for the circulation had apparently started to decrease just before the heat current was switched on. The initial deflection of the transients and the steady deflection are in the same direction, as they should be, and the transient oscillation which accompanies the start of the steady deflection is also visible. The steady deflection itself lasts for about a second until the onset of turbulence. The circulation deduced by equation (4.54) from the last transient before the steady heat current is

$$\gamma_{transient} = 0.11 \text{ quanta.}$$

The circulation deduced from the steady deflection, assuming that the superfluid velocity profile is flat, is

$$\gamma_{steady} = 0.5 \pm 0.1 \text{ quanta.}$$

Hence

$$\gamma_{steady} / \gamma_{transient} = 4.5 \pm 1 \qquad (7.3)$$

If the optical axis and the axis of the tunnel are not exactly parallel, part of the apparent transverse deflection of the bob will be due to its downstream deflection by the normal fluid, and so this comparison will be in error. It is believed that the angle between the two axes is not greater than 2°, which would lead to a maximum error in the measured, steady transverse deflection equivalent to about 0.1 quanta of circulation at 1.3°K, and falling to 0.02 quanta at 2.1°K. That the misalignment is certainly no worse than this is confirmed by the fact that normally no steady deflection is detectable when a large heat current is switched on at 1.3°K, and that there is no response detected to the majority of heat pulses.

With fibre I and heater I it has been found that in undisturbed

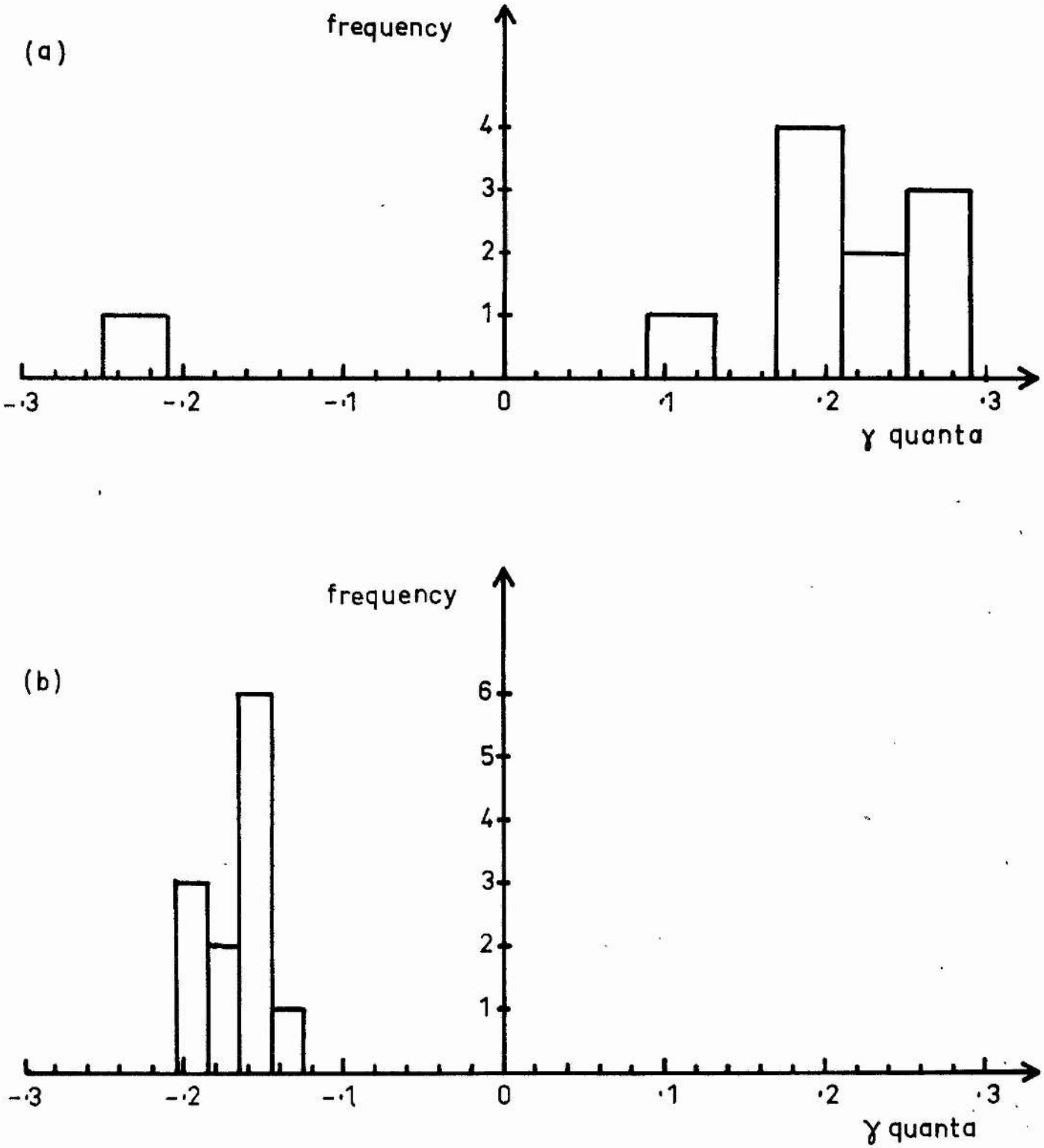

Figure 7.5. Histograms of persistent circulations at 1·3°K

(a) with heater I and fibre I;

(b) with heater II and fibre II.

helium (apart from disturbance due to the pulses themselves) there may be no detectable circulation about the fibre for long periods. A small circulation will eventually appear and gradually grow, sometimes decaying again, but often attaining a large value which then persists with some variation through perhaps twenty pulses or, if the pulses are interrupted, for a minute or more without pulses, before gradually decaying. Apart from their persistence the most striking aspect of the observed circulations is their directional bias: almost all are in the positive direction, corresponding, that is, to clockwise circulation about the fibre (viewed from above). The only exceptions occurred soon after a steady heat current in the tunnel.

Circulations which remain above 50% of their maximum value for more than thirty seconds are judged to be particularly persistent. A histogram of the apparent circulation deduced from the largest transient deflection attained by such circulations is given in figure 7.5(a). Some results obtained during very low, steady heat currents are also included on this histogram (see Section (c) below). The longest time for which a circulation has been observed to persist at above half-maximum is four and three quarter minutes.

There is a possible systematic error in the results of up to perhaps 25%, due to inaccurate calibration of the recording system and error in the weight of the nylon bob, while variation in the sensitivity of the system during the run leads to a random error of about 10%. There is a further possible random error of the same magnitude due to

instability in the length and height of the pulses. The spread of the values of γ within the maximum of the histogram is therefore hardly significant, and we may suppose that there is a single particularly persistent circulation, of apparent size

$$\gamma = (0.23 \pm 0.01) \text{ quanta}, \qquad (7.4)$$

the mean of the maximum of the histogram. There is an indication that $\gamma = -0.23$ quanta may also be persistent, once it has been established against the general bias. The value $\gamma = 0.12$ quanta is perhaps a sport.

Although it does not appear as such on the histogram, zero circulation is also a particularly stable value. No circulation, persistent or non-persistent, larger than the largest shown on the histogram has been observed with fibre I and heater I.

With fibre II and heater II similar results have been obtained at 1.3°K. The persistence of circulations is not quite so marked, and their bias is in the opposite direction. Circulations of opposite sense to the general bias in undisturbed helium again occur after steady heat currents. A histogram of the maximum value attained by circulations which remained above 50% of their maximum for thirty seconds or more is shown in figure 7.5(b). This criterion for persistence (slightly less stringent than that used with fibre I and heater I) is not ideal, although simple to apply, for some of the circulations satisfying it vary in a rather random way, while many of the largest circulations of

both senses grow and decay very smoothly, but do not persist long enough to satisfy the criterion. Nevertheless no circulation larger than the largest on the histogram has been observed. With this fibre and heater the longest time for which a circulation remained above half-maximum was two minutes.

Apart from the change of sign, the difference between the mean value of the maximum of this histogram

$$\gamma = -(0.17 \pm 0.01) \text{ quanta}, \qquad (7.5)$$

and that of the previous one (equation (7.4)) is not significant, as it could be due to errors in calibration and in the weights of the nylon bobs on fibres I and II.

(iii) Stability and persistence of circulation.

To facilitate comparison between results in different conditions a single number is required to express the stability and persistence of circulation. Such a statistic should preferably be independent of the average magnitude and bias of the circulation, reasonably stable in given conditions, and easy to calculate. It should not be too much affected by the fact that small circulations are lost in the noise. A suitable statistic has been found to be

$$r^* = \frac{\sum_n (x_n x_{n+1})}{\sum_n (x_n^2)}, \qquad (7.6)$$

where x_n is the peak-to-peak deflection of the nth transient (with appropriate sign). Equation (7.6) is a slightly modified serial correlation coefficient with lag one (Hoel 1954, p. 299). In the usual form of this coefficient the x_n would be measured from their mean value, but in the present case there is a known true zero, and we wish the results to be unaffected by bias about this zero. The modified form is therefore preferable.

r^* can vary from +1 (all x_n equal and in the same direction) to -1 (x_n equal and alternating in direction). If there were no directional bias the expectation value of r^* would be zero for completely random x_n. If there is bias the expectation value is finite and positive even when the x_n are random, although it is arguable whether the x_n can meaningfully be said to be both biased in direction and completely random. Ignoring this problem, it is easily shown that r^* is a measure of the persistence of circulation. For consider the series [0, 1, 0]. Here $r^* = 0$. For the series [0, 1, 1, 0] $r^* = \frac{1}{2}$; for [0, 1, 1, 1, 0] $r^* = \frac{2}{3}$; and so on. Hence $\frac{1}{1 - r^*}$ measures the average number of pulses for which circulation persists.

As a measure of the directional bias of circulation the statistic

$$S = \frac{\sum_n x_n}{\sum_n |x_n|} \qquad (7.7)$$

has been computed at the same time as r^*.

At 1.30°K, with no steady heat current flowing in the tunnel, the

following values of r^* and S have been obtained (in chronological order). With fibre I and heater I:

r^*	0.81	0.83†	0.86	0.94	0.69†	0.94
S	+1	-0.23	+0.52	+1	+0.41	+1

Results marked † were obtained immediately after the passage of a steady heat current. The last pair of results but one was obtained during the 200 sec immediately following a 2.9 mW/cm^2 heat current, and the last pair in the succeeding 300 sec. With fibre II and heater II:

r^*	0.92	0.82	0.92	0.90	0.84†
S	-0.97	-1	-1	-1	-0.38

The high values of r^* which can be obtained, and the opposite directional biases in the two apparatuses, are clear. There seems to be a definite association between low values of r^*, departures of S from its undisturbed value (+1 or -1), and heat currents in the helium. Towards the end of both runs, after many turbulent heat flows, the values of r^* and S characteristic of undisturbed helium, were not regained, even after waiting some hundreds of seconds.

(iv) Results at 1.64°K.

Typical transient forms appear in figure 7.2(a). Again the period and the damping are as expected, but the beginning of the transient is

not. The apparent circulation γ is estimated as before from the peak-to-peak transient deflection, and again we attempt to compare transient and steady deflections due to the same circulation. The one satisfactory comparison, using fibre I and heater II, is shown in figure 7.4(b). A heat pulse after the start of the steady heat current shows that the circulation is still there and probably not much reduced in size. We may therefore have confidence in the comparison, which gives, using equation (4.55),

$$\gamma_{steady}/\gamma_{transient} = 1.9 \pm 0.8, \qquad (7.8)$$

the uncertainty being mainly due to noise.

The observed apparent circulations range in size from zero up to about 0.1 quanta. Even allowing for the expected underestimation and possible calibration errors they fall short of one quantum. Except in a few instances the circulation about the fibre in apparently undisturbed helium was not very persistent, so that a histogram of the type plotted at 1.3°K is not possible. Nor was the directional bias very pronounced; indeed in the second run at this temperature it seems to have reversed during the run. Results from the first run are rather scanty because for long periods it proved difficult to observe any measurable circulation. The values of r^* and s are, in chronological sequence, with heater II and fibre I:

r^*	0.85	0.80	0.75
s	-0.37	-0.09	-0.34

with heater II and fibre II:

r^*	0.91†	0.72	0.80	0.79
S	−1	+0.03	+0.17	+0.97

The result marked † was obtained at the beginning of the run, before any steady heat current had flowed.

(v) Results at 2.10°K and 1.84°K.

At 2.10°K the theoretical peak-to-peak transient deflection is, by equation (4.58),

$$0.80\,\frac{D v_s \tau\,(1-e^*)}{B}.$$

On this basis apparent circulations of up to about $\frac{1}{3}$ quanta were observed at the start of the run with fibre I. For most of the remainder of the run very little circulation could be seen, so that there are too few data for reliable calculation of r^* and S. In favourable circumstances however high values of r^* were possible, although probably not as high as at the lower temperatures. With fibre I and heater II:

r^*	0.88	0.76	0.86
S	−0.63	−0.01	−1

The first pair of results was obtained near the beginning of the run.

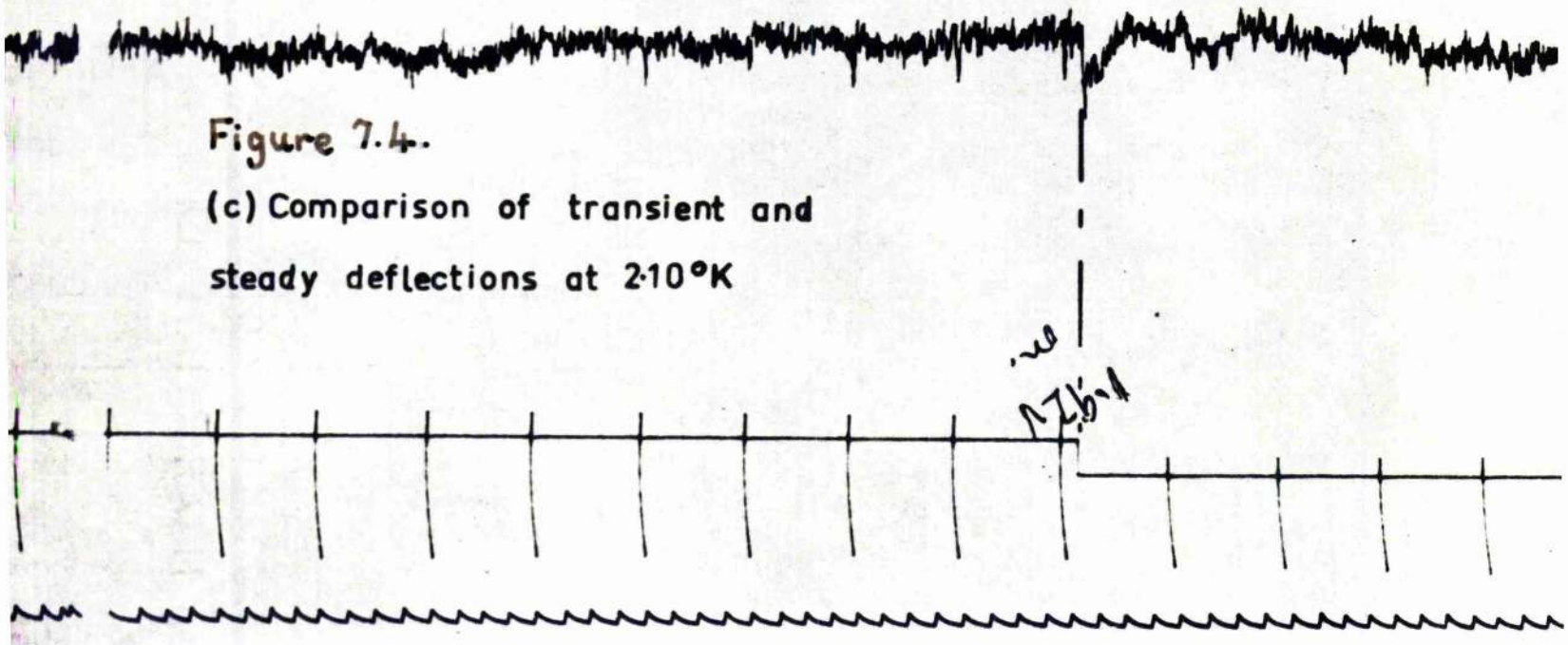

Figure 7.4.

(c) Comparison of transient and steady deflections at 2·10°K

In the run with fibre II no circulation was detected with subcritical heat pulses, although apparent circulations of 0.1 quanta would have been just visible above the noise. Since however the observations at this temperature were not begun until after a series of readings at 1.64°K, it is probable that the helium was already in the disturbed state, noticed at 1.64°K and in the previous run at 2.10°K, which is characterised by low values of r^* and rather small circulation about the fibre. Some circulation was present, for transients were sometimes seen when a heat current was switched on, but the transient response to subcritical heat pulses was lost in the noise. This lack of sensitivity arises because near the λ-point the passage between the Scylla of the noise level and the Charybdis of the critical pulse height is very narrow. In an effort to detect and measure circulation the temperature was reduced to 1.84°K, without success.

At 2.10°K there are three possible comparisons of the steady and transient deflections due to the same circulation. Of these one, shown in figure 7.4(c), is very satisfactory; the other two are consistent with it, but only their steady deflections are visible, the transients being below noise level. In the figure, after three similar transients, corresponding to an apparent circulation of 0.13 quanta, a steady heat current is switched on. After the initial transient there is a steady deflection, corresponding to a circulation of (0.55 ± 0.18) quanta, which lasts for about a second before falling smoothly to zero in a further second. The next heat pulse confirms that there is very little

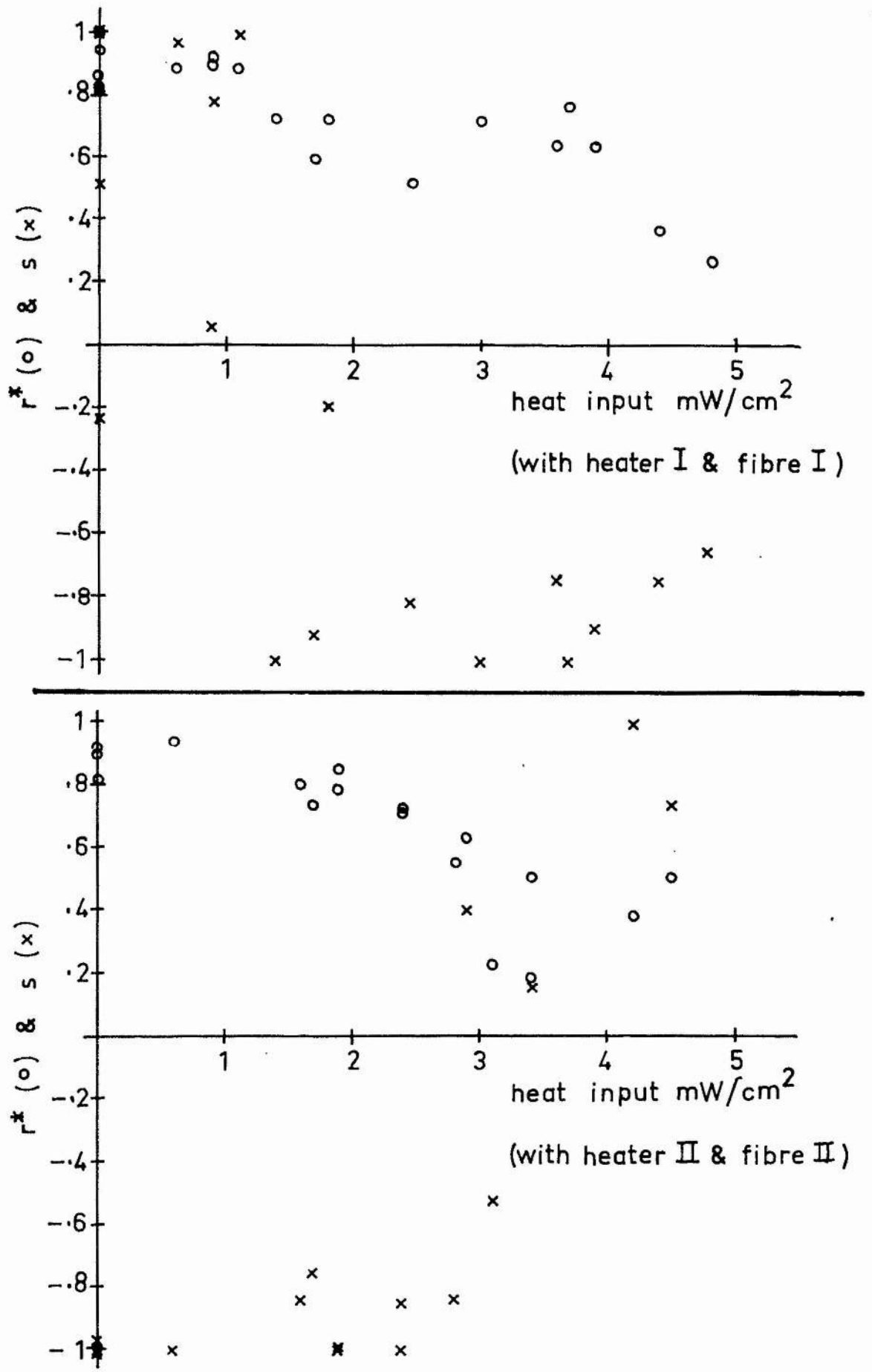

Figure 7.6(a). Circulation bias & correlation in heat currents at 1·30°K

remaining circulation, and the trace then becomes rather more disturbed. The ratio deduced from this comparison is

$$\gamma_{\text{steady}} / \gamma_{\text{transient}} = 4.2 \pm 1.4, \qquad (7.9)$$

which is similar to the value at 1.30°K (equation (7.3)).

The largest observed circulation, which is the maximum value attained by a circulation that remained above half-maximum for seventy seconds, one of the very few persistent circulations, occurred near the start of the run with fibre I. Its apparent size was 0.33 quanta, corresponding to a true circulation, by equation (7.9), of (1.4 ± 0.5) quanta. Within experimental error this may have been a single quantum of circulation, but if so it is the only example. All other circulations were less than $\frac{3}{4}$ of this size.

(c) Observations during steady heat currents

(i) Results at 1.30°K.

At this temperature very small heat currents have no detectable effect on the helium. The bob is not agitated and in tunnel II circulations of magnitude and directional bias similar to those in undisturbed helium have been detected by superimposed heat pulses; τ^* is at least as high as when there is no heat current. In heat currents above about $1\frac{1}{2}$ mW/cm^2[4] the circulation about the fibre is less persistent and the directional bias is reversed. This occurred in both runs at 1.3°K although the bias in undisturbed helium was opposite in the two cases.

[4] in tunnel I; 3 mW/cm^2 in tunnel II.

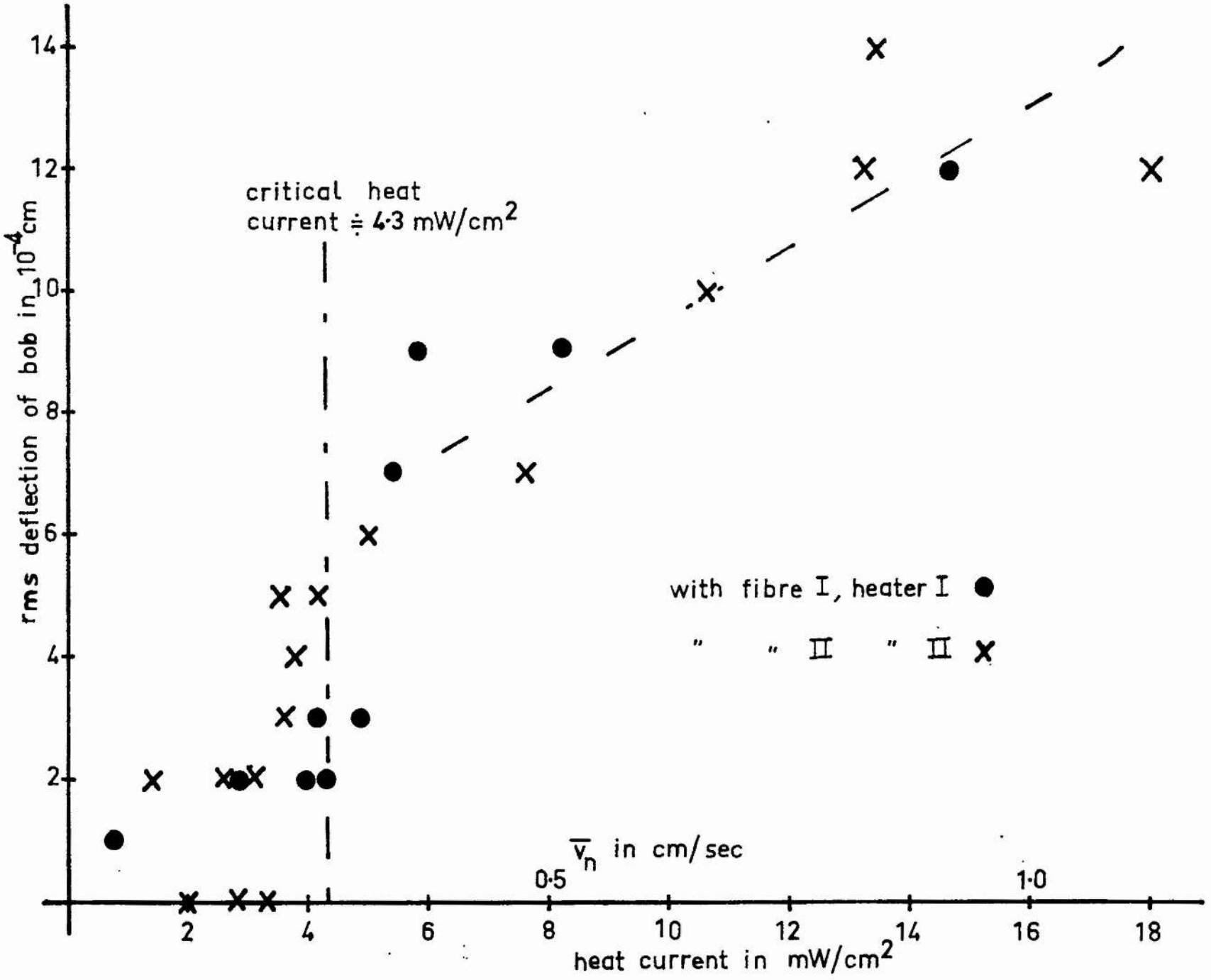

Figure 7.7 (a). rms deflection of bob vs. heat current at 1·30°K

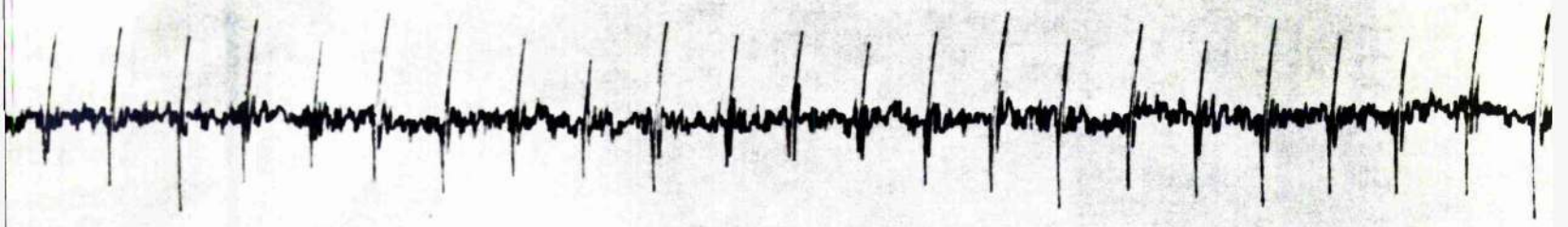

Figure 7·10. (a) Persistent circulation at 1·30°K

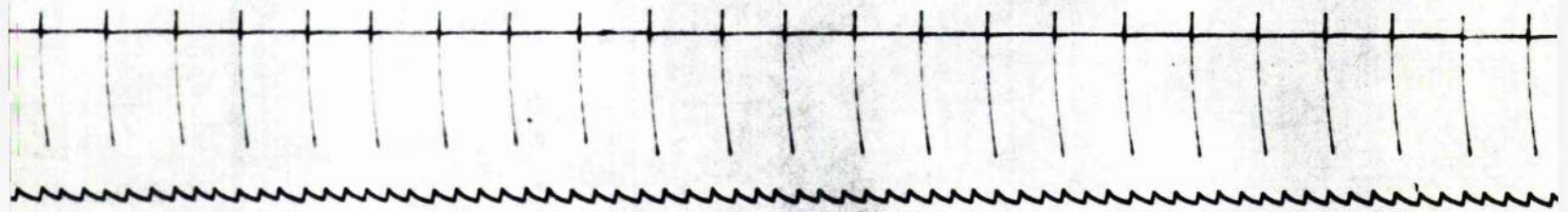

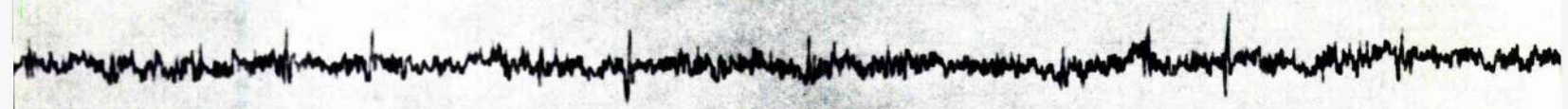

(b) Variable circulation during a heat current ($3{\cdot}1\ mW/cm^2$) at 1·30°K

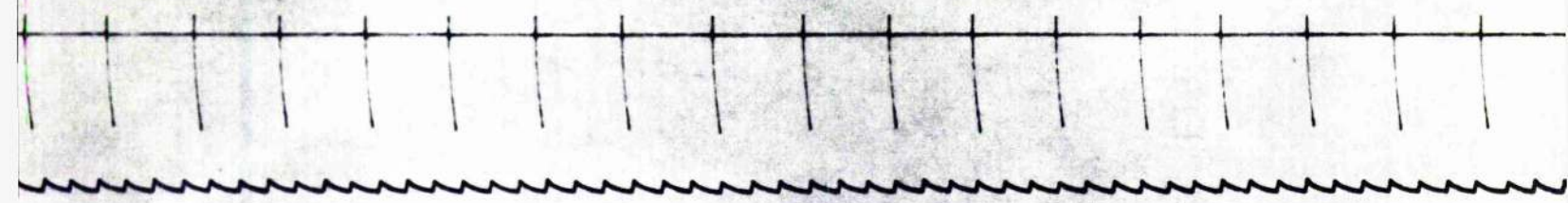

With increasing heat currents scattered values of r^* are obtained, with a general downward trend (see figure 7.6(a)), and the bob begins to be agitated between pulses. Eventually, over a short range of heat currents, any transient response to heat pulses becomes invisible in the random agitation of the bob, loosely referred to as turbulence. This turbulence increases in intensity with further increase of the heat current.

The rms deflection of the bob, which has been rather laboriously determined by sampling the pen records at 50 or 60 points for each heat current, is plotted against the heat current in figure 7.7(a). The mean square noise has been subtracted from the mean square signal-plus-noise, and the results from the first run have been scaled down by the factor (0.17/0.23 = 0.74) which is necessary to make the two circulation histograms agree (see equations (7.4) and (7.5)), and which we have ascribed mainly to calibration errors. The results in the two runs are in good agreement at high heat currents, and in both there is a sharp increase in the rms deflection of the bob at a heat current of 4 or 5 mV/cm^2. The difference between the two transitions is probably due to differences in the asymmetry of heaters I and II, as well as to the uncertain resistance of heater I (see above). Some of the points were obtained with superimposed pulses, some without. Just below the transition the pulses certainly contribute to the general agitation of the bob, as well as causing transient deflections. Well above the transition they have no detectable effect. Very near the transition

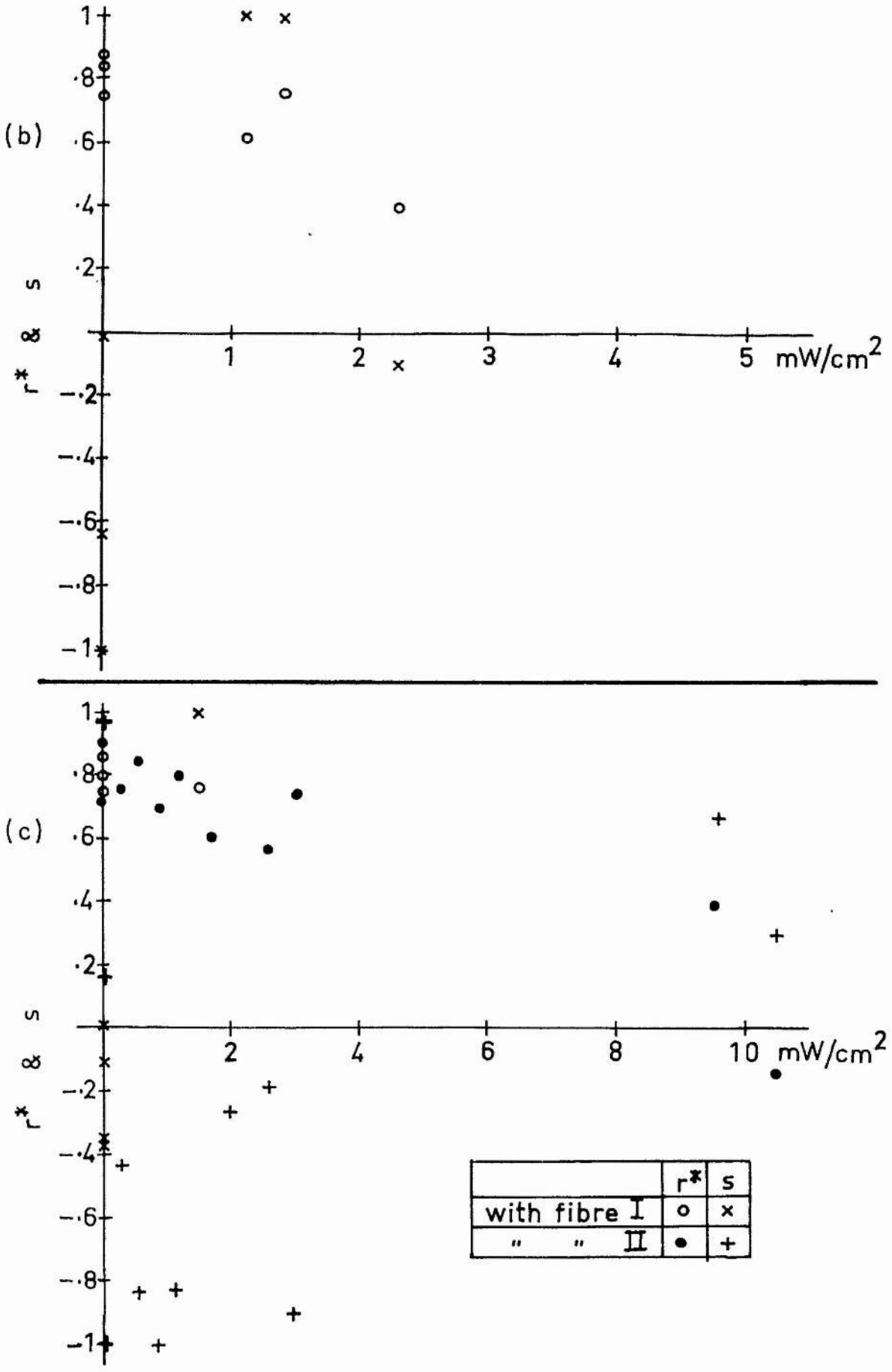

Figure 7.6. Circulation bias & correlation (b) at 2·10°K; (c) at 1·64°K

they reduce the delay time necessary for the development of turbulence (see below), and possibly are able to make heat flows turbulent which would not otherwise be so.

The scatter of the points below the transition can be accounted for by fluctuations in the noise level, and any genuine agitation of the bob is unfortunately masked. Inspection of the pen records suggests however that there is some agitation below the transition. This would not be surprising, for we know from the circulation results that the helium is modified below the transition. Even so, there is a definite, sharp increase in the rms deflection at a mean heat current of (4.3 ± 0.8) mW/cm^2. We shall refer to this as the transition to turbulence, and to the heat current at which it occurs as the critical heat current.

(ii) Results at 2.10°K.

At this temperature circulation correlation data during heat currents are scanty, and hence confused and unreliable. They are plotted in figure 7.6(b). Some of the points are based on as few as thirteen significant responses to heat pulses (repeated zeroes are ignored).

Turbulent agitation of the bob is detectable in heat currents above 80 mW/cm^2 (see figure 7.7(b)). The results of the two runs, in which different fibres but the same heater (II) were used, agree well with each other, but in both cases the noise level is such that the transition to turbulence, if it exists, is not detectable. A considerable amount of the rather high, variable noise level was due to low-frequency drift of the DC amplifier. It was this, rather than the photomultiplier noise,

Figure 7.7(b). rms deflection of bob vs. heat current at 2·10°K

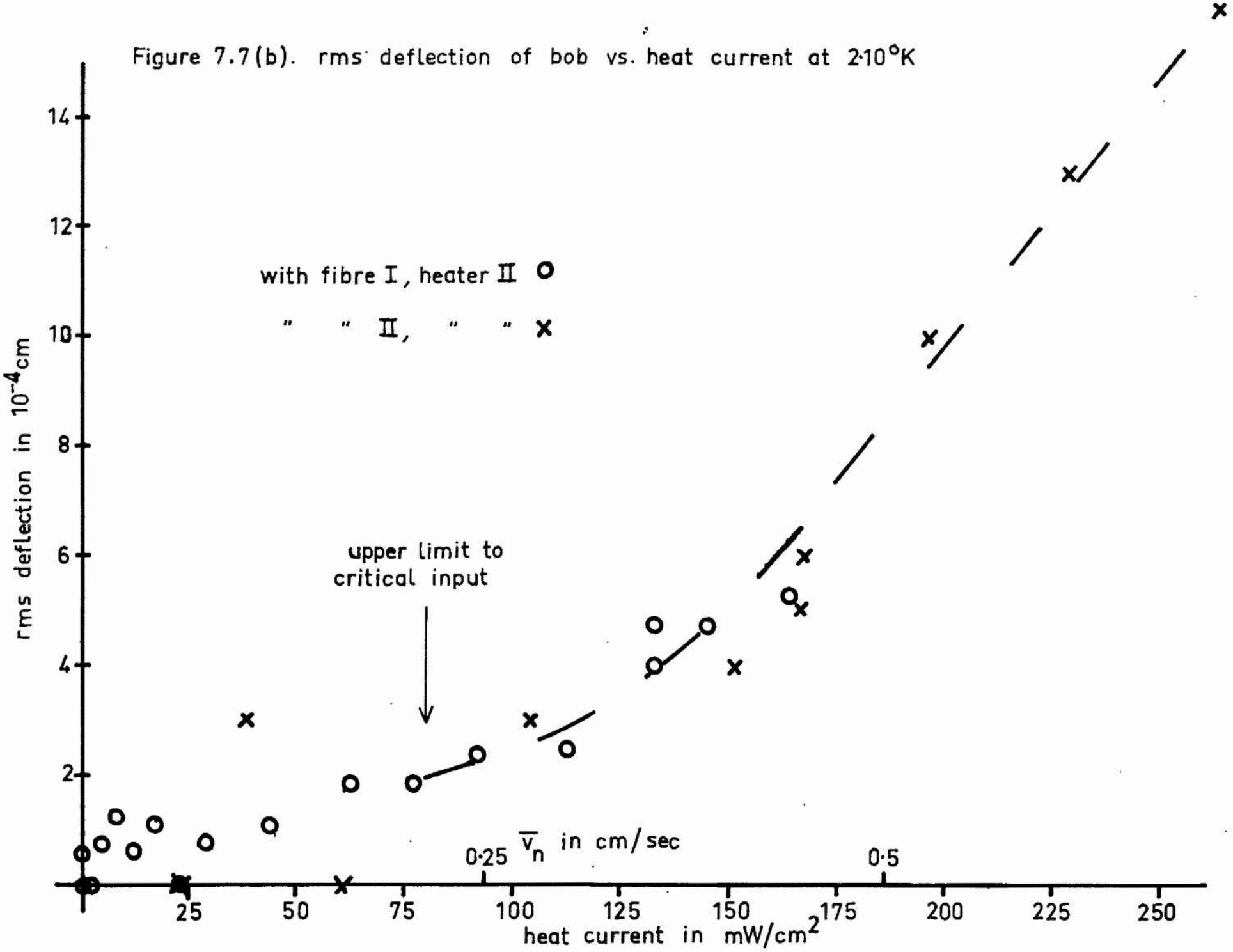

which limited the sensitivity of the apparatus at low heat currents.

(iii) Results at 1.64°K.

Circulation correlation results during heat flows are here confused because conditions with no heat current flowing were not reproducible. r^* and s are plotted against heat current in figure 7.6(c) for the two runs, with different fibres but the same heater (II). In both cases conditions at the beginning of the run are similar to those in the run at 1.3°K with heater II. The same high values of r^* and the same directional bias occur; there is slight evidence for a change in the bias in heat currents above about $1\frac{1}{2}$ mW/cm^2. The results from the rest of the two runs confuse this picture, but confirm that r^* tends to decrease with increasing heat current.

In heat currents above 10 mW/cm^2 random agitation of the bob is detectable, but increase of the heat current does not always increase the rms deflection of the bob. The flow is uneven, with bursts of violent agitation separated by long periods of relative quiescence. Agitation always occurs soon after switching on, usually after switching off, and occasionally during the flow, apparently at random. This behaviour is reflected in the scatter of the points in figure 7.7(c). Nevertheless the two runs gave consistent results, although the rms deflections deduced from the second run are uniformly higher than those from the first by a factor of about 1.4, ascribed to calibration errors. In heat flows above about 70 mW/cm^2 the bob is agitated continuously and uniformly, just as at 1.3°K and 2.1°K.

Figure 7.7 (c). rms deflection of bob vs. heat current at 1·64°K

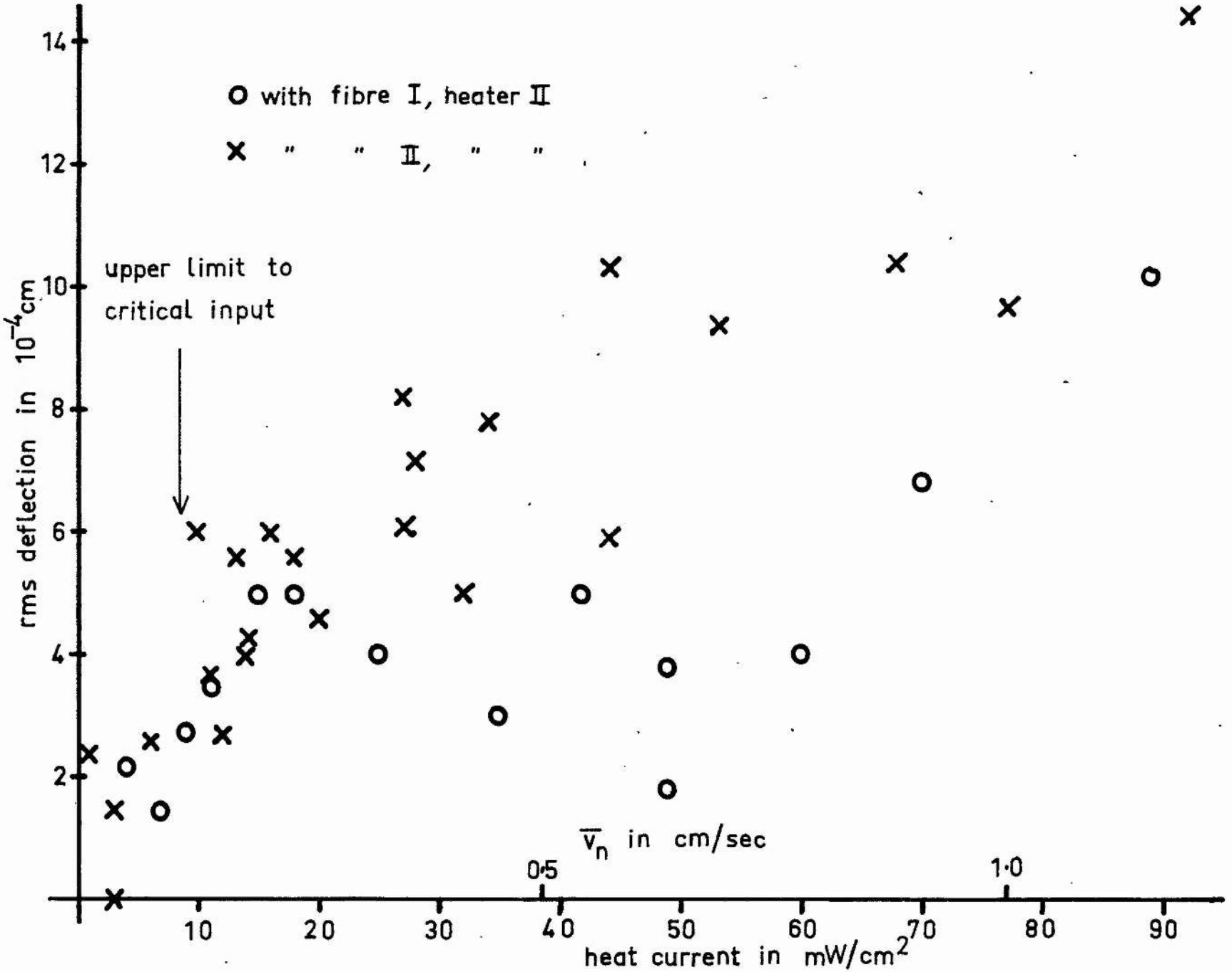

It has been confirmed by checking the calibration of the recording system during the heat current that the periods of quiescence are not caused by reduced sensitivity due, for example, to the bob's moving out of the illumination under the influence of normal-fluid drag. An example of a trace with quiescent periods is shown in figure 7.8, together with a fully turbulent one for comparison.

There is no conclusive indication of a sharp transition to turbulence at this temperature, but, if it exists, it must occur at a heat current below 10 mW/cm^2.

(iv) Results at 1.84°K.

At this temperature there are results from one run only, using fibre II and heater II. No circulation data have been obtained (see Section (b) (v)). The lowest heat current in which there is definite evidence of random agitation of the bob is 29 mW/cm^2, as shown in figure 7.7(d), where the rms deflection is plotted against the heat current. The general behaviour is similar to that at 1.64°K. In some heat currents above 29 mW/cm^2 the quiescent regime is so dominant that hardly any agitation of the bob can be detected above the noise. Even the initial and final bursts of turbulence are hardly visible. Again fully-developed turbulence seems to be established at very high heat inputs.

(v) Comparison with results in other wind tunnels.

In the original viscosity experiment which suggested the present experiment the observations on turbulence are not detailed. Turbulence

Figure 7.7 (d). rms deflection of bob vs. heat current at 1·84°K

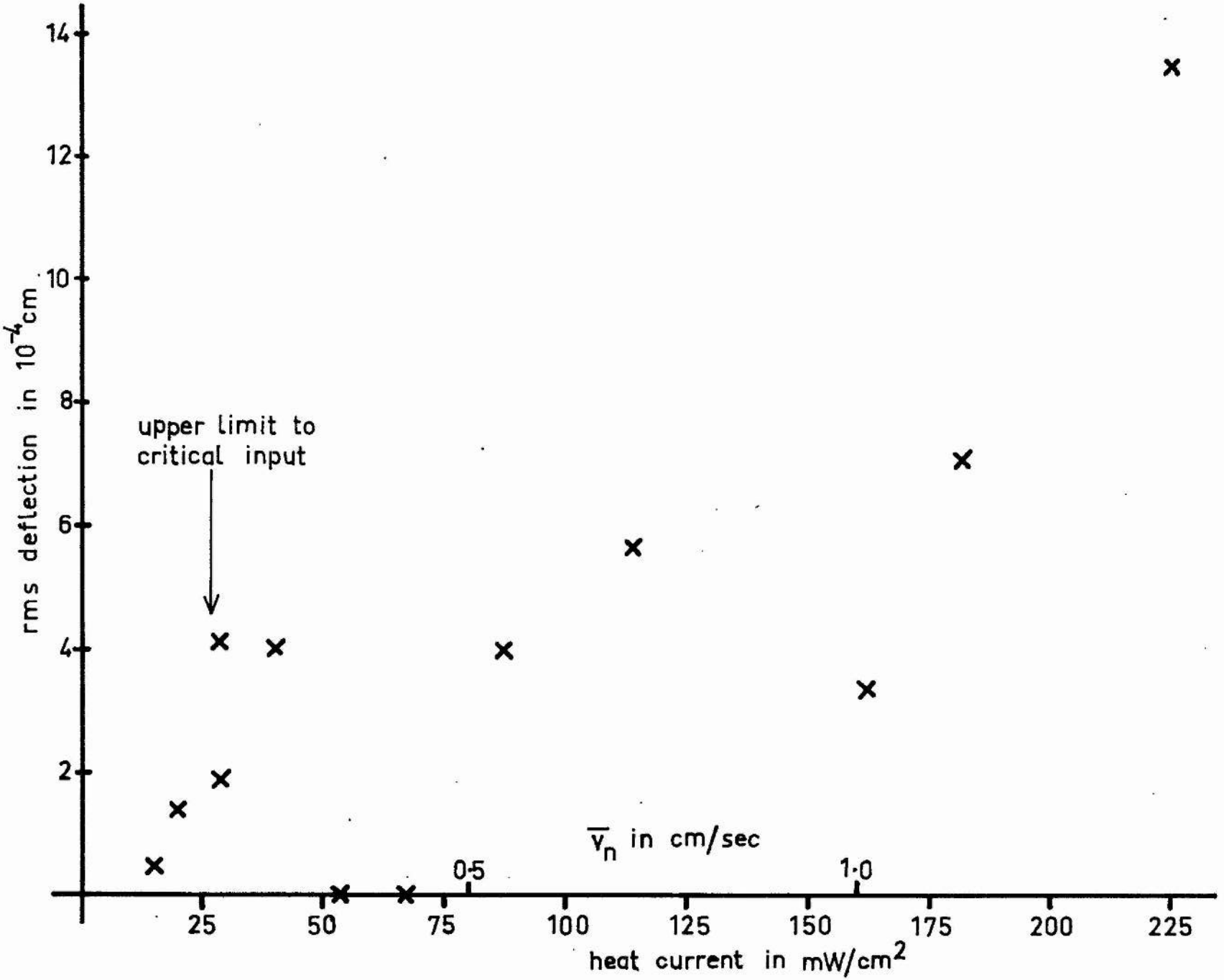

certainly occurred at heat inputs of a similar order of magnitude, and it was noted that the largest random deflections were of the same order of magnitude as the mean steady deflection due to viscous drag. All these deflections were of course in the direction parallel to the heat flow. A transition to turbulence was looked for, but if present it was at the extreme limit of sensitivity, and the viewing system was poor, since ripples on the helium surface introduced spurious movement of the image.

With tunnel I, described in chapter 6, in which transverse motion of the fibre was visually observed, the turbulent transition was again at or below the limit of sensitivity. It was found that at 1.3°K random motion of the fibre could just be detected down to 2 mW/cm^2. In very much higher heat currents the sizes of the largest sudden movements of the bob were noted. It was found that, within the rather large scatter of results, these jumps were proportional to the normal-fluid velocity, with a constant of proportionality not varying greatly with temperature between 1.25°K and 2.0°K. The characteristic alternation at intermediate temperatures of bursts of agitation with periods of quiescence was observed in this tunnel also.

From the results with tunnel II given above we find that the rms deflection of the bob in fully turbulent heat currents is roughly proportional to the heat current, with a constant of proportionality that is approximately

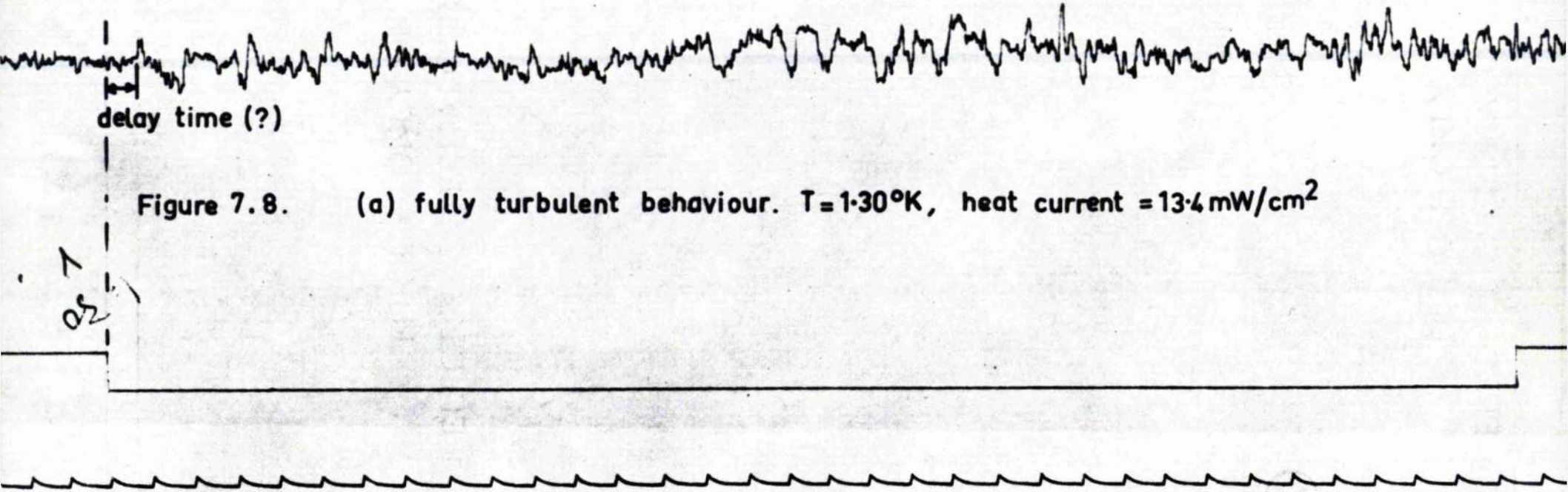

Figure 7.8. (a) fully turbulent behaviour. T = 1·30°K, heat current = 13·4 mW/cm^2

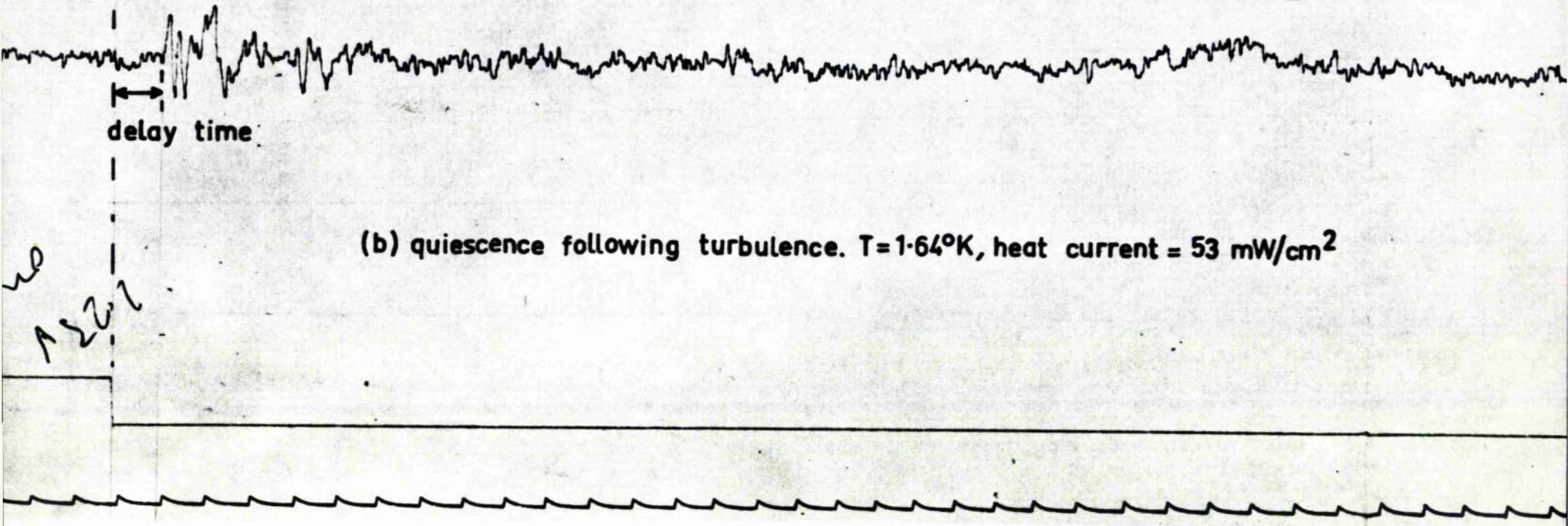

(b) quiescence following turbulence. T = 1·64°K, heat current = 53 mW/cm^2

$$\left.\begin{array}{l} 1.10^{-4} \text{ cm/mWcm}^{-2} \text{ at } 1.30^{\circ}\text{K} \\ 0.13.10^{-4} \text{ cm/mWcm}^{-2} \text{ at } 1.64^{\circ}\text{K} \\ 0.06.10^{-4} \text{ cm/mWcm}^{-2} \text{ at } 1.84^{\circ}\text{K} \\ 0.05.10^{-4} \text{ cm/mWcm}^{-2} \text{ at } 2.10^{\circ}\text{K} \end{array}\right\} \qquad (7.10)$$

Expressed in terms of mean normal-fluid velocity the constant of proportionality is

$$\left.\begin{array}{l} 1\tfrac{1}{2}.10^{-3} \text{ cm/cmsec}^{-1} \text{ at } 1.30^{\circ}\text{K} \\ 1.10^{-3} \text{ cm/cmsec}^{-1} \text{ at } 1.64^{\circ}\text{K} \\ 1.10^{-3} \text{ cm/cmsec}^{-1} \text{ at } 1.84^{\circ}\text{K} \\ 2.10^{-3} \text{ cm/cmsec}^{-1} \text{ at } 2.10^{\circ}\text{K} \end{array}\right\} \qquad (7.11)$$

In agreement with the observations in the other tunnels, (7.11) is almost independent of temperature.

(d) Delay and decay times for turbulence

When a supercritical heat current is switched on the bob is not immediately agitated (unless there is a transient followed by a steady deflection, associated with superfluid circulation about the fibre), but there is a delay time of the order of a second before turbulence is established (see figure 7.8). Since this delay is of the order of the period of the main turbulent fluctuations, the rms deflection does not rise smoothly to the value characteristic of the heat current, but

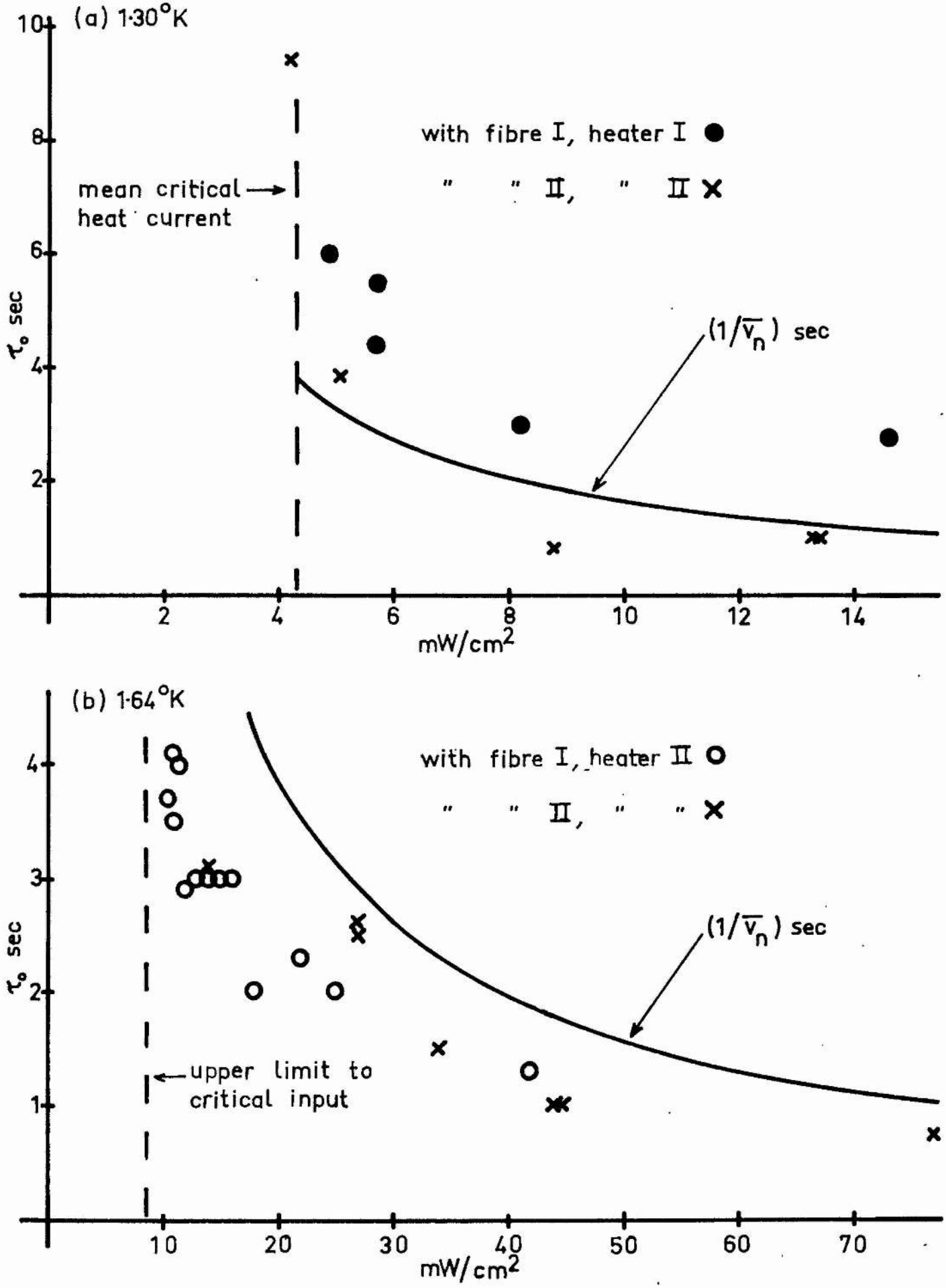

Figure 7.9. Delay time τ_o for turbulence vs. heat current

rather the first perceptible movement is in favourable circumstances the sudden onset of a large fluctuation. The delay time τ_0 is then well defined.

At 1.30°K τ_0 is not very reproducible, although there is a clear trend towards higher values as the heat current approaches the turbulent transition from above. There is some evidence that τ_0 is smaller when the helium has been recently disturbed by a heat current. In figure 7.9(a) only values obtained after the helium had remained undisturbed for more then 100 sec are plotted. It is possible that, by allowing the helium to remain undisturbed for much longer times, less scattered points could be obtained, but more likely that τ_0 is by its definition rather irreproducible, since it depends on detection of the bob's initial movement, which may sometimes be small.

At 1.64°K τ_0 is usually well-defined, and quite reproducible provided the helium has not been disturbed for a time of the order of twenty seconds. The values obtained are shown in figure 7.9(b). At the higher temperatures, where the ratio of the superfluid to the normal-fluid velocity is high, the Magnus force acting on the circulation about the fibre when the heat current is switched on may be large. It is often difficult to separate the effect of this force, which will vary if the circulation changes, from the onset of true turbulence. The delay time is therefore often ill-defined. It is possible to say only that at 1.84°K and 2.10°K the delay times τ_0 are probably of the same order of magnitude as at the lower temperatures.

When a turbulent heat current is switched off the large fluctuations of the bob die out in a time of order one to three seconds, often leaving a slow drift which lasts for about ten seconds. Although no further agitation of the bob can be seen, a time of 100 sec or more elapses at 1.3°K before the circulation correlation r^* and bias s return to the values characteristic of undisturbed helium. At higher temperatures the situation is more confused, and similar observations are not possible. During this period after a turbulent heat current, the little circulation that is visible is fleeting and of no clear directional bias. At 1.3°K after a medium heat current is switched off (i.e. a non-turbulent current in which r^* is low and the sign of s is reversed), the circulation correlation remains low and the bias reversed or uncertain for a time also of the order of 100 sec.

IV

Discussion and interpretation

These are deep waters; rest not there - reject
Conclusion ...

(Purgatorio VI, 43-44)

8. Discussion of results

(a) Superfluid circulation

(i) The form of the transient response to a heat pulse.

The variability of the form of the transient responses is not surprising, since we expect that a given fractional apparent circulation can arise in different ways, according to the position of the partly attached vortex line. It is more disturbing that even the transients associated with circulations which are believed to be quite close to one quantum have a form different from that predicted in chapter 4. The obvious explanation is that our small-circulation approximation is not valid and that precession is changing the form of the transient, but since even the smallest transients differ in a similar way from the predicted form, this explanation seems implausible.

Another possibility is that the viscous drag on the bob, which was neglected in the boundary condition for the free end of the fibre, equation (4.11), is not in fact negligible. Remembering from chapter 4 that the principal period of the fibre is about $\sqrt{2}$ times that of a simple pendulum of the same length, the approximate equation of motion of the bob is

$$M\ddot{y} + C\dot{y} + \frac{T}{2l}y = 0 \qquad (8.1)$$

with the notation of chapter 4, where C is the viscous drag coefficient which was there neglected. For low Reynolds' numbers $C = 6\pi\eta_n a$,

where $a \doteq 0.6.10^{-2}$ cm is the radius of the spherical bob. Hence $C \sim 1.10^{-6}$ to 2.10^{-6} dyne-sec/cm between 1.3°K and 2.1°K, while $\frac{4MT}{2L} \sim 2.10^{-9}$ [dyne-sec/cm]^2. Therefore

$$C^2 \ll \frac{4MT}{2L}, \tag{8.2}$$

which implies that the bob is very lightly damped. The viscous drag on it can therefore safely be neglected.

Associated with partly attached quanta of circulation are free vortex lines which terminate on the fibre. These lines behave as if they are under a tension (Hall 1958) which must deflect the fibre and might alter the form of the transient. The tension is equal to

$$\pi \rho_s \kappa^2 \ln b/a_0 , \tag{8.3}$$

where $2\pi\kappa = h/m$ is the circulation about the vortex line, b is a macroscopic dimension, and a_0 is the effective vortex-core radius. Typically the tension is about 2.10^{-7} dyne, which could deflect the bob at the most only two or three microns, an almost undetectable movement. This tension could not significantly alter the form of the transient.

A possible cause of departure from the theoretical behaviour is the short stub of fibre (about $\frac{1}{2}$ mm) unavoidably left projecting below the nylon bob. This must increase the damping and also sometimes the

Magnus force, when there is circulation about it. It is difficult to see how it could greatly alter the form of the transient.

The most likely cause of the unexpected transient form is the following. The viscous drag on a long, circular cylinder depends on the establishment of a rather special flow pattern round the cylinder (Lamb 1945, p. 614). In oscillatory motion the flow pattern and the drag coefficient are functions of frequency (see equation (4.42)), and their establishment at the start of the oscillation must take a time of the order of the period of oscillation ($\frac{1}{5}$ sec in the experimental conditions). Until then the damping varies with time in a complicated way (e.g. Fromm and Harlow 1963). It seems plausible that such a complication could partly suppress the first maximum, and reduce the scale and alter the phase of the remainder of the transient. At 1.30°K the fact that the mean free path of the phonons is about equal to the fibre diameter may introduce additional complications (see appendix I).

(ii) The directional bias of circulation.

In undisturbed helium at 1.5°K the circulation bias was reversed when the heater and fibre were changed. Results at higher temperatures suggest that the bias is associated with the heater rather than with the fibre. It was at first thought that the bias might depend on the overall asymmetry of the heater. The resistance of the left side of heater I, and hence the heating there, is greater than the resistance of the right side (see figure 8.1(a)). At the heater the mean superfluid velocity must be greater in the left half of the tunnel than in the

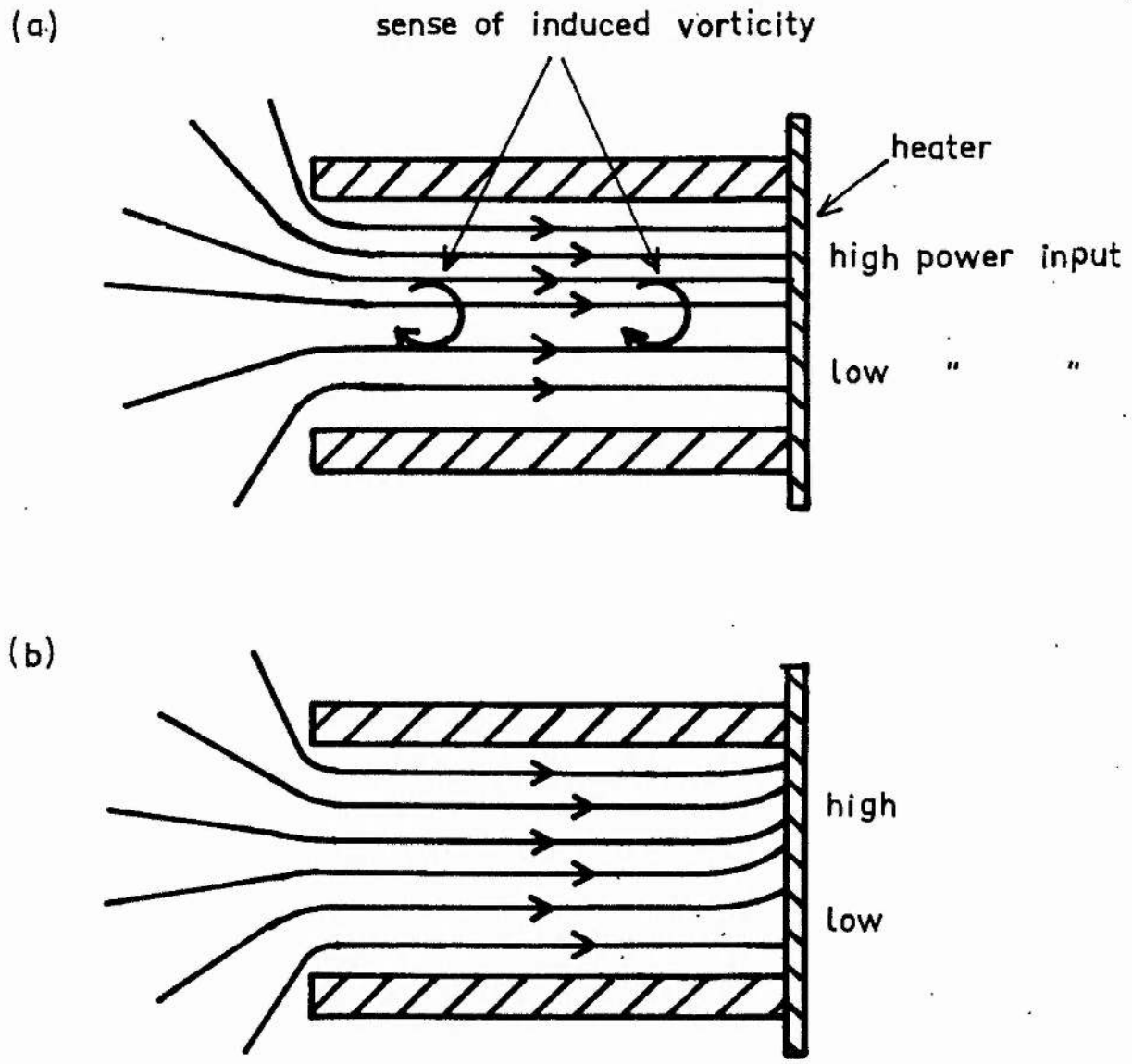

Figure 8.1. Possible superfluid flow patterns in a tunnel with an asymmetrical heater :

(a) flow without change of velocity profile, showing induced vorticity ;

(b) potential flow, showing curvature of streamlines

right. If this velocity difference is propagated along the tunnel in the heat pulses, vorticity is generated in the superfluid, and vortex lines might be formed with a preferred orientation by a mechanism of the sort suggested in chapter 9(b). This idea predicts the correct bias for heater I, but with heater II, which has similar asymmetry, circulations of opposite bias are observed. The bias must therefore depend on less obvious aspects of the heater geometry, although it is suggested that there must be some generation of superfluid vorticity by the heat pulses to explain the results.

An allied problem is that of the superfluid velocity profile. If the heater were uniform the profile would be flat. There is no reason for it to depart from flatness unless mutual friction operates, and since it is the contention of this thesis that mutual friction is associated with turbulence of the whole fluid, which probably does not occur in subcritical heat pulses, no mutual friction is expected in such pulses. However the heater is not uniform, and we do not know whether the velocity profile at the heater is propagated along the tunnel unaltered, or whether the superfluid is able to flow without vorticity, which would imply the gradual flattening of the profile as the pulse propagated along the tunnel. Hence the superfluid velocity at the fibre, and therefore the circulation, are uncertain.

(iii) The size of observed circulations.

Problems of deduction of the size of circulations from the observed transients can be overcome if accurate comparison of steady and transient

deflections can be made. Apart from the practical difficulties there is again the difficulty that for a non-uniform heater the superfluid velocity profile at the fibre is not accurately known. Since steady deflections can be measured only in non-turbulent conditions, mutual friction is again unable to distort the velocity profile.

The one comparison (equation (7.3)) of steady and transient deflections at 1.3°K is not very trustworthy. Nevertheless it is possible, within the experimental error, that the two particularly persistent circulations which appear on the histograms (figure 7.5 and equations (7.4) and (7.5)) correspond to true circulations of one quantum in opposite senses. On the vortex-line hypothesis such circulations are stable because a short, straight length of vortex line can carry the circulation about the fibre from the bob to the floor of the tunnel, while for smaller circulations the vortex line has to take up a configuration similar to that considered in appendix II(d), where it is shown that in the experimental apparatus such configurations are probably less stable.

Although this piece of evidence for quantization of circulation is too qualitative to be conclusive, it must be emphasised that the general behaviour is exactly as predicted on the vortex-line hypothesis by the calculations of chapter 3. Circulations up to, but probably no greater than, one quantum have been observed from 1.3°K to 2.1°K, and have persisted for up to four and three-quarter minutes. The sizes of the circulations are such that the superfluid velocity at the surface of the fibre is several cm/sec. It has been confirmed by observing the steady

deflection of the bob in heat currents that the transients are indeed due to circulation about the fibre. The slow variation in the size of a given circulation can plausibly be interpreted as the pealing of a vortex line on and off the fibre, aided by the repeated disturbance due to the measurement process itself.

(b) Subcritical heat currents and superfluid vorticity

(i) The effect of heat currents on the observed circulation.

At 1.3°K the behaviour of circulation in heat currents from zero up to $1\frac{1}{2}$ mW/cm^2 is constant. The superfluid is apparently moved bodily along the tunnel without essential modification, that is, without generation of extra vorticity. Because of the bias of the observed circulations, the vortex lines in the superfluid must have a preferred orientation. There can therefore be few of them, since otherwise they would quickly become tangled and randomly orientated, and, by chapter 3(e), the mean circulation about the fibre would be both small and variable.

In heat currents above $1\frac{1}{2}$ mW/cm^2 the circulation does become more variable. This would not in itself be remarkable, if it were not for the simultaneous reversal of bias. The clear implication is that superfluid vorticity is being generated, and the fact that it is not randomly orientated, but of the opposite sense to the natural bias with both heaters, suggests that not turbulence but secondary flow is occurring in the superfluid. The orientation of the superfluid vorticity generated in the secondary flow probably depends on the same aspects of the heater asymmetry as does the natural bias in undisturbed helium, and may be

$\frac{1}{4}$ in tunnel I; 3 mW/cm^2 in tunnel II.

associated with a progressive change in velocity profile as the superfluid approaches the irregularities of the heater. Any such change of profile involves flow of the superfluid across the tunnel, as shown in figure 8.1(b), and it is known from classical hydrodynamics that such a situation favours secondary flow.

The mean superfluid velocity corresponding to a heat input of 3 mW/cm^2 at 1.3°K is 10^{-2} cm/sec. There is slight evidence for similar behaviour above a heat input of $1\frac{1}{2}$ mW/cm^2 in tunnel II at 1.64°K, corresponding to a superfluid velocity of 5.10^{-3} cm/sec. It therefore appears that secondary superfluid flow occurs in the experimental apparatus at mean superfluid velocities above about 10^{-2} cm/sec, depending perhaps on temperature and probably upon the geometrical details and imperfections of the apparatus, since the higher velocity is associated with the more symmetrical heater. It is likely that the subcritical turbulence detected by Vinen (1957d) was also superfluid vorticity generated by secondary flow. His published results suggest that between 1.4°K and 1.6°K secondary flow occurred in his apparatus no. 1 at mean superfluid velocities above 0.04 cm/sec. This apparatus was a long counterflow tunnel of rectangular cross-section 0.24 x 0.645 cm, opening at one end into a chamber in which was a heating coil. Its geometry is therefore quite different from that of the present apparatus.

(ii) The decay of superfluid vorticity.

At 1.3°K the reverse bias and low correlation of the circulation about the fibre remain for 100 sec or more after the end of a heat

current in which superfluid vorticity has been generated. This time is similar to that noted by Vinen (1957b) for the complete decay of turbulence in the helium. After a fully turbulent heat current the circulation is small, variable and of uncertain bias for a similar time. According to chapter 3(e), this indicates that a tangled array of vortex lines is present, taking at least 100 sec to decay. In runs at higher temperatures initial conditions were similar, but, once generated, superfluid vorticity decayed very slowly, if at all. This may be due to the inevitable steady heat leak into the helium, whose disturbing effect could well increase with temperature and with decreasing volume of helium - i.e. towards the end of runs, as observed.

(c) Supercritical phenomena

(i) Nature of the turbulence.

A Fourier analysis of the deflection of the bob in fully turbulent heat currents has not been attempted, but it is clear that a large contribution to the rms deflection comes from fluctuations which have a period comparable with D/v_n, where D is the width of the tunnel ($\sim$1 cm) and v_n is the mean normal-fluid velocity. D/v_n is of the order of 1 to 10 sec at all temperatures in the supercritical heat currents observed experimentally, while the comparable quantity for the superfluid, D/v_s, varies from ~ 0.1 sec at 1.3°K to $\sim$10 sec at 2.1°K. There is no sign of such a temperature dependence in the experimental

results.

The relation (7.11) of the rms deflection of the bob to the normal fluid velocity is almost exactly that given in equation (5.7), which was calculated on the assumption that the normal fluid was turbulent. Even the temperature variation due to the viscosity is reproduced, probably fortuitously. It follows that at the transition the normal fluid becomes turbulent. The observation reported in Section (b) (ii) that random vorticity is present in the superfluid after a supercritical heat current suggests that the superfluid also becomes turbulent at the transition. The implication is that in supercritical heat currents the whole fluid is turbulent.

(ii) Quiescence in supercritical heat currents.

The alternation of bursts of fully-developed turbulence with periods of quiescence was observed in supercritical heat currents at 1.64°K and 1.84°K. The fibre is more sharply tuned at these temperatures that at 1.3°K and 2.1°K (see equation (5.2)), because of the variation of viscosity with temperature. Nevertheless it is difficult to see how this could produce such a marked effect.

Quiescent behaviour would occur if the turbulence in the normal fluid were for some reason not fully-developed, so that it contained no large eddies, but only a large number of smaller ones, whose average effect on the fibre would be small. It is possible that quiescence is related to the observations by Vinen (1957a-d) and Chase (1962) that the critical heat input was less well defined in this temperature region,

especially in wide channels. Chase found that the critical heat input again became sharp near the λ-point; similarly, no quiescent behaviour was observed at 2.1°K.

(iii) Delay times for turbulence.

The history-dependence of the delay time τ_0 for the onset of turbulence is behaviour well-known in classical hydrodynamics. The delay times measured at 1.3°K and plotted in figure 7.9(a) are believed to be characteristic of undisturbed helium. The dependence of τ_0 on the heat current is qualitatively similar to that found by Vinen (1957b) but the absolute magnitude is uniformly lower by a factor of about 20. At 1.64°K it is believed that the superfluid was nearly always slightly disturbed. The behaviour of τ_0 is however quite reproducible, and similar to that at 1.3°K (see figure 7.9(b)).

It has been reported by Mendelssohn and Steele (1959) that turbulence fronts are propagated from the heater along a rather narrow counterflow channel in supercritical heat currents. If a similar phenomenon occurs in the present experiment the delay time is simply the time taken for the turbulence front to reach the fibre. In order to explain the results the velocity of propagation of the front must depend on the heat current and the history of the helium, and we should expect the delay time to depend on the distance between the fibre and the heater. This could be checked experimentally.

The large difference between τ_0 in the present apparatus and in Vinen's apparatus is probably due to differences in geometry, and also

in the definition of τ_0, since his delay time is obtained by measurement of second-sound attenuation, while in the present experiment is found by direct observation of the onset of normal-fluid turbulence. If the idea of a turbulence front is correct it would take a longer time to fill Vinen's long channel with turbulence than to reach the fibre in the present apparatus.

During the heat pulses which are used to measure circulation about the fibre a highly supercritical heat current flows. Associated with this must be a short delay time τ_0 for the onset of turbulence. Clearly, if the length τ of the pulse is greater than τ_0, the pulse will disturb the helium. It seems likely that this is the explanation of the critical pulse height reported in chapter 7(b) (i), equation (7.1). If turbulence is propagated from the heater behind a front, all reasonably large pulses will generate some turbulence near the heater, and the apparent critical pulse height will be reached when this turbulence extends as far as the fibre. On the other hand, if turbulence builds up throughout the fluid, the critical pulse height will be genuinely characteristic of the helium: in subcritical pulses no turbulence occurs, in supercritical pulses it does occur. In this case we would expect a sharp increase in the attenuation of pulses at the critical height. Such an increase should have been detected by second-sound techniques; that it has not been detected, as far is known, supports the idea of a turbulence front. It should be mentioned that the rise-time of the pulses is deliberately made too long for shock-wave phenomena of the

type described by Osborne (1951) to occur.

In classical turbulent flow turbulence usually builds up in the following way. At the inlet to the channel the flow is laminar, and it remains so until after a certain 'inlet length', turbulence suddenly sets in (Prandtl 1952, p. 167). The inlet length depends not only on the diameter of the channel and the Reynolds' number of the flow, but also very markedly on the perturbations which are impressed on the flow at the inlet to the channel. In short channels turbulence cannot be observed in nominally supercritical flows unless the inlet length L is less than the length of the channel. Because fluid entering the channel does not become turbulent until it has travelled a distance L, the delay time τ_0 for the build-up of turbulence at the start of the flow must be of order L/v, where v is the mean velocity of the fluid (Vinen 1957b). i.e.

$$L \sim v\tau_0 \quad . \qquad (8.4)$$

In Vinen's experiment the quantity $v_n\tau_0$ was always comparable with or greater than the length of the channel. Therefore, he argued, there can be no inlet length associated with the normal fluid. The quantity $v_s\tau_0$ was less than the length of his channel, and he suggested that any inlet length must be associated with the superfluid, and that therefore the turbulence associated with supercritical heat currents was in the superfluid. Yet we shall see that the normal fluid was almost

certainly turbulent in this experiment too. It is therefore suggested that the concept of an inlet length is not applicable in counterflow tunnels, and that the idea of a turbulence front is more fruitful.

In the present experiment the quantity $v_n \tau_0$ was of the order of 1 cm, the distance from the heater to the fibre, as shown in figures 7.9(a) and (b), where the quantity $1/v_n$ sec is plotted along with the observed values of τ_0. This suggests that in supercritical currents the turbulence front is propagated downstream with a velocity similar, but not exactly equal, to the mean normal fluid velocity.

(iv) The decay of turbulence in the normal fluid.

After a turbulent heat current is switched off the major fluctuations of the bob die out in a time which is not very well defined or reproducible, but which lies between one and three seconds, independently of the value of the preceding heat current. There sometimes remains a slow fluctuation which decays in about ten seconds, and thereafter only the superfluid vorticity, which has already been discussed, is present. If we make the reasonable assumption that these times are all much longer than the time taken to discharge the thermal capacity of the heater when the current is switched off, this behaviour must be characteristic of the decay of turbulence in helium.

According to Batchelor (1953, p. 92; and others), in a turbulent classical fluid it is the smallest eddies which decay first, eventually leaving only the very largest (and hence most slowly varying). From our observations, turbulence in the normal component of helium II behaves

in just this classical way: after the decay of the small, fast eddies the remnants of the largest eddies originally present in the flow cause the slow fluctuation of the bob.

(d) The critical heat input

The results of Staas, Taconis and van Alphen (1961), referred to as STA, have been outlined in chapter 2(b). They measured the pressure gradient in various types of flow and found that their results fitted the known empirical relation between pressure gradient and mean velocity for a turbulent classical liquid of viscosity η_n, density ρ and mean velocity v_n. By equation (2.5) the pressure gradient is not directly dependent on the mutual friction. STA also measured the temperature gradient in turbulent flow and showed that mutual friction was necessary to explain the results (see equation (2.6)): normal-fluid turbulence alone was insufficient. They found that the flow was always potentially turbulent, independent of superfluid velocity, if the Reynolds' number Re_v exceeded 1200. Re_v, which is defined in equation (2.14), depends ~~not~~ on the normal fluid velocity, but the total fluid density.

Chase's (1962) results have also been noted in chapter 2(b). He found that the critical velocity for turbulent flow was given by

$$Re_v \doteq 2600\text{--}2300 \qquad (8.5)$$

from 1.2°K to 1.6°K. Above 1.6°K the critical value of Re_v fell roughly linearly with temperature to zero at the λ-point. In fact most

of the results were obtained not by direct measurement of the temperature gradient, but by a rather sophisticated technique involving the measurement of the delay time for the build-up of mutual friction in a highly supercritical heat current. This technique, which is due to Vinen (1957b,d), is described in chapter 2(b). The results were confirmed by direct measurement of the temperature gradient in the smallest channel (0.08 cm diameter), and it was found that no mutual friction was detectable below the critical heat input. Chase's tentative conclusion was that below 1.6°K mutual friction is associated with turbulence in the normal fluid or in both fluids, with possibly another mechanism operative near the λ-point. The observed blurring of the transition in the middle temperature range would then be associated with the change-over from one mechanism to the other.

Chase has pointed out in a private communication, and as far as possible it has been confirmed by the present author, that for the published measurements of mutual friction in heat currents Re_v is greater than the critical value. This is certainly true of nearly all the results quoted by Gorter and Mellink (1949) in wide ($>10^{-3}$ cm) capillaries. In one of their sets of results, in a capillary of 0.34 mm diameter at 1.61°K, a sharp decrease in the mutual friction below $Re_v \doteq 2500$ is clearly visible. In some other measurements in narrow capillaries, where a critical velocity for the onset of mutual friction has been determined, the critical value of Re_v calculated from the published data seems rather low: e.g. $Re_v^{\text{critical}} \doteq 150$ at 1.72°K in a

capillary of diameter $2.4.10^{-4}$ cm (Winkel et.al. 1955); $Re_v^{critical} \doteq$ 240 at 1.84°K in a capillary of diameter 5.10^{-3} cm (Brewer, Edwards and Mendelssohn 1956). The critical values of Re_v calculated from Vinen's (1957a,b) detailed measurements of mutual friction in wide, rectangular channels are as follows:

In apparatus no. 1 (0.240 x 0.645 cm)

$$Re_v \doteq 1500 \text{ at } 1.295°K$$
$$\doteq 2100 \text{ at } 1.400°K$$
$$\doteq 2100 \text{ at } 1.500°K$$

In apparatus no. 2 (0.400 x 0.783 cm)

$$Re_v \doteq 1700 \text{ at } 1.304°K$$
$$\doteq 2300 \text{ at } 1.400°K$$

For these calculations the effective diameter of the channel is taken, as in chapter 5, as $4A/P$, where A is the area and P the perimeter of its cross-section. Values of the viscosity have been interpolated from those used in chapter 4(b). They are rather uncertain, and the apparently low values of the critical Reynolds' number near 1.3°K may be due to overestimation of the viscosity coefficient at that temperature.

In the present experiment the critical heat input for the onset of turbulence in tunnel II is (4.3 ± 0.8) mW/cm^2 at 1.30°K. Therefore the mean critical velocity of the normal fluid is (0.27 ± 0.05) cm/sec. The effective diameter of the tunnel is 0.75 cm. With the value of the viscosity used in chapter 4, $\eta_n = 22.10^{-6}$ poise, the critical Reynolds' number at 1.3°K is

$$Re_v = 1350 \pm 250 , \qquad (8.6)$$

in good agreement with the STA value. At the higher temperatures the actual turbulent transition is not visible, but from the lowest heat current in which there is definite evidence of turbulence an upper limit to the critical Reynolds' number can be deduced:

$$\left.\begin{aligned} Re_v &\leqslant 1450 \text{ at } 1.64°K) \\ &\leqslant 1750 \text{ at } 1.84°K) \\ &\leqslant 1500 \text{ at } 2.10°K) \end{aligned}\right\} \qquad (8.7)$$

In tunnel I at 1.3°K turbulence was observed visually down to the limit of sensitivity, 2 mW/cm^2, corresponding to a Reynolds' number $Re_v \doteq 1100$.

The agreement of these results with those of STA inspires confidence in them, although they were obtained in a short and geometrically imperfect wind tunnel. Within the experimental error the fluid becomes

turbulent at the lowest possible value of R_{e_v} , 1200 according to STA. In Chase's and Vinen's results the transition is delayed until a higher Reynolds' number, approximately equal to the classical value of 2300, is reached. The difference probably lies in the normal fluid inlet to the channel, which in their experiments was connected to a chamber in which the heater was placed, while in the present apparatus the heater, with its irregularities, covered one end of the tunnel. In STA's apparatus the transition may have sometimes occurred at the lower Reynolds' number because of the middle section of the channel, which, although of wider diameter than the rest, was curved. However the transition could sometimes be delayed until a Reynolds' number of 5000.

The transition to turbulence observed in the present experiment is therefore identified with the onset of mutual friction previously determined by Vinen, Chase and others. It appears that mutual friction in heat currents in wide channels is in fact associated with turbulence in both the normal fluid and the superfluid, as suggested by Chase. It is unfortunate that the sensitivity of the apparatus is not high enough to determine whether the critical Reynolds' number falls to zero at the λ-point, or whether it is roughly independent of temperature, as seems to be implied by STA.

(e) Summary of main conclusions

In a short counter flow wind tunnel at 1.3°K two "critical" heat currents are observed. Below the lower of these the normal fluid flows in a laminar way and the superfluid contains only a little vorticity,

which may be produced by the measurement process itself. There is some rather qualitative experimental evidence that under these conditions the superfluid circulation about a fibre immersed in the helium is quantized. In the flow regime between the two critical heat currents, which is probably related to Vinen's "subcritical turbulence", the superfluid contains extra, not entirely random, vorticity, and the normal fluid, although possibly slightly disturbed, is not fully turbulent. The lower critical heat current can be described as a critical superfluid velocity whose value, about 10^{-2} cm/sec in the present experiment, probably depends strongly on the geometry of the apparatus. Above the upper critical heat current, which is that for the onset of mutual friction determined by previous authors, the normal fluid is fully turbulent. This behaviour can be described by a Reynolds' number depending on the velocity and viscosity of the normal fluid but the total fluid density. The critical value (1350 ± 250) of this Reynolds' number is approximately equal to that of the Reynolds' number for the onset of turbulence in a classical fluid. At temperatures higher than 1.3°K the results, although for experimental reasons less clear-cut, are consistent with this interpretation.

It seems that the transition to turbulence in helium may be essentially classical, so that calculations of the critical velocity for the onset of mutual friction in terms of the creation of vortex rings are incorrect. However, Vinen's (1957d) calculation of the critical behaviour in terms of the amplification of existing superfluid

vorticity gives good qualitative agreement with experiment, and may have more in common with the present approach than is at once apparent.

9. Further suggestions and speculations

(a) Mutual friction and turbulence

Referring back to equations (2.5) and (2.6), we see that, if there is no mutual friction,

$$\text{grad } p = \rho S \text{ grad } T \tag{9.1}$$

in a heat current, whether the normal fluid is turbulent or not. We know that mutual friction is not detectable unless the normal fluid is turbulent, but it cannot be identical with normal fluid turbulence because the relation (9.1) is not satisfied. When turbulence sets in grad p rises above the value expected in laminar flow, but $\rho S \text{ grad } T$ rises even more, and the difference between them increases with increasing heat current (e.g. STA 1961). Therefore not only must the normal fluid be turbulent, but some other force must act specifically on the temperature gradient. It is tempting to identify this force with the Gorter-Mellink mutual friction, which is known to be a good approximation in wide channels and at high velocities. Like Vinen (1957c) we assume that the mutual friction is caused by superfluid turbulence, which we now believe to be accompanied by turbulence in the normal fluid.

The suggested flow equations are therefore:

$$\left.\begin{aligned} \text{grad } p &= \eta_n \nabla^2 \underset{\sim}{v}_n \\ \rho S \text{ grad } T &= \eta_n \nabla^2 \underset{\sim}{v}_n \end{aligned}\right\} \tag{9.2}$$

in subcritical heat currents, where $\nabla^2 \underset{\sim}{v}_n$ is to be calculated for Poiseuille flow, and any small, subcritical mutual friction is neglected; and

$$\overline{\text{grad } p} = \underset{\sim}{f}\left(\overline{\underset{\sim}{v}_n}, \eta_n, \rho\right)$$

$$\rho S \text{ grad } T = \underset{\sim}{f}\left(\overline{\underset{\sim}{v}_n}, \eta_n, \rho\right) + A \rho_s \rho_n \left|\overline{\underset{\sim}{v}_s - \underset{\sim}{v}_n}\right|^2 \left(\overline{\underset{\sim}{v}_s - \underset{\sim}{v}_n}\right) \tag{9.3}$$

in supercritical heat currents, where $\underset{\sim}{f}\left(\overline{\underset{\sim}{v}_n}, \eta_n, \rho\right)$ is the known mean pressure gradient in classical turbulent flow, and A is the Gorter-Kellink constant, whose value according to Vinen (1957a) ranges from 30 cm-sec/gm at 1.3°K to 100 cm-sec/gm at 1.9°K. The averages are to be taken over the channel cross-section and in time.

We can apply classical theory to these results. For Poiseuille flow $\eta_n \nabla^2 \underset{\sim}{v}_n = \dfrac{32 \eta_n \overline{\underset{\sim}{v}_n}}{d^2}$. Therefore by (9.2)

$$\text{grad } p = \rho S \text{ grad } T = \frac{32 \eta_n \overline{\underset{\sim}{v}_n}}{d^2} \tag{9.4}$$

in subcritical heat currents. This relation has been confirmed by numerous authors, who have used it to deduce η_n (e.g. STA). In turbulent flow the mean pressure gradient is (Prandtl 1952, p. 162)

$$f\left(\overline{v}, \eta, \rho\right) = \tfrac{1}{2} \frac{\lambda_1}{d} \rho \overline{v}^2 \quad , \tag{9.5}$$

where λ_1 is a slowly varying function of the Reynolds' number. For Reynolds' numbers Re up to 80,000 Blasius's formula

$$\lambda_1 \doteqdot 0.32/Re^{\frac{1}{4}} \tag{9.6}$$

is correct in smooth pipes.

SFA find that the pressure gradient in helium is given by Blasius's results if the Reynolds' number Re_v (equation (2.14)) is used. Hence we have that, in supercritical heat currents,

$$\rho S\,\overline{\text{grad}\,T} = \overline{\text{grad}\,p} + A\rho_s\rho_n\left|\overline{\underset{\sim}{v}_s - \underset{\sim}{v}_n}\right|^3$$
$$\overline{\text{grad}\,p} = \tfrac{1}{2}\frac{\lambda_1}{d}\rho\,\overline{v_n}^2 , \tag{9.7}$$

where $\lambda_1 = 0.32/Re_v^{\frac{1}{4}}$. Therefore $\overline{\text{grad}\,p} \propto \overline{v_n}^{1.75}/d^{1.25}$, while the mutual-friction contribution to $\rho S\,\overline{\text{grad}\,T}$ is proportional to $\left|\overline{\underset{\sim}{v}_s - \underset{\sim}{v}_n}\right|^3$, and independent of d. It follows that in sufficiently wide channels or at high enough velocities the mutual-friction contribution to $\rho S\,\overline{\text{grad}\,T}$ will be dominant, and the Gorter-Mellink equation will appear to be sufficient to describe the results. In narrow channels and at low velocities $\overline{\text{grad}\,p}$ will become important, and departures from the Gorter-Mellink equation will be observed if no account is taken of turbulence in the normal fluid. The departures will take the form of deviations from the cube law of velocity, and apparent dependence of the constant A on

channel diameter. This is exactly the position in practice.

For a just supercritical heat current ($Re_v \doteq 2000$) in a 1 cm channel at 1.3°K

$$\overline{\text{grad } p} \doteq 3.10^{-4} \text{ dyne/cm}^3, \tag{9.8}$$

while

$$A \rho_s \rho_n \left| \overline{\underset{\sim}{v}_s - \underset{\sim}{v}_n} \right|^3 \doteq 9.10^{-4} \text{ dyne/cm}^3. \tag{9.9}$$

The normal-fluid contribution to $\rho S \, \text{grad} \, T$ is therefore significant just above the transition, but insignificant for heat currents greater than a few times the critical value. In a 1 mm channel the normal-fluid contribution is dominant in heat currents from the critical value up to several times critical, and so, if it is not taken into account, considerable divergences from the Gorter-Mellink equation should occur.

In view of this, previous determinations of the form of the Gorter-Mellink friction, especially at low velocities and in narrow channels, are untrustworthy. It would be worthwhile to recalculate the mutual friction from all previous results, allowing for normal-fluid turbulence, and see if they thereby became more consistent, and whether the simple Gorter-Mellink form suggested for the mutual friction in equation (9.3) is correct. In the measurements of mutual friction which have been deduced from the attentuation of second sound, turbulence in the normal

fluid must lead to some extra attenuation, which may possibly be large enough to confuse the results. No estimate of the size of this effect has been made.

The problem of explaining mutual friction has now altered slightly. It is known (Vinen 1957c) that the presence of vortex lines in the superfluid offers a plausible approach; previously the problem was to explain why vorticity appeared in the superfluid above a certain critical velocity and how it could be maintained at a constant level. Now it must be explained why the superfluid becomes turbulent when the normal fluid does: why the critical Reynolds' number contains the total fluid density and not that of the normal fluid alone. STA have put forward some ideas on this subject. It is tentatively suggested by the present author that normal-fluid turbulence may automatically induce vortex lines or vorticity in the superfluid. In this way difficulties in the maintenance of superfluid vorticity (Townsend 1963) can be avoided, and it is not necessary to rely on the amplification of existing vorticity, or on the creation of vortex lines at the wall of the channel, which we know from chapter 3(c) to be extremely difficult. On the other hand the real difficulty is brought right into the foreground. This is that the creation of a complete, quantized vortex line, of macroscopic length, and having a velocity field which extends in theory throughout the whole helium bath, is virtually impossible. We shall discuss this problem in Section (b).

(b) Superfluid vorticity and the quantization of circulation

Vinen's (1961b) experiment on the detection of single quanta of circulation provides fairly firm evidence for the quantization of circulation, particularly with the interpretation in terms of classical vortex-line theory put forward in appendix II. Some further support is given by the circulation measurements made in the present experiment. It is therefore probable that the superfluid circulation about a solid body is quantized. However, superfluid circulation may not always be a good quantum number. We know (Landau 1941) that the three components of curl $\underset{\sim}{v}_s$ at a point do not commute with each other; that is, they cannot be simultaneously defined. It follows by a simple argument that the superfluid circulations about two linked circuits do not commute. Since $\underset{\sim}{v}_s$ can only be defined by an average over at least one atomic volume, we must count two circuits as linked if they anywhere approach closer than the interatomic distance. Hence, if the circulation is defined or measured about a given circuit, there is a whole class of circuits whose circulation is uncertain: the circulation about these circuits is not a good quantum number.

At absolute zero the whole superfluid is in a single quantum state, which in the quasi-classical approximation is specified by the configuration of all the vortex lines in it. In general this configuration is not steady, but changes with time in a way which can be calculated classically. The circulation about any given circuit therefore changes in general with time. In quantum-mechanical language, it does not

commute with the Hamiltonian; that is, if the total energy of the helium is specified†, the superfluid circulation about any circuit cannot in general be exactly defined. The total energy and the circulation can be simultaneously defined only if the vortex-line configuration is steady. Possible steady configurations can be found classically, as in appendix II.

When the circulation cannot be defined, neither can the vortex-line configuration be exactly specified. This quantum-mechanical uncertainty can be introduced into the quasi-classical approximation by allowing the superfluid to occupy mixed quantum states, built up by the superposition, with varying probabilities, of a large number of pure states in which the vortex-line configuration is exactly specified. The quasi-classical description of such mixed states must be in terms of distributed vorticity; that is, laminar flow of the superfluid.

We have therefore reached the conclusion that, although the superfluid circulation about any circuit is quantized, so that its value when measured must be an integral multiple of h/m, it need not be a good quantum number, and so the superfluid can flow, in the quasi-classical approximation, with distributed vorticity. We shall assume that this result applies at all temperatures below the λ-point.

It is plausible that the creation of distributed, unquantized vorticity is much easier than the creation of a complete vortex line. In turbulent flow for example it could be produced by a weak interaction between the normal fluid and the superfluid, probably essentially

†Classically any vortex configuration has constant energy at 0°K.

quantum-mechanical in origin, and possibly connected with the fact that, when the normal fluid is turbulent, there are no steady vortex-line configurations by superposition of which the superfluid vorticity can be built up. Mutual friction can then occur because at every point there is a finite probability of finding a vortex-line core, which may scatter normal-fluid excitations.

Once the turbulence has decayed and the normal fluid is at rest it is again possible to find states in which the total energy and the superfluid circulation can be simultaneously defined. Many of these states will be too different from the initial distribution of vorticity to be accessible. We expect that the occupation probability of the accessible state of lowest energy will grow at the expense of the remainder. That is, the superfluid vorticity will appear, classically, to crystallize out in a certain steady vortex-line configuration: distributed, unquantized vorticity (superfluid turbulence) will be destroyed, as suggested by Townsend (1963).

The model meets some of Townsend's other criticisms of the vortex-line theory of mutual friction. Because in turbulent flow the vortex lines are not localised, the mutual friction is now a volume force instead of the awkwardly localised force of the usual theory; also, since we are postulating creation of superfluid vorticity by normal-fluid turbulence, there is no difficulty in the maintenance of the vorticity at an equilibrium level.

The effect of this modification of vortex-line theory on the capture

and loss of superfluid circulation by a fibre or wire has not yet been considered. It seems possible that the matrix elements for the various processes may be small unless vorticity is sufficiently concentrated near the fibre to resemble a classical vortex line. In this case the usual theory will remain a good approximation.

Distributed superfluid vorticity may prove a useful idea in other situations where the creation of classical, quantized vortex lines is an embarrassment. For example it is postulated that there is an array of vortex lines in a rotating bucket of helium, but the creation of these lines at the wall of the bucket when rotation is started is impossible, by the results of chapter 3(c). If however the turbulence induced in the normal fluid at the start of the rotation creates superfluid vorticity the vortex lines can be formed by its subsequent concentration. It is also easier to understand the production of vortex lines of a preferred orientation in short heat pulses and the occurrence of vorticity associated with secondary flow of the superfluid, both of which are believed to have been observed in the present experiment, if relatively easy creation of distributed superfluid vorticity is possible.

(c) Suggestions for further work

Apart from theoretical investigation in the direction indicated by Section (b) and a recalculation of the published results on mutual friction (see Section (a)), it is suggested that the following experimental work might be of value.

Firmer evidence for or against the quantization of circulation

could be obtained with more reliable calibration of the apparatus and more and better comparisons of transient and steady deflections. If the signal/noise ratio of the recording system were improved the temperature dependence of the critical Reynolds' number for turbulence could be measured, and an attempt could be made to detect the effect of subcritical turbulence on the fibre.

It would be useful to try to find out what controls the observed bias of superfluid circulation, both in undisturbed helium and in what we have called secondary flow of the superfluid; also to see whether the critical velocity for this secondary flow is reproduced in other apparatuses and, if so, what governs it.

It would be relatively simple and very interesting to repeat the present experiment with a wind tunnel in which the normal fluid was held at rest by filters permeable to the superfluid. We should then have $\overline{\underset{\sim}{v}_n} = 0$, so that $Re_v = 0$. According to ST' the normal fluid should not become turbulent whatever the superfluid velocity. Probably in practice some sort of secondary flow would develop, and might eventually become turbulent (cf. Kidder and Fairbank 1962).

Some possible experimental tests of the theory of quantized vortex lines are outlined at the end of appendix II.

Appendix 1: Measurement of the normal viscosity of helium II

The object of this experiment was to estimate the mean free path of the normal-fluid phonons by measurement of the viscous drag on a fine fibre. The normal viscosity is the sum of two parts, due respectively to rotons and phonons (e.g. Atkins 1959, p. 106). The phonon viscosity and mean free path (which is normally terminated by a roton) increases steeply with decreasing temperature. It was believed that the apparent viscosity would fall below the expected value when the phonon mean free path was larger than the fibre diameter. The roton mean free path is smaller by two orders of magnitude and the roton viscosity is independent of temperature.

The experiment was carried out in an apparatus very similar to that described in chapter 6(e). The wind tunnel had a rectangular cross-section 0.5 x1.0 cm and two fibres were used, both of diameter 0.9 μ and length just less than 1 cm. The first had a shellac bob of rather uncertain weight and the second, a nylon bob of weight 0.8 μgm. From the downstream deflection of the bob, measured in steady heat currents, the apparent viscosity was deduced using equation (4.2) and the classical results for the viscous drag on a circular cylinder. The small viscous drag on the bob was neglected, and it was assumed that the velocity profile of the normal fluid was flat.

For Reynolds' numbers $Re' = \frac{v_n d \rho_n}{\eta_n} < 0.4$, where d is the diameter of the fibre, Lamb's (1945, p. 616) formula (5.3) was used to calculate the viscosity. For $Re' \geq 0.4$, the classical result was

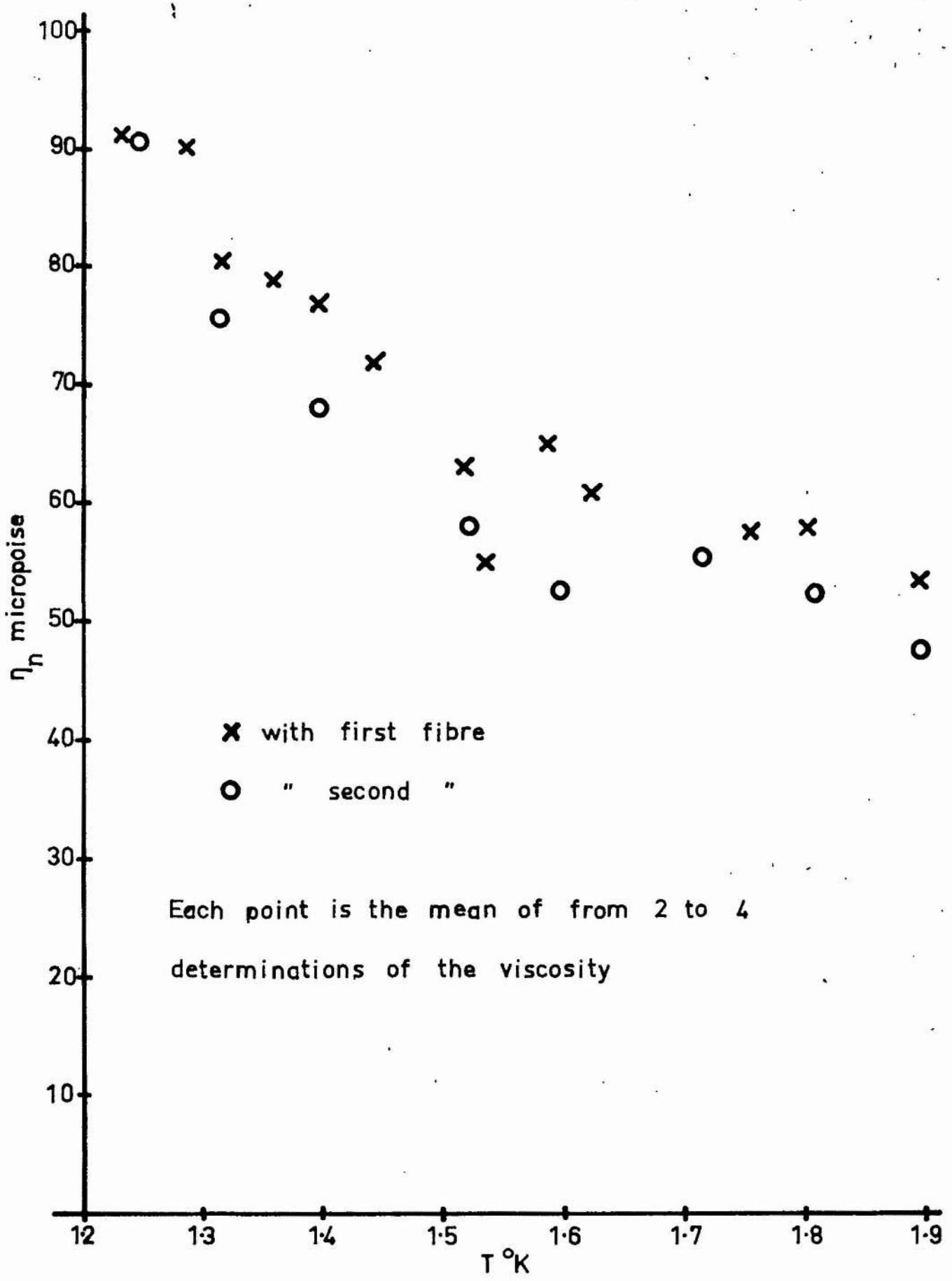

Figure I.1. Measured viscosity as a function of temperature

found by interpolation from the results given by Prandtl (1952, p. 190). The calculated effective viscosity of helium is shown in figure I.1. The scatter of the points is within the experimental error, but the approximate agreement between the results with the two fibres is largely fortuitous because of the uncertain weight of the shellac bob. The temperature variation of the effective viscosity is very similar to that of the known, true viscosity, but its absolute value is higher by a factor of 5, well outside the experimental error.

The phonon mean free path is expected to become equal to the fibre diameter between 1.3°K and 1.4°K. The experiment was discontinued because no anomaly in the effective viscosity could be seen near this temperature. Because of the curious form (5.3) of the drag on a cylinder, it is not even certain that the effective viscosity ought to fall when the mean free path becomes larger than the fibre diameter. For low stream velocities the viscous drag is lower than the drag that would occur in open-gas flow. The effective viscosity might therefore tend to rise. In the original formulation of the theory of the normal viscosity the phonon mean free path seemed well defined (Landau and Khalatnikov 1949a,b) but Khalatnikov's later work (1956a,b) it becomes a vaguer concept, so that it is not clear what relation even a clear-cut experimental measurement of the mean free path would have to the theory.

No convincing explanation of the anomalously high effective viscosity has been found. The heat current was supercritical for all the measurements, so that the normal fluid was turbulent and the assumption

of a flat velocity-profile not too poor (random deflections due to the turbulence contributed to the scatter of the results). In any case this assumption could hardly cause an error of more than a factor 2. It is possible, but rather implausible, that both the bobs were much lighter than expected. It seems more likely that the classical results for the viscous drag on a cylinder in steady flow broke down in the experimental circumstances, perhaps because of mean-free-path effects or the turbulence in the normal fluid. It is known that the drag is very easily altered if the aspect ratio of the cylinder is too low (Prandtl 1952, p. 190), if the walls of the containing vessel are not very distant indeed (White 1945), or if the flow velocity is not steady but oscillatory (see equation (4.42) and chapter 8(a) (i)): too much faith should therefore not be placed in the applicability of the classical results without more experimental investigation.

Appendix II: Vinen's experiment to detect single quanta of circulation

In this appendix Vinen's (1961b) experiment, outlined in chapter 2(b), is interpreted in terms of the quasi-classical theory of quantized vortex lines. Most of his observations can be accounted for in this way, and some difficulties in the original interpretation overcome. In particular it is found unnecessary to postulate, as Vinen did, an anomalously large vortex-core radius.

(a) The action of a straight wire on parallel vortex lines

(i) The hydrodynamical approach.

It was pointed out in chapter 3(a) that the results of that chapter could be applied to interactions in the array of parallel vortex lines present in rotating helium. If, as in Vinen's experiment, a fine wire is stretched along the axis of a rotating vessel of helium, the results of chapter 3(b) are at once applicable.

When there is no circulation about the wire neighbouring vortex lines are subject to the induced velocity (3.7), which must lead to the capture by the wire of one quantum of circulation, as in chapter 3(b). Thereafter the neighbouring vortex lines are subject to the velocity field (3.9), which far from the wire is identical to the velocity induced by a free vortex line. Hence, provided that the equilibrium line spacing λ is much greater than the radius R of the wire, the presence of the wire will disturb the regular array of vortex lines very little. For when one quantum has been captured its induced velocity field (3.9) remains similar to that of a free vortex line.

Hence the remaining vortex lines will take up their normal equilibrium positions with respect to it and to each other, and no further circulation will be captured. However, if λ were comparable with R it would be possible to capture a second quantum. The maximum positive (repulsive) value of (3.9), which occurs at $r \doteqdot 2R$ and is of magnitude about $K/3R$ (see figure 3.4), could just be overcome by the velocity field of a vortex line a further distance $3R$ from the wire. Hence, neglecting the second-order effect of other vortex lines, a second quantum could be captured when $\lambda \sim 3R$. But $\lambda \sim (\pi K/\omega)^{\frac{1}{2}}$ (II.1) (see chapter 2(b)), where ω is the angular velocity of rotation, and so the criterion for the capture of two quanta is in order of magnitude

$$(\pi K/\omega)^{\frac{1}{2}} \sim 3R$$

or

$$\omega \sim K/3R^2 \qquad \text{(II.2)}$$

$\doteqdot 30$ rad/sec if $R = 1.3.10^{-3}$ cm.

The criteria for the capture of further quanta could be similarly derived.

(ii) The connection between the energetic and hydrodynamical approaches.

Vinen deduced the expected equilibrium circulation about the wire by direct calculation of the free energy of various configurations. In simple cases it is possible to calculate free-energy changes hydrodynamically, to show that they agree with the directly calculated values,

and to demonstrate the possibility or impossibility of attaining equilibrium. The vortex lines are treated as bound; that is, fixed at rest in the coordinate system. The Magnus forces acting upon them may then be integrated to find the change in energy as their positions are varied.

Consider the case of a wire with no circulation about it and a parallel vortex line in otherwise undisturbed helium. The free energy of the line when it is far from the wire is (e.g. Vinen 1961a)

$$q_1 = \pi \rho_s \kappa^2 \ln b'/a_0 \text{ per unit length,} \qquad \text{(II.3)}$$

where $b' \sim b$, the radius of the containing vessel, and a_0 is a cut-off parameter depending on the structure of the core of the vortex line. In the simplest case, where the core is just a hole in the liquid which contributes nothing to the energy if surface tension is neglected, a_0 is equal to the radius of the hole.

The free energy per unit length after the vortex line has been captured by the wire is

$$q_2 = \pi \rho_s \kappa^2 \ln b''/R , \qquad \text{(II.4)}$$

where R is the radius of the wire, and $b'' \sim b'$. The change in free energy per unit length is therefore

$$\Delta g = g_1 - g_2 = \pi \rho_s \kappa^2 \ln a_0 b'' / R b'$$

$$\doteq -\pi \rho_s \kappa^2 \ln R/a_0 \text{ for } R \gg a_0 . \qquad \text{(II.5)}$$

Hydrodynamically the free-energy change is calculated as follows. The Magnus force per unit length is

$$\underset{\sim}{f} = 2\pi \rho_s \underset{\sim}{q_t} \times \underset{\sim}{\kappa} \quad \text{(equation (3.1))}.$$

$$q_t = \frac{-\kappa R^2}{r(r^2 - R^2)} \quad \text{(equation (3.7))}.$$

Therefore $$f = \frac{2\pi \rho_s \kappa^2 R^2}{r(r^2 - R^2)} , \qquad \text{(II.6)}$$

Since $\underset{\sim}{f}$ is directed inwards, Δg is negative for the capture process, and

$$\Delta g = -\int_d^D f \, dr , \qquad \text{(II.7)}$$

where D is the initial distance between wire and vortex, assumed large, and d is a lower limit, unknown because the form of f for $r < a_0$ is unknown. An estimate of Δg is found by integrating until the core just touches the surface of the wire.

i.e.

$$\Delta g \sim -\int_{R+a_0}^{D} f \, dr$$

$$= -\pi \rho_s \kappa^2 \left(\ln \frac{D^2 - R^2}{R^2} + \ln \frac{(R+a_0)^2}{(R+a_0)^2 - R^2} \right). \qquad (II.8)$$

Taking the limit as $D \to \infty$, and assuming that $R \gg a_0$, we have

$$\Delta g \sim -\pi \rho_s \kappa^2 \ln R/2a_0 . \qquad (II.9)$$

This agrees with the directly calculated value (II.5) when account is taken of an extra contribution of $\pi \rho_s \kappa^2 \ln 2$ from the integration through the vortex core.

A more interesting case is that of a wire with unit circulation and a parallel vortex line. When the separation is large we have

$$g_1 = \pi \rho_s \kappa^2 (\ln b'/a_0 + \ln b''/R) , \qquad (II.10)$$

and after capture

$$g_2 = \pi \rho_s (2\kappa)^2 \ln b'''/R . \qquad (II.11)$$

Therefore $$\Delta g = g_2 - g_1 \doteq \pi \rho_s \kappa^2 \ln a_0 b^2/R^3 , \qquad (II.12)$$

taking $b' = b'' = b''' = b$ with sufficient accuracy.

From equation (3.10) we know that the interaction is repulsive for

$r > \sqrt{2}R$ and attractive for $R < r < \sqrt{2}R$. The energy change therefore falls naturally into two parts, divided at the critical radius. Now

$$q_t = \frac{\kappa(r^2 - 2R^2)}{r(r^2 - R^2)} \quad \text{(equation (3.9))}.$$

Therefore
$$\Delta g_1 = 2\pi\rho_s\kappa \int_{\sqrt{2}R}^{D} q_t \, dr$$
$$= \pi\rho_s\kappa^2 \ln \frac{D^4}{4R^2(D^2 - R^2)}. \qquad \text{(II.13)}$$

Δg_2 is negative and

$$\Delta g_2 \sim -2\pi\rho_s\kappa \int_{R+a_0}^{\sqrt{2}R} |q_t| \, dr$$
$$= -\pi\rho_s\kappa^2 \ln \frac{(R+a_0)^4}{4R^2[(R+a_0)^2 - R^2]}$$
$$\doteq -\pi\rho_s\kappa^2 \ln R/8a_0 \text{ for } R \gg a_0. \qquad \text{(II.14)}$$

Therefore $\Delta g_1 + \Delta g_2 \sim \pi\rho_s\kappa^2 \ln \frac{2a_0 D^4}{R^3(D^2 - R^2)}$. (II.15)

This expression diverges as $D \to \infty$, but it is natural to take $D \doteq b$, the radius of the containing vessel. Therefore, assuming $b \gg R$,

$$\Delta g_1 + \Delta g_2 \sim \pi\rho_s\kappa^2 \ln 2a_0 b^2/R^3, \qquad \text{(II.16)}$$

which agrees with the directly calculated value (II.12) if the core contribution $\pi\rho_s\kappa^2 \ln 2$ is added as before.

Because Δq_1 is strongly positive there is a potential barrier to be overcome in the capture by the wire of a second quantum of circulation. Extension of the argument shows that the capture of further quanta is similarly hindered. States with integral circulation about the wire, between which the barriers occur, will be called quasi-equilibria. It is assumed that the calculations remain qualitatively valid in rotating helium.

The total energy change $\Delta q_1 + \Delta q_2$ is also positive, but small. The differences in energy between the quasi-equilibria are therefore small, and may be reversed in sign by relatively minor changes in conditions, in particular by rotation at low angular velocity. Of all the possible quasi-equilibrium states the true equilibrium is that of lowest free energy. Vinen (1961b) has calculated the equilibrium circulation for a wire of radius $1.3.10^{-3}$ cm in a cylindrical vessel 0.2 cm in radius, and finds that it rises from zero to one quantum and again to two quanta at angular velocities in the range from 10^{-2} to 10^{-1} rad/sec. The system cannot reach its true equilibrium from a quasi-equilibrium of lower circulation however, for the angular velocity necessary to overcome the potential barriers involved is by equation (II.2), of the order of $\kappa/3R^2$, which is about 30 rad/sec if $R = 1.3.10^{-3}$ cm.

Just as Δq_1 prevents the capture of vortex lines, so Δq_2 prevents their loss. In chapter 3(c) the condition necessary for the

creation of a vortex line at a fibre, or any other solid surface, was determined. It is so stringent that normally such creation is impossible, and so in a quasi-equilibrium state the wire is unable to lose circulation.

(iii) Summary.

The equilibrium state of a rotating vessel of helium contains an array of vortex lines parallel to the axis of rotation. If a fine wire is stretched along this axis a quasi-equilibrium state will be attained in which there is unit circulation about the wire, except possibly at such low rates of rotation that no vortex lines are present in the vessel. The attainment of the true equilibrium, if that should require two or more quanta of circulation about the wire, is opposed by energy barriers which can be overcome only by very rapid rotation of the helium. If on the other hand too high a circulation were somehow established about the wire, equilibrium could not be attained because of an energy barrier opposing the loss of circulation. There is no possibility of the annihilation of circulation by the capture of vortex lines of opposite sense, so that the circulation could fall only if superfluid were made to stream past the fibre faster than the critical velocity found in chapter 3(c), for example by vibrating the wire. It is clear that in quasi-equilibrium states the energy barriers prevent not only the simultaneous change of circulation along the whole wire, but also the capture or loss of circulation over short lengths (which would lead to the partial attachment of vortex lines to the wire). Quasi-equilibrium

states are therefore metastable. If however a state with a vortex line partly attached to the wire could be established, we might expect equilibrium to be approached by the peeling of the vortex line on or off the wire until the nearest quasi-equilibrium was reached. This process does not require the creation or destruction of a complete length of vortex line but only the stretching or shortening of existing line, and so it is not opposed by the energy barriers of (ii). States with partly attached vortex lines may nevertheless be metastable. Before this can be decided a technique for treating the behaviour of curved vortex lines must be developed.

(b) Partly attached vortex lines

(i) The self-induced velocity of a curved vortex line.

Let $\underset{\sim}{q}(\underset{\sim}{x})$ be the fluid velocity at point $\underset{\sim}{x}$ in an unbounded fluid. Then the vorticity

$$\underset{\sim}{\zeta}(\underset{\sim}{x}) = \nabla \times \underset{\sim}{q}(\underset{\sim}{x}) , \qquad \text{(II.17)}$$

and the velocity $d^3\underset{\sim}{q}_{ik}$ induced at $\underset{\sim}{x}_i$ by the volume element $d^3\tau_k$ at $\underset{\sim}{x}_k$ is given by

$$d^3\underset{\sim}{q}_{ik} = d^3\tau_k \frac{\underset{\sim}{\zeta}_k \times (\underset{\sim}{x}_i - \underset{\sim}{x}_k)}{4\pi |\underset{\sim}{x}_i - \underset{\sim}{x}_k|^3} . \qquad \text{(II.18)}$$

Suppose that all vorticity is concentrated in the core of a single vortex line of radius a_0.

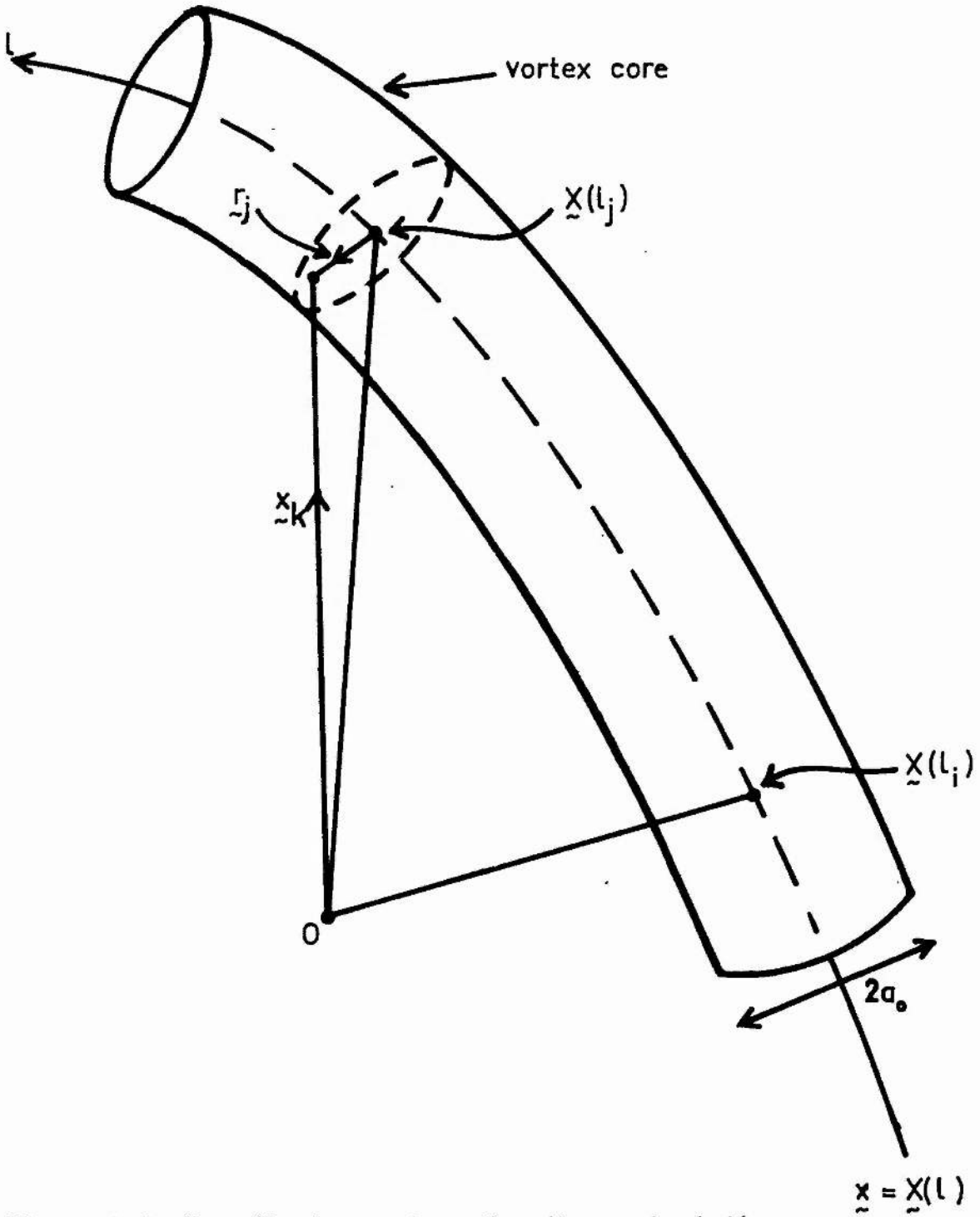

Figure II.1. Coordinate system for the calculation of the self-induced velocity of a curved vortex line

Then

$$\underset{\sim}{q}_i = \iiint_{\text{all space}} d^3 \underset{\sim}{q}_{ik}$$

$$= \iiint_{\text{vortex core}} d^3 \underset{\sim}{q}_{ik} \qquad \text{(II.19)}$$

Let $\underset{\sim}{x} = \underset{\sim}{X}(l)$ be the equation of the vortex line axis, where l denotes distance measured along the axis from a given origin, and let $\underset{\sim}{x}_i = \underset{\sim}{X}(l_i)$. Then $\underset{\sim}{q}_i$ is the self-induced velocity of the vortex line at $\underset{\sim}{X}(l_i)$. We may take

$$\underset{\sim}{x}_k = \underset{\sim}{X}(l_j) + \underset{\sim}{r}_j \qquad \text{(II.20)}$$

for points lying inside the core, where $\underset{\sim}{r}_j$ is a variable vector in the plane of the cross-section of the line at $\underset{\sim}{X}(l_j)$, of magnitude not greater than a_0, as shown in figure II.1. Provided the radius of curvature ρ_j of the vortex line is large compared with a_0, $\underset{\sim}{r}_j$ is unique for every $\underset{\sim}{x}_k$ inside the core.

Let the element of area in the cross-section at $\underset{\sim}{X}(l_j)$ be d^2S_j. Then

$$d^3\tau_k \doteq dl_j \, d^2S_j \quad \text{, with} \quad \rho \gg a_0 \, . \qquad \text{(II.21)}$$

Therefore from equation (II.18)

$$d\underset{\sim}{q}_{ij} = \frac{dl_j}{4\pi} \iint_{\substack{\text{cross-}\\ \text{section}}} d^2S_j \; \frac{\underset{\sim}{\zeta}(\underset{\sim}{r}_j) \times \left[\underset{\sim}{X}_i - (\underset{\sim}{X}_j + \underset{\sim}{r}_j)\right]}{\left|\underset{\sim}{X}_i - (\underset{\sim}{X}_j + \underset{\sim}{r}_j)\right|^3} \qquad \text{(II.22)}$$

writing $\underset{\sim}{X}(l_i) = \underset{\sim}{X}_i$, $\underset{\sim}{X}(l_j) = \underset{\sim}{X}_j$ for convenience, where $d\underset{\sim}{q}_{ij}$ is the velocity induced at $\underset{\sim}{X}_i$ by the length dl_j of vortex line at $\underset{\sim}{X}_j$.

Now

$$\iint_{\substack{\text{cross-}\\ \text{section}}} d^2S_j \; \underset{\sim}{\zeta}(\underset{\sim}{r}_j) = 2\pi \underset{\sim}{K}_j , \qquad \text{(II.23)}$$

where $2\pi\underset{\sim}{K}_j$ is the vector circulation about the vortex line at $\underset{\sim}{X}_j$.

Therefore, if

$$\left|\underset{\sim}{X}_i - \underset{\sim}{X}_j\right| \gg a_0 ,$$

$$d\underset{\sim}{q}_{ij} = dl_j \; \frac{\underset{\sim}{K}_j \times (\underset{\sim}{X}_i - \underset{\sim}{X}_j)}{2\left|\underset{\sim}{X}_i - \underset{\sim}{X}_j\right|^3} . \qquad \text{(II.24)}$$

Hence the velocity contributions from distant parts of the line depend on K but not on the core structure. Comparison of equations (II.22) and (II.24) shows that the effect of finite core size is to remove the singularity which occurs in (II.24) when $\underset{\sim}{X}_i = \underset{\sim}{X}_j$. To a good approximation the total velocity

$$\underset{\sim}{q}_i = \int_{\text{all } l} d\underset{\sim}{q}_{ij} \qquad \text{(II.25)}$$

can be evaluated by using the approximate expression (II.24) and cutting off the integration at a lower limit $\varepsilon \sim a_0$. Since $dq_{ij} \sim |\underset{\sim}{X}_i - \underset{\sim}{X}_j|^{-2}$, a further approximation may be obtained by retaining only the leading term in the Taylor expansion of $(\underset{\sim}{X}_i - \underset{\sim}{X}_j)$ about $\underset{\sim}{X}_i$ (Hama 1962). To this order

$$q_i = \frac{\kappa}{2\rho_i} \ln \frac{\rho_i}{\varepsilon}, \qquad \text{(II.26)}$$

where q_i is in the direction of the binormal at $\underset{\sim}{X}_i$. The integral relation (II.25) is thus replaced by a differential relation. In this, which is Hama's localised-induction approximation and also the approximation used by Hall (1958) in his discussion of the behaviour of curved vortex lines, q_i is equal to the self-induced velocity of a circular vortex ring of radius ρ_i, tangent to the line at $\underset{\sim}{X}_i$ and lying in the osculating plane.

In order to see how good the localised-induction approximation is we examine the separate contributions of the various parts of the circumference of a circular vortex ring to its total self-induced velocity. Clearly, if the major contribution to the velocity at a given point comes from neighbouring parts of the circumference, the fact that in an

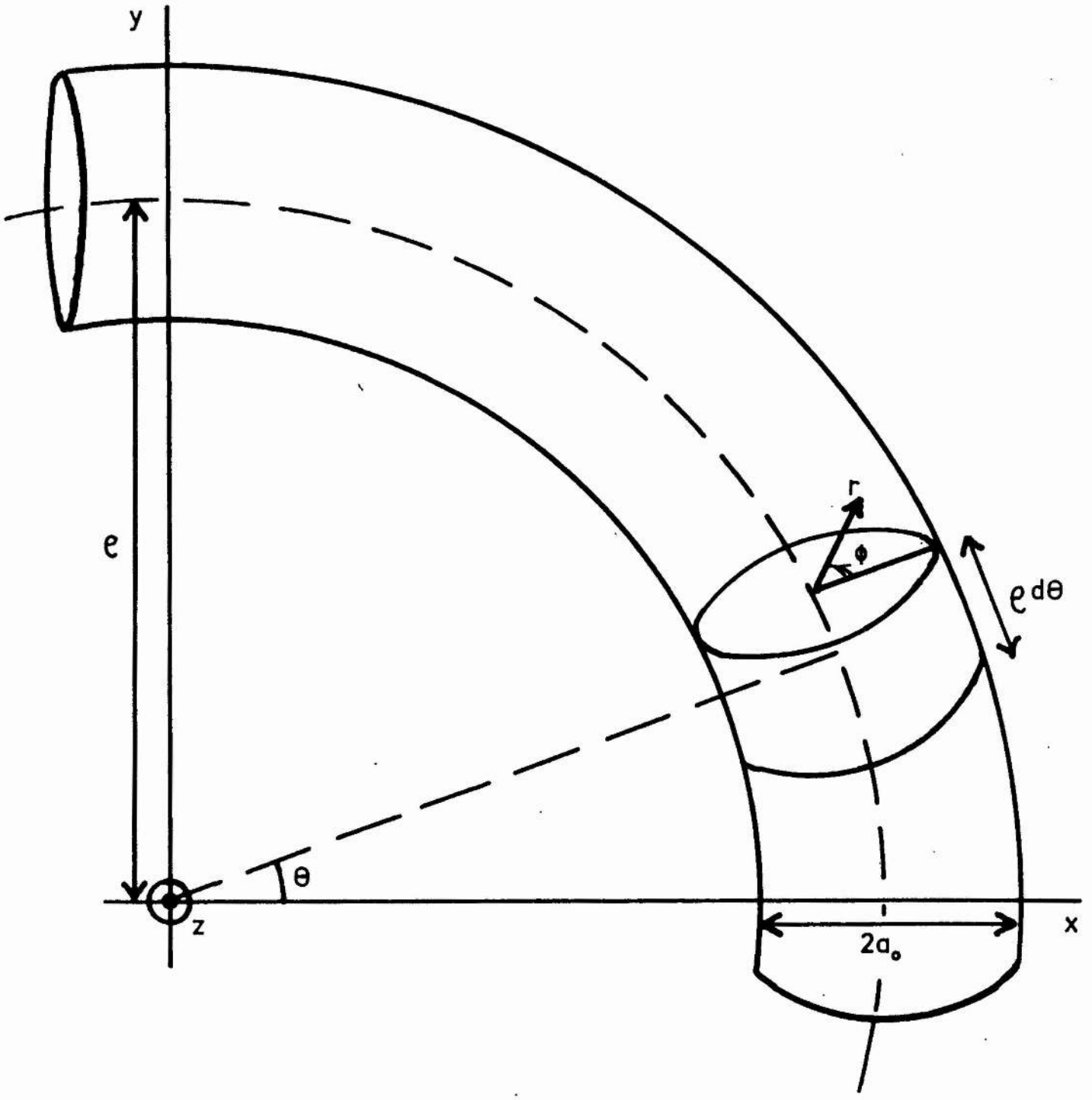

Figure II.2. Coordinate system for the description of a vortex ring

arbitrary configuration distant parts of the vortex line depart from the circular configuration will have little effect on the velocity, and so the localised-induction approximation will be good. Conversely, if the whole circumference contributes significantly to the self-induced velocity, the approximation will be a poor one.

Suppose that the vortex core has a circular section of radius a_0, within which there is vorticity $\zeta(r)$ depending only on the distance $r = |\underset{\sim}{r}_j|$ from the axis of the core. A coordinate system is set up as in figure II.2 and we take

$$\left.\begin{aligned} &\underset{\sim}{X}_i = (\varrho, 0) \\ \text{and} \quad &\underset{\sim}{X}_j = (\varrho, \theta) . \\ \text{Then} \quad &\underset{\sim}{r}_j = (r, \phi) , \\ &dl_j = \varrho\, d\theta \quad \text{with} \quad \varrho \gg a_0 , \\ \text{and} \quad &d\underset{\sim}{q}_{ij} = d\underset{\sim}{q}(\theta) , \end{aligned}\right\} \qquad \text{(II.27)}$$

where $d\underset{\sim}{q}(\theta)$ is the velocity contribution at $(\varrho, 0)$ from the element $\varrho\, d\theta$ at (ϱ, θ). Since the total self-induced velocity of the ring is known to be in the z-direction, only the components $dq_z(\theta)$ need be considered. From equation (II.22)

$$dq_z(\theta) = \frac{\varrho\, d\theta}{4\pi} \int_0^{a_0} dr \int_0^{2\pi} r\, d\phi\, \zeta(r)\, \frac{d' \sin\theta/2}{d^3} \qquad \text{(II.28)}$$

where $d = \left| \underset{\sim}{X}_i - \left(\underset{\sim}{X}_j + \underset{\sim}{r}_j \right) \right|$, and d' is the projection of d on to the x-y plane. Now

$$d^2 = \left[\varrho - (\varrho + r\cos\phi)\cos\theta \right]^2 + \left[(\varrho + r\cos\phi)\sin\theta \right]^2 + \left[r\sin\phi \right]^2$$

$$= 4\varrho(\varrho + r\cos\phi)\sin^2\theta/2 + r^2, \qquad \text{(II.29)}$$

and

$$d' \sin\theta/2 = (\varrho + r\cos\phi) - \varrho\cos\theta$$

$$= 2\varrho\sin^2\theta/2 + r\cos\phi. \qquad \text{(II.30)}$$

Also $r \leqslant a_0 \ll \varrho$, and $|\cos\phi| \leqslant 1$.

Therefore $$|r\cos\phi| \ll \varrho \ . \qquad \text{(II.31)}$$

Therefore $$d^2 \doteq 4\varrho^2\sin^2\theta/2 + r^2. \qquad \text{(II.32)}$$

Therefore

$$dq_z(\theta) = \frac{\varrho d\theta}{4\pi} \int_0^{a_0} dr \int_0^{2\pi} d\phi \ \frac{r\zeta(r)(2\varrho\sin^2\theta/2 + r\cos\phi)}{(4\varrho^2\sin^2\theta/2 + r^2)^{3/2}}$$

$$= \varrho^2 d\theta \int_0^{a_0} dr \ \frac{r\zeta(r)\sin^2\theta/2}{(4\varrho^2\sin^2\theta/2 + r^2)^{3/2}} \ . \qquad \text{(II.33)}$$

Therefore the total self-induced velocity at $(\varrho, 0)$ is given by

$$q = \int_{\theta=-\pi}^{\pi} dq_2(\theta)$$

$$= \rho^2 \int_{-\pi}^{\pi} d\theta \int_0^{a_0} dr \frac{r\,\zeta(r)\,\sin^2\theta/2}{(4\rho^2\sin^2\theta/2 + r^2)^{3/2}} \qquad \text{(II.34)}$$

If $\zeta(r)$ is taken as constant for $r < a_0$, and equation (II.23) is used, the value of this integral is (Lamb 1945, p. 241)

$$q = \frac{K}{2\rho}\left(\ln\frac{8\rho}{a_0} - \frac{1}{4}\right), \text{ with } \rho \gg a_0 ,$$

$$\doteq \frac{K}{2\rho}\ln\frac{6.2\rho}{a_0} . \qquad \text{(II.35)}$$

If the core is not circular and of uniform vorticity the numerical factor inside the logarithm is altered.

By equation (II.33) the contribution from the element $d\theta$ of the circumference of the vortex ring to the total velocity q is given by

$$dq_2(\theta) = \rho^2\, d\theta \int_0^{a_0} dr \frac{r\,\zeta(r)\,\sin^2\theta/2}{(4\rho^2\sin^2\theta/2 + r^2)^{3/2}} . \qquad \text{(II.36)}$$

Now $r \leqslant a_0 \ll \rho$, and so for $\theta \gg a_0/\rho$

$$4\rho^2\sin^2\theta/2 \gg r^2 . \qquad \text{(II.37)}$$

Therefore

$$dq_2(\theta) = \varrho^2 \, d\theta \int_0^{a_0} dr \, \frac{r\zeta(r) \sin^2 \theta/2}{8\varrho^3 \left|\sin^3 \theta/2\right|} \quad \text{for } \theta \gg a_0/\varrho$$

$$= \frac{\kappa \, d\theta}{8\varrho \left|\sin \theta/2\right|} \, . \qquad \text{(II.38)}$$

Hence, as in the general case (II.22) to (II.25), the core structure affects only the contributions from the nearest parts of the circumference. It is taken into account when equation (II.38) is used by cutting off the integration over θ at a lower limit θ_0, given by

$$\theta_0 \doteq 4a_0/6.2\varrho \, . \qquad \text{(II.39)}$$

The contribution to q from the part of the circumference beyond an angle θ_1 from the origin is

$$2\int_{\theta_1}^{\pi} dq_2(\theta) \doteq \frac{\kappa}{4\varrho} \int_{\theta_1}^{\pi} \frac{d\theta}{\left|\sin \theta/2\right|}$$

$$= \frac{\kappa}{2\varrho} \ln \cot \theta_1/4. \qquad \text{(II.40)}$$

If we put $$\theta_1(n) = (4a_0/6.2\varrho)^{\frac{1}{n}} \, , \qquad \text{(II.41)}$$

then, provided $$1 \gg \theta_1 \gg a_0/\varrho \, ,$$

$$2\int_{\theta_1}^{\pi} dq_2(\theta) \doteq \frac{\kappa}{2\pi\rho} \ln \frac{6.2\rho}{a_0}$$

$$= q/n . \qquad \text{(II.42)}$$

i.e. $(1 - 1/n)q$ is contributed by elements within an angle $|\theta_1| = (4a_0/6.2\rho)^{\frac{1}{n}}$ from $\theta = 0$. With $n = 6$, and taking as typical values $a_0 = 10^{-7}$ cm, $\rho = 10^{-1}$ cm, we see that $\frac{5}{6}q$ is contributed by elements within 0.1 radians of the point considered; that is, by 1/30 of the circumference of the ring. The required fraction becomes larger as ρ decreases, but, provided ρ is reasonably large, q is a mainly local velocity. In non-circular configurations, therefore, if ρ varies slowly enough in magnitude and direction, the localised induction approximation is good. More precisely, $|\Delta\underset{\sim}{\chi}| / |\underset{\sim}{\chi}|$ taken over an angular distance $\theta_1(n)$ must be small for reasonably large n, where $\underset{\sim}{\chi}$ is the curvature of the vortex line. Since $|\underset{\sim}{\chi}| = \rho^{-1}$, the criterion in planar configurations is that $\Delta\rho/\rho$ should be small. i.e.

$$\frac{1}{\rho}\left(\frac{d\rho}{dl}\cdot\rho\theta_1\right) = \theta_1 \frac{d\rho}{dl} \ll 1. \qquad \text{(II.43)}$$

Hence the approximation can be tested by solving for n the relation

$$\theta_1 \frac{d\rho}{dl} = \left(\frac{4a_0}{6.2\rho}\right)^{\frac{1}{n}} \frac{d\rho}{dl} \sim 1. \qquad \text{(II.44)}$$

The larger the value of n, the better the approximation.

(ii) Steady configurations in an apparatus of Vinen's geometry.

The self-induced velocity $\underset{\sim}{q}$ at any point on a vortex line can be written as

$$\underset{\sim}{q} = \underset{\sim}{q}_L(\ell) + \underset{\sim}{q}_c , \qquad (II.45)$$

where $\underset{\sim}{q}_L(\ell)$ is the velocity given by the localised-induction approximation, and $\underset{\sim}{q}_c$ is the correction due to departures of the configuration from a circle, the presence of solid boundaries, and superimposed flow of the superfluid. In a steady configuration $\underset{\sim}{q} = 0$. i.e.

$$\underset{\sim}{q}_L(\ell) + \underset{\sim}{q}_c = 0 \qquad (II.46)$$

In any specific problem configurations satisfying this equation may be sought by successive approximations. An initial configuration I, compatible with the boundary conditions, is assumed, and $\underset{\sim}{q}_c$ calculated. The radius of curvature at each point is then adjusted so that in the new configuration II

$$\underset{\sim}{q}_L^{II}(\ell) + \underset{\sim}{q}_c^{I} = 0 . \qquad (II.47)$$

$\underset{\sim}{q}_c^{II}$ may then be calculated and the procedure repeated, and so on. The convergence of this process needs further discussion.

Figure II.3. Vortex line partly attached to a wire in a cylindrical vessel ; detail (a): idealised roughness on the wall ; detail (b): junction of vortex line with circulation about wire

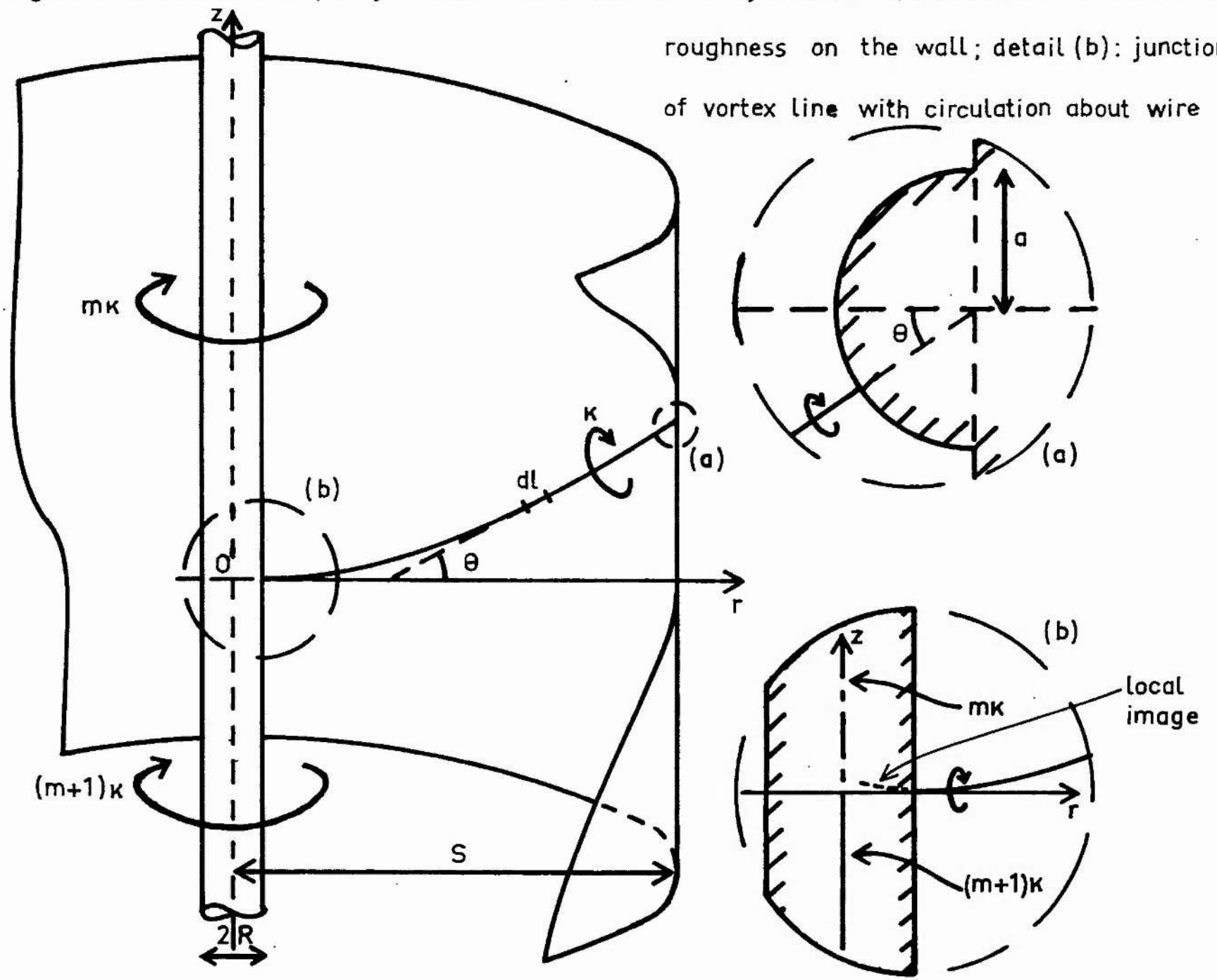

Suppose that the wire in Vinen's apparatus has m complete quanta of circulation about it, and that there is one partly attached vortex line, of which the far end is attached to the wall of the vessel and which lies in a plane containing the axis of symmetry, as shown in figure II.3. We wish to know whether such a configuration can be steady.

The general boundary condition is that the perpendicular velocity component must vanish on all surfaces. Now, suppose that the vortex line meets a surface whose radius of curvature is large compared with a_0. Then the surface may be treated as planar for discussion of behaviour in the vicinity of the attachment point, and so a local image system may be set up as in figure II.4. If the vortex line were ideal the radius of curvature ϱ of the line-image system at the attachment point would be infinitesimal for non-zero Θ, and the self-induced velocity would be singular there. Because a real vortex line has a finite core ϱ cannot vanish, but $\varrho \sim a_0$. Although our approximations break down in these conditions it is clear that the induced velocity is very large, of the order of κ/a_0, at the attachment point. Since this quasi-singularity is removed if $\Theta = 0$, in steady configurations the vortex line must meet the surface normally. The curvature $d\Theta/dl$ continues smoothly through the boundary, without necessarily vanishing.

In the successive approximations the junction of the vortex line with the wire is treated in the simplified manner shown in figure II.3, detail (b). The partly attached quantum of circulation is supposed to

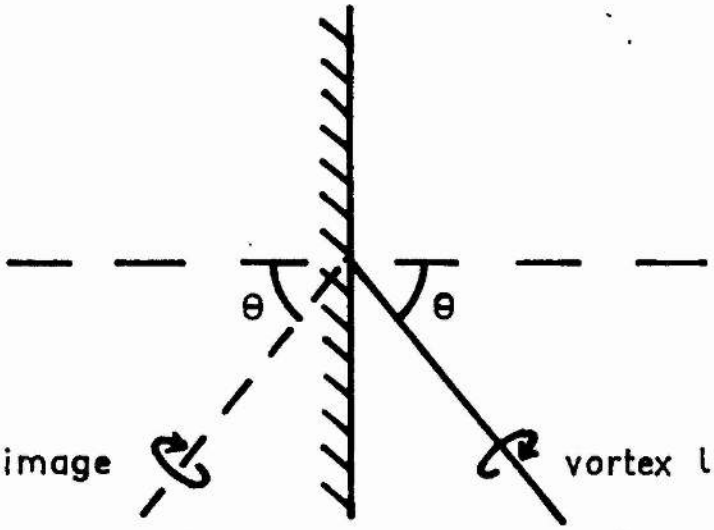

Figure II.4. Image of a vortex line in a plane boundary

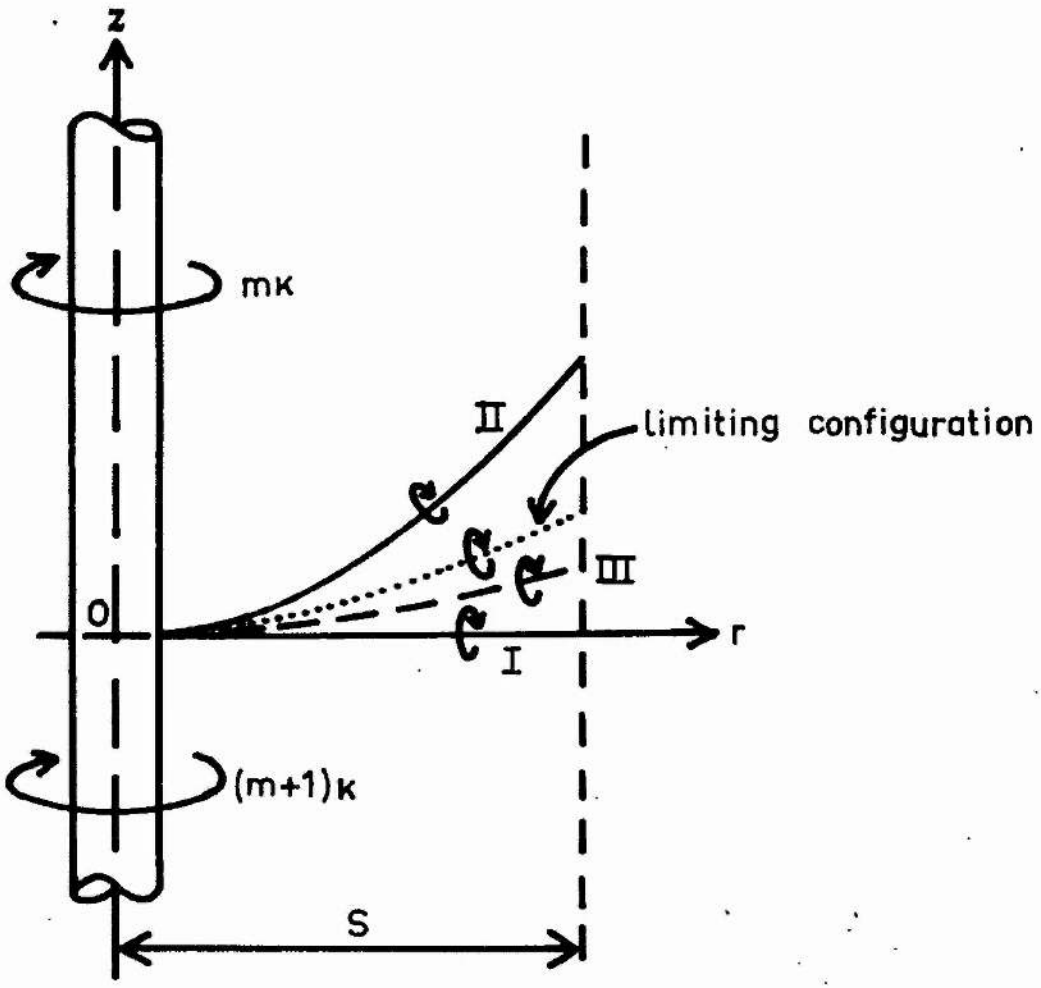

Figure II.5. Successive approximations to the limiting loose-end configuration in the apparatus of figure II.3.

extend from $z = -\infty$ to $z = 0$ exactly, and the vortex line to leave the wire normally at the point $(R, 0)$. In the neighbourhood of this point the concept of the local image of the line in the surface of the wire is valid. Any further contribution from the junction to the velocity field is neglected.

Let the velocity field due to the circulation about the wire alone (i.e. excluding that due to the vortex line) be $q_K(r,z)$, and let the vortex line lie along $z = 0$ in configuration I, as in figure II.5. Then the boundary conditions on Θ are satisfied, and

$$q_c^I(r) = q_K^I(r) , \qquad \text{(II.48)}$$

where $q_K^I(r) = q_K(r,0)$ is the form taken by $q_K(r,z)$ in configuration I. It is easy to show that

$$\left.\begin{aligned} q_K(r,z) &\sim (m+1)K/r \text{ as } z \to -\infty \\ &\sim mK/r \quad \text{as } z \to \infty \\ &= (m+\tfrac{1}{2})K/r \text{ when } z = 0 \end{aligned}\right\} \qquad \text{(II.49)}$$

Hence $q_c^I(r) = (m+\frac{1}{2})K/r$ perpendicular to the r-z plane.

Now from equation (II.35)

$$q_L(\ell) = \frac{K}{2\ell} \ln \frac{6.2\ell}{a_0} . \qquad \text{(II.50)}$$

In configuration II

$$\left| q_L^{II}(r) \right| = \left| q_c^{I}(r) \right| .$$

i.e. $$\frac{K}{2\rho} \quad \frac{6.2\rho}{a_0} = (m + \tfrac{1}{2}) K/r . \tag{II.51}$$

i.e. $$\frac{\rho}{r} = \frac{1}{2m+1} \ln \frac{6.2\rho}{a_0} . \tag{II.52}$$

But $$\rho = \frac{dl}{d\theta} = \frac{dr}{d\theta} \sec\theta . \tag{II.53}$$

Therefore $$\frac{dr}{r} = \frac{\cos\theta \, d\theta}{2m+1} \ln \frac{6.2\rho}{a_0} . \tag{II.54}$$

Since the logarithm is slowly varying we may replace ρ by a mean value $\bar{\rho}$ and integrate with the boundary condition $\theta = 0$ when $r = R$.
Whence

$$\sin\theta = (2m+1) \frac{\ln r/R}{\ln 6.2\bar{\rho}/a_0} \tag{II.55}$$

in configuration II. Inspection of signs shows that the direction of curvature is as shown in figure II.5. Now either the vortex line does not meet the wall, or it meets it at a non-zero angle $\theta = \theta_S$, so that the boundary condition at $r = S$ is not satisfied. The second possibility is considered further since it is the more promising.

If the effect of the wall, including the boundary condition, is

temporarily neglected, the line being treated as if it had a loose end at $r = S$, configuration II is given by equation (II.52). By equation (II.45)

$$q_c^{II}(r) = q_L^{II}(r) - q_c^{II}(r) , \qquad (II.56)$$

where modulus signs have been omitted. The correction velocity may itself be written as

$$q_c^{II}(r) = q_K^{II}(r) + \Delta q^{II}(r) . \qquad (II.57)$$

where $q_K^{II}(r) = q_K(r,2)$ in this configuration. $\Delta q^{II}(r)$, which is associated with the section of free vortex line between $r = R$ and $r = S$, and may be positive or negative, arises because $q_L^{II}(r)$ expresses only approximately the effect of its curvature. To the extent that q_L is a good approximation Δq can be neglected. This point is examined below. There is also a contribution to q_c from the surface of the wire. It is minimised by our choice of boundary condition and otherwise neglected. With these approximations

$$q_L^{III}(r) = q_K^{II}(r) . \qquad (II.58)$$

$q_K(r,2)$ is a monotonically decreasing, positive function of z for given r. Therefore, since from figure II.5

$$\varrho^{II}(r) < \varrho^{I}(r) = \infty \,, \tag{II.59}$$

$$0 < q_K^{II}(r) < q_K^{I}(r) \quad \text{for} \quad r > R \,. \tag{II.60}$$

Therefore, using equations (II.47), (II.48) and (II.58),

$$0 < q_L^{III}(r) < q_L^{II}(r) \,. \tag{II.61}$$

But q_L is a monotonically decreasing, positive function of ϱ, and $q_L(\varrho) \to 0$ as $\varrho \to \infty$. Therefore

$$\varrho^{I}(r) = \infty > \varrho^{III}(r) > \varrho^{II}(r) \,. \tag{II.62}$$

Pursuing this argument we find the nest of inequalities

$$\varrho^{I}(r) > \varrho^{III}(r) > \ldots > \varrho^{IV}(r) > \varrho^{II}(r) \tag{II.63}$$

and infer that the approximation procedure converges on some $\varrho(r)$ for which $q_L(r) = q_K(r)$. However, this configuration is not completely steady. There remains the small velocity Δq, whose magnitude is estimated by solving relation (II.44) for h, in configuration II for convenience.

In this configuration

$$\frac{\rho}{r} = \frac{1}{2m+1} \ln 6.2\rho/a_0 \text{ (equation II.52)}$$

Therefore $$\frac{d\rho}{dr} = \frac{1}{\ln 6.2\rho/a_0} + \frac{1}{2m+1} \ln 6.2\rho/a_0 . \qquad \text{(II.64)}$$

With $a_0 = 10^{-7}$ cm, we find that,

$$\left.\begin{aligned} &\text{when } r = 10^{-3} \text{ cm}, \quad \rho \sim 10^{-2}/(2m+1) \text{ cm} \\ &\text{when } r = 10^{-1} \text{ cm}, \quad \rho \sim 1/(2m+1) \text{ cm} \end{aligned}\right\} \qquad \text{(II.65)}$$

(The chosen values of r are the approximate radii of the wire and of the containing vessel in Vinen's apparatus). For values of ρ in this range

$$\ln 6.2\rho/a_0 \sim 15 , \qquad \text{(II.66)}$$

provided m is a small integer. Substituting this value in equation (II.64) we find $d\rho/dr \sim 15/(2m+1)$ for small, integral m. (II.67)
Hence, taking $d\rho/dr \doteq d\rho/dl$, (II.44) becomes

$$\left(\frac{10^{-7}}{\rho}\right)^{\frac{1}{h}} \frac{15}{2m+1} \sim 1 . \qquad \text{(II.68)}$$

With the values of ρ given by (II.65) the solution of (II.68) is

$$\left.\begin{aligned} n \sim 4, \text{ when } m = 0 \text{ and } r = 10^{-3} \text{ cm} \\ n \sim 6, \text{ when } m = 0 \text{ and } r = 10^{-1} \text{ cm} \\ n \sim 7, \text{ when } m = 1 \text{ and } r = 10^{-3} \text{ cm} \\ n \sim 10, \text{ when } m = 1 \text{ and } r = 10^{-1} \text{ cm} \\ \text{and so on.} \end{aligned}\right\} \qquad \text{(II.69)}$$

We expect that $|\Delta q| / q_L \sim n^{-1}$. Although n is not as large as could be hoped, particularly when $m = 0$, it does appear that there exists a steady, loose-end configuration not very different from the one to which the successive approximations lead.

When the effect of the wall is considered q_c is altered everywhere, but the main change may be found through a local image system near the attachment point, which causes q_c to increase strongly as $r \to S$. If the curvature is increased in an attempt to keep the configuration steady, the angle θ_s becomes larger, the increase in q_c is more marked, and the boundary condition is still further from being satisfied. There is therefore no steady state satisfying the given conditions.

In practice the wall and the wire are not perfectly smooth but, even if they are optically polished, may have roughness of up to about 10^{-6} cm in scale. Suppose that the wall is covered with idealised roughness in the form of hemispherical pimples of radius a, as shown in figure II.3, detail (a). Then if $a \gg a_0$ the vortex line can

meet the boundary normally, although $\theta_s \neq 0$. The image in the bulk of the wall remains, and so q_{V_c}, and hence the curvature, must be larger than in the loose-end configuration. We therefore expect that with roughness of this scale ($\sim 10\, a_0$) on the wall a steady configuration exists provided θ_s is not too large. If it is large the roughness must be correspondingly greater for the existence of a steady configuration. Since $\theta_s^{\text{II}} > \theta_s$ in the steady loose-end configuration, we take as a convenient criterion

$$\theta_s^{\text{II}} \leqslant 30^\circ \,. \qquad \text{(II.70)}$$

Just as roughness on the wall permits the boundary condition there to be apparently violated, so roughness on the wire allows non-zero values of θ on $r = R$. Again very large angles are not advantageous because the curvature has to be increased to compensate for the increase in q_{V_c} caused by the image system in the wire. If we assume again that a reasonable criterion for steadiness is

$$|\theta| \leqslant 30^\circ \text{ on } r = R \,, \qquad \text{(II.71)}$$

then the limiting steady configuration will have $\theta = -30^\circ$ on $r = R$. This may be approximately taken into account by modifying equation (II.55) to read

$$\sin \Theta^{II} = (2m+1) \frac{\ln r/R}{\ln 6.2\bar{\ell}/a_0} - \tfrac{1}{2} . \qquad \text{(II.72)}$$

The value of r for which $\Theta^{II} = 30°$ is given by equation (II.72) as

$$r_{30} = R(6.2\,\bar{\ell}/a_0)^{\frac{1}{2m+1}} \qquad \text{(II.73)}$$

This is also the value of r for which $\Theta^{II} = 90°$ if $\Theta = 0$ on $r = R$. The results are therefore not too sensitive to the correctness of our criteria.

If the geometric mean of the extreme values given in (II.65) is taken as a reasonable estimate of $\bar{\ell}$, i.e.

$$\bar{\ell} = 10^{m-1}/(2m+1) \text{ cm}, \qquad \text{(II.74)}$$

then, with $a_0 = 10^{-7}$ cm, $R = 10^{-3}$ cm and no quantum of circulation wholly attached to the wire ($m = 0$),

$$r_{30} \sim 10^{4} \text{ cm}. \qquad \text{(II.75)}$$

Taking the smallest possible estimate $\bar{\ell} = R$, again with $m = 0$,

$$r_{30} \sim 10^{2} \text{ cm}. \qquad \text{(II.76)}$$

Since even the smaller of these two estimates is far larger than the radius ($S = 0.2$ cm) of the containing vessel, the vortex line meets the wall at an angle θ_s^{II} which is considerably less than 30°. Hence the criterion (II.70) is easily satisfied and the existence of a steady configuration is assured, provided only that the solid surfaces are rough on a scale large compared with 10^{-7} cm.

When there is one quantum of circulation wholly attached to the wire and one partly attached vortex line, $m = 1$, and by equation (II.74)

$$\overline{\ell} = 3.10^{-2} \text{ cm.}$$

Therefore $$r_{3o} \sim 10^{-1} \text{ cm.} \qquad \text{(II.77)}$$

Since this is of the order of the radius S the criterion (II.70) is satisfied only with difficulty, if at all. Because of our approximations we can say only that, if a steady state exists, it is on the verge of instability. It is probably very sensitive to the scale of the roughness on the solid surfaces and easily disturbed by small perturbations.

With two wholly attached quanta and one partly attached vortex line, $m = 2$. By equation (II.74)

$$\overline{\ell} = 2.10^{-2} \text{ cm.}$$

Therefore $r_{3_0} \sim 10^{-2}$ cm. (II.78)

Since $S = 0.2$ cm, θ^{II} becomes equal to 30° far from the wall in this case. It can further be seen from equation (II.72) that $\theta^{\mathrm{II}} = 90°$ when $r \sim 10^{-1}$ cm, and so the vortex line can in fact hardly reach the wall at all. (II.70) cannot be satisfied. The theory therefore predicts that there is no steady configuration of this type in Vinen's apparatus. With more quanta wholly attached to the wire the impossibility of any steady configuration involving a partly attached vortex line is even more certain.

The stability of the predicted steady configurations has not been proved, but the agreement of the energetic and hydrodynamical approaches in the simple cases of Section (a) supports the belief that steadiness and stability are so linked that surface roughness not only allows steady configurations to exist, but also ensures their metastability.

It can be shown that, to the extent that the localised-induction approximation is correct, the angle θ_s at which the vortex line meets the wall of the containing vessel has a minimum value in planar configurations of the type so far considered. To this extent then a planar configuration is the most favourable for steadiness. In configurations which depart greatly from a plane the approximation is not good. Such complicated configurations will not be considered however, as it seems both energetically and hydrodynamically improbable that

they could be steady.

(c) Comparison with experiment

Vinen (1961b) measured the superfluid circulation about a wire of radius $1.3.10^{-3}$ cm stretched along the axis of a cylindrical vessel of helium of radius 0.2 cm by observing changes in the vibrational modes of the wire. After steady rotation just above the λ-point followed by slow cooling to 1.3°K, the apparent circulation was measured. During rotation there was no sign of quantisation, while the variability of the results showed that equilibrium was not attained. Large-amplitude vibration of the wire had no definite effect on the apparent circulation and so did not aid the attainment of equilibrium. Eventually a plot of the mean apparent circulation against the angular velocity of rotation was obtained, which corresponded in some respects to a smoothed version of the stepwise variation predicted by Vinen's free-energy calculations.

The variation of the apparent circulation with time after stopping rotation was also observed, and in particular its stability against large-amplitude vibration of the wire. In the undisturbed system there was little variation. Large-amplitude vibration temporarily reduced circulations of less than one quantum, although their long-term stability was unaffected. Circulations between one and two quanta were permanently reduced, and with repeated strong vibration they fell either to less than one quantum or sometimes to exactly this value, which then persisted unchanged by further vibration. It proved impossible to

establish circulations of more than two quanta.

From comparison of the results (principally the failure to attain equilibrium and the fact that the mean apparent circulation never rose to two quanta) with the equilibrium circulation, calculated as a function of the angular velocity and the effective vortex core radius a_0, it was deduced that a_0 must be greater than 10^{-4} cm, a value in complete disagreement with that suggested by Feynman (of the order of the interatomic spacing, 4.10^{-8} cm) and that obtained by Hall (1958) from measurements of the velocity of propagation of waves on vortex lines ($6.8.10^{-8}$ cm). The analysis took very little account of the mechanism by which equilibrium was to be attained. The existence of metastable, non-equilibrium states provides an alternative explanation for the failure to reach equilibrium.

When rotation ceases, turbulence is generated in the normal fluid, accompanied, according to chapter 9(b), by randomly orientated vorticity in the superfluid. As equilibrium is re-established this vorticity should crystallize out into a steady vortex-line configuration, in which the circulation about the wire could in principle be smaller than it was during rotation. Classically we would say that part of it had been annihilated. In fact this happened apparently only to a limited extent, if at all. No doubt the rates of rotation were so low that too little vorticity was induced in the superfluid for annihilation to be a probable process. Rather similar were the observations that, when rotation was started below the λ-point, the superfluid remained apparently at rest,

and that reverse rotation of the apparatus did not necessarily destroy established circulation. The classical explanation of all three observations is simply that the creation of vortex lines is a difficult process.

Whatever the true explanation, after the cessation of rotation and the decay of the associated turbulence, the superfluid circulation about the wire is substantially the same as it was during rotation. If the mean circulation is fractional there must be one or more partly attached vortex lines in metastable configurations. If it is integral there are probably no partly attached vortex lines, and so the superfluid is in a quasi-equilibrium state, which we know from Section (a) to be highly metastable. This is in agreement with the experiment, where it was found that the two observable integral circulations, zero and one quantum, were the only circulations consistently stable against large-amplitude vibration of the wire.

In fact vibration of the wire with velocity amplitude up to $60\pi\kappa/R$ was insufficient to disturb the stability of a completely attached quantum of circulation. In the absence of more positive information we can tentatively infer an upper limit to the core radius a_0. For, assuming that the frequency of vibration (about 1 kc/s) was not too high to permit the creation of a vortex line at the surface of the wire, it follows from relation (3.11) that, in order of magnitude,

$$60\pi\kappa/R < \kappa/2a_0$$

i.e. $$a_0 < R/120\pi$$

$$\doteq 3.10^{-6} \text{ cm.} \qquad \text{(II.79)}$$

The fact that this upper limit is consistent with other estimates of a_0, but not with the lower limit of 10^{-4} cm suggested by Vinen, supports the interpretation of his experiment here put forward.

In considering the behaviour of partly attached vortex lines after cessation of rotation we take $a_0 = 10^{-7}$ cm as a reasonable estimate. The numerical calculations of Section (b) (ii) are immediately applicable since the dimensions used there are approximately equal to those of the experimental apparatus, and there was certainly roughness of at least 10^{-6} cm in scale on both wire and wall. The results of the calculations are now summarised.

With a single vortex line partly attached to the wire and no wholly attached quanta ($m = 0$) the criterion (II.70) for steadiness is easily satisfied, and so steady, stable configurations should be formed without difficulty. With one wholly and one partly attached quantum ($m = 1$) the existence of a steady configuration is more doubtful, probably depending critically on the roughness of the wire and the wall. If it does exist it is probably easily disturbed. Steady configurations of

this type, but with more than one wholly attached quantum ($m \geq 2$), are most improbable.

These results are in good agreement with the experimental observations after cessation of rotation. It appears that, as Vinen suggested, large-amplitude vibration of the wire is able to move only the end of the vortex line attached to the wire when $m = 0$: the other end remains anchored to roughness on the wall, and so the vortex line eventually returns to its initial steady configuration. When $m = 1$ the configuration is so nearly unsteady that, although the vibration involved in measurement of circulation does not affect it, large-amplitude vibration dislodges both ends of the vortex line and it moves towards equilibrium. The apparent circulation therefore falls. Fractional circulations with $m \geq 2$ were not observed. This is at least consistent with the unsteadiness of such states, which implies that they decay into accessible, metastable states of lower circulation by the peeling-off of partly attached vortex lines. However, the absence of circulations of exactly two quanta suggests that such states were never formed, possibly for some different reason.

During rotation of the apparatus the theoretical analysis is apparently little altered. States with integral circulation are still metastable below an angular velocity of about 30 rad/sec, by (II.2). The configuration of a partly attached line may be distorted out of the plane by the presence of other vortex lines, but, since to first order these lines only cause the superfluid to rotate with the walls and

normal fluid, they do not alter the argument. Hence apart from the possible effect of Coriolis forces the situations during and after rotation seem to be similar. We therefore do not expect any tendency towards equilibrium at 1.3°K. Rather must the measured circulations depend on the conditions near the λ-point, when the superfluid was created. In the λ-transition some turbulence is almost certainly generated, so that the created circulation differs from that which would occur in perfect rotational equilibrium. The variability of the observed circulation and the fact that there was often circulation about the wire even when the cooling was done without rotation confirm this. Deduction of the expected circulation, in particular of whether it should exceed two quanta, is therefore difficult.

Up to this point theory and experiment are consistent. However, during rotation large-amplitude vibration of the wire had very little effect on circulations of any value. This behaviour is quite different from that in the non-rotating case; the system seems to possess unexpected extra stability. Clearly this may be due to the breakdown of our approximations in the conditions of rotation. Non-planar configurations should be considered, as well as the effect of Coriolis forces, which appears to increase the stability of partly attached vortex lines. Nevertheless it is difficult to understand why, even with greater stability, large-amplitude vibration of the wire should not move the point of attachment of the vortex line to the wire at least temporarily. There may therefore be some more fundamental short-

coming in the theory.

(d) Application of the theory to the present experiment

Unlike the wire in Vinen's apparatus, a hanging fibre in a wind tunnel does not render the helium truly doubly connected. The complete attachment of quanta of circulation to the fibre is therefore impossible in the sense of Section (a), for circulation about the fibre must always be completed by a free vortex line running from the fibre to one of the fluid boundaries. Clearly stability is greatest, and the ideal of complete attachment most nearly approached, when the vortex line extends from the lower end of the fibre to the floor of the tunnel in the same straight line as the fibre. For this reason we expect a mean circulation of one quantum to be fairly stable. The stability of other values can be judged by investigating the steadiness of vortex lines partly attached to the fibre, and terminating on the wall of the wind tunnel.

The measurements of circulation were made in tunnel II, in which the perpendicular distance between the fibre and the side wall was about 0.3 cm. The radii of both fibres I and II were $0.35.10^{-4}$ cm. In configuration II of the theory of Section (b) (ii), the radius of curvature of the partly attached vortex line is given by equation (II.52) as

$$\left.\begin{aligned} \rho &\sim 3.10^{-4}/(2m+1) \text{ cm when } r = 3.10^{-5} \text{ cm} \\ \rho &\sim 10/(2m+1) \text{ cm when } r = 3.10^{-1} \text{ cm,} \end{aligned}\right\} \qquad \text{(II.80)}$$

taking $a_0 = 10^{-7}$ cm. Again $\ln 6.2\ell/a_0 \sim 15$ if m is a small integer, so that relation (II.68) is unchanged:

$$\left(\frac{10^{-7}}{\ell}\right)^{\frac{1}{n}} \frac{15}{2m+1} \sim 1 . \qquad \text{(II.81)}$$

With $m = 0$ and $r = 3.10^{-5}$ cm the solution is $n = 3$, so that the localised-induction approximation is poorer than for Vinen's apparatus (see (II.69)).

If the quartz fibre is rough enough, either naturally or because of dust particles, equations (II.72) and (II.73) are valid. The geometric mean of the values given in (II.80) is

$$\bar{\ell} \doteq 5.10^{-2}/(2m+1) \text{ cm} . \qquad \text{(II.82)}$$

Therefore, with $a_0 = 10^{-7}$ cm and $m = 0$,

$$r_{30} \sim 10^2 \text{ cm} , \qquad \text{(II.83)}$$

while, with $m = 1$,

$$r_{30} \sim 3.10^{-3} \text{ cm} . \qquad \text{(II.84)}$$

With one "completely attached" quantum of circulation a partly attached vortex line could not possibly, by (II.84), reach the tunnel wall at a

sufficiently obtuse angle to satisfy criterion (II.70). There is therefore no possibility that fractional mean circulations greater than one quantum would be metastable, even if they could be established. With a single, partly attached vortex line it is, by (II.83), possible to satisfy the steadiness criterion, although much less easily than in Vinen's apparatus. Despite the very approximate nature of the theory we might expect sometimes to find persistent, fractional circulations of less than one quantum. That such circulations have very rarely been observed may be due partly to the measurement process itself, which causes a disturbance at least as great as the large-amplitude vibration of the wire carried out in Vinen's apparatus.

(e) Summary of conclusions

In Vinen's apparatus, provided that all the existing vortex lines have a preferred orientation with respect to the wire so that no annihilation can take place, there exist metastable states of two kinds. Any state with integral, non-zero circulation about the wire is metastable, and, if the apparatus has sufficiently rough surfaces, so are states with fractional apparent circulations arising from the partial attachment of vortex lines to the wire. The existence of the latter depends critically not only on the dimensions of the apparatus but on the total circulation about the wire. States with a single partly attached vortex line are certainly metastable; those with one wholly and one partly attached vortex line, more doubtfully so. A partly attached vortex line is almost certainly unstable if there are two or

more complete quanta on the wire: it is expected to peel off. The theory agrees well with the published experimental results in the case where the apparatus is no longer rotating. The interpretation of the observations in terms of quasi-classical vortex lines here seems to be quite adequate. On the other hand the agreement in the rotating case is less happy. It is not clear whether this is due to the breakdown of the approximations used or to some inadequacy in the quasi-classical vortex-line model, perhaps of the sort suggested in chapter 9(b).

For the apparatus of the experiment described in the body of this thesis the approximations made in this theory are rather drastic. Nevertheless it is expected that a single, partly attached vortex line could be metastable. Hence fractional mean circulations of less than one quantum should sometimes be persistent. Such circulations have been observed very rarely (one example appears on the histogram in figure 7.5(a)). A circulation of one quantum is expected to be especially stable, in agreement with the interpretation in chapter 8(a) (iii) of the histograms of persistent circulations (Figure 7.5 (a) and (b)). Fractional circulations of more than one quantum would be unstable if they could be created. The agreement between these predictions and the experimental results is as good as can be expected, although not particularly convincing.

By performing Vinen's experiment in apparatuses of varying dimensions and establishing larger circulations about the wire the predictions of the theory could be checked more rigorously. It should also be

possible with larger circulations to demonstrate the quantization of circulation more convincingly and test the theory of quasi-classical vortex lines more thoroughly than has so far been done. For partly attached vortex lines would then be unstable, and only integral circulations should be persistent. Such large circulations could be established by rotation at an angular velocity high enough to overcome the potential barriers opposing the capture of successive vortex lines. The experimental measurement of this angular velocity, which is expected to be of the order of κ/R^2, where R is the radius of the wire, would provide a further test of the theory.

The features of his experimental results, in particular the failure to attain equilibrium, which Vinen suggested might be explained by assuming that vortex lines had a larger core (that is, lower energy) than had previously been supposed, are now ascribed to the trapping of vortex lines in metastable states. His suggested lower limit to the core radius, $a_0 > 10^{-4}$ cm, is therefore unreliable, especially as it is inconsistent with the upper limit tentatively inferred from the observations of the stability of a completely attached quantum of circulation, $a_0 < 3.10^{-6}$ cm.

References: original papers.

Allen, J. F. and Misener, A. D. (1938) Nature, Lond., 141, 75.

Brewer, D. F. and Edwards, D. O. (1957) Proc. Vth International Conference on Low Temp. Physics and Chemistry (Madison, U.S.A.), p. 12.

Chase, C. E. (1962) Proc. VIIIth International Congress on Low Temp. Physics (London).

Dash, J. G. and Taylor, R. D. (1957) Phys. Rev. 105, 7.

Fairbank, H. A., Buckingham, M. J. and Kellers, C. F. (1957) Proc. Vth International Conference on Low Temp. Physics and Chemistry (Madison, U.S.A.), p. 50.

Fromm, J. E. and Harlow, F. H. (1963) Phys. Fluids 6, 975.

Gorter, C. J. and Mellink, J. H. (1949) Physica 15, 285.

Hall, H. E. and Vinen, W. F. (1956) Proc. Roy. Soc. A238, 204.

Hall, H. E. (1958) Proc. Roy. Soc. A245, 546.

Hama, F. R. and Nutant, J. (1961) Phys. Fluids 4, 28.

Hama, F. R. (1962) Phys. Fluids 5, 1156.

Hung, C. S., Hunt, B. and Winkel, P. (1952) Physica 18, 629.

Kapitza, P. L. (1938) Nature, Lond., 141, 74.

Khalatnikov, I. M. (1956a) Usp. Fiz. Nauk 59, 673.

Khalatnikov, I. M. (1956b) Usp. Fiz. Nauk 60, 69.

Kidder, J. N. and Fairbank, W. M. (1962) Phys. Rev. 127, 987.

Landau, L. D. (1941) J. Phys., Moscow, 5, 71.

Landau, L. D. (1947) J. Phys., Moscow, 11, 91.

Landau, L. D. and Khalatnikov, I. M. (1949a,b) J. Exp. Theor. Phys. U.S.S.R. 19, 637, 709.

Lin, C. C. (1943) Quart. Appl. Math. 1, 43.

London, H. (1939) Proc. Roy. Soc. A171, 484.

Mendelssohn, K. and Steele, W. A. (1959) Proc. Phys. Soc. A73, 144.

Onsager, L. (1949) Nuovo Cim. 6, Suppl. 2, 249.

Osborne, D. V. (1950) Proc. Phys. Soc. A63, 909.

Osborne, D. V. (1951) Proc. Phys. Soc. A64, 114.

Palevsky, H., Otnes, K., Larsson, K. E., Pauli, R. and Stedman, R. (1957) Phys. Rev. 108, 1346.

Pellam, J. R. (1962) Phys. Rev. Letters 9, 289.

Pellam, J. R. (1963) Phys. Rev. Letters 10, 82.

Sewell, C. J. T. (1910) Phil. Trans. A210, 239.

Staas, F. A., Taconis, K. W. and Van Alphen, W. M. (1961) Physica 27, 893.

Tisza, L. (1940) J. Phys. Radium 1, 165, 350.

Townsend, A. A. (1963) J. Fluid Mech. 15, 262.

Vinen, W. F. (1957a) Proc. Roy. Soc. A240, 114.

Vinen, W. F. (1957b) Proc. Roy. Soc. A240, 128.

Vinen, W. F. (1957c) Proc. Roy. Soc. A242, 493.

Vinen, W. F. (1957d) Proc. Roy. Soc. A243, 400.

Vinen, W. F. (1961b) Proc. Roy. Soc. A260, 218.

Walmsley, R. H. and Lane, C. T. (1958) Phys. Rev. 112, 1041.

White, C. M. (1945) Proc. Roy. Soc. A186, 472.

Winkel, P., Broese van Groenou, A. and Gorter, C. J. (1955) Physica 21, 345.

Yarnell, J. L., Arnold, G. P., Bendt, P. J. and Kerr, E. C. (1959) Phys. Rev. 113, 1379.

References: books and review articles.

Atkins, K. R. (1959) Liquid Helium. Cambridge University Press.

Batchelor, G. K. (1953) Homogeneous Turbulence. Cambridge University Press.

Birkhoff, G. (1950) Hydrodynamics. Princeton University Press.

Chester, G. V. (1961) Proc. International School of Physics "E. Fermi", Course XXI (Varenna, Italy), p. 51.

Feynman, R. P. (1955) Prog. Low Temp. Phys., Vol. I, p. 36. Amsterdam: North-Holland Publishing Co.

Fineman, J. and Chase, C. E. (1959) Tables of some properties of liquid helium. Massachusetts Institute of Technology, Group Report #46-46.

Hall, H. E. (1960) Adv. Phys. 9, 89.

Hoel, P. G. (1954) Introduction to Mathematical Statistics (2nd ed.) New York: Wiley.

Jaeger, J. C. (1951) Laplace Transformation. London: Methuen.

Lamb, H. (1945) Hydrodynamics (6th ed.). New York: Dover.

Landau, L. D. and Lifshitz, E. (1959) Fluid Dynamics. Oxford: Pergamon Press.

Lane, C. T. (1962) Superfluid Physics. New York: McGraw-Hill.

Lin, C. C. (1961) Proc. International School of Physics "E. Fermi", Course XXI (Varenna, Italy), p. 93.

London, F. (1954) Superfluids, Vol. II. New York: Wiley.

Milne-Thomson, L. M. (1960) Theoretical Hydrodynamics (4th ed.). London: Macmillan.

Prandtl, L. (1952) Fluid Dynamics. London: Blackie.

Strong, J. (1938) Modern Physical Laboratory Practice. London: Blackie.

Tighe, N. J. (1956) Fused-Quartz Fibers. NBS Circular 569, U.S. Department of Commerce.

Vinen, W. F. (1961a) Prog. Low Temp. Phys., Vol. III, p. 1.